University of Essex

School of Biological Sciences

Date of Submission: April 2019

Characterisation of Androgen Receptor Signalling and Metabolism in Prostate Cancer

Eleanor Rees

Supervisor: Dr Greg Brooke

A thesis submitted in accordance with the requirements of the University of Essex for the degree of MSc by Dissertation in Cell and Molecular Biology

Statement of Originality

I clarify that this thesis is the result of my own work. All sources used have been acknowledged

Abstract

Prostate cancer (PCa) is a prevalent disease which affects men worldwide. The Androgen Receptor (AR) is responsible for driving disease progression, therefore therapies often target this signalling axis. Eventually, these treatments fail and the cancer progresses to an aggressive stage known as castrate-resistant prostate cancer (CRPC) for which very few therapies exist. Therefore, understanding and characterising AR signalling may aid in the development of novel therapeutics, especially for incurable, advanced stages of disease. Fused in Sarcoma (FUS) (a co-regulator protein of the AR) and Hox Transcript Antisense Intergenic RNA (HOTAIR) (a long noncoding ribonucleic acid [RNA]) can interact with the AR and are found to be elevated in CRPC. To investigate their effect on AR activity, luciferase reporter assays were performed. Results demonstrated that both factors can repress AR activity.

The AR drives prostate cancer growth through the regulation of genes and protein involved in, for example, the cell cycle and metabolism. Metabolism is augmented in cancer cells to support their elevated growth and division. One such pathway is haem synthesis, which supplies haem for several proteins that assist in maintaining cellular homeostasis and protect against cell stress. Previously, using an siRNA screen, haem synthesis was identified as a potential therapeutic target for prostate cancer and the pathway was therefore further investigated. The results demonstrated that inhibiting haem synthesis, using succinylacetone, significantly reduced PC3 cell proliferation in crystal violet growth assays. Furthermore, small interfering RNA (siRNA) knockdown of aminolevulinate synthase-1, involved in the first step of the haem synthesis pathway, significantly reduced cell proliferation by approximately 60 %. Interestingly, inhibition of haem synthesis sensitised PC3 cells to ROS. In preparation for crystallography assays, ALAS1 and ALAS2 were cloned and expressed in *Escherichia coli* BL21(DE3). Further investigation of co-factors which interact with the AR and downstream metabolic pathways will aid in the development of novel therapeutic strategies for PCa patients in the future.

Acknowledgements

A thesis becomes possible when one is surrounded by great people. I would like to take this opportunity to express my sincere thanks and gratitude towards them.

Firstly, I would like thank my supervisor Dr Greg Brooke for his continuous support, encouragement, positivity and enthusiasm - it was greatly appreciated. I truly enjoyed the laboratory work and feel I gained excellent experience. Appreciation goes towards Anatastios Bamplilis for his data contribution and support. Also, thank you to all my colleagues in Team GB especially Mohammad Alkheilwi, Dr Amna Allafi, Angela Pine and Ryan Cronin. I will miss all our laughter and banter in our happy laboratory.

I would also like to thank Mrs Julie Arvidson for continual encouragement. Also, Miss Amanda Clements and Mrs Vicky Hall for all their hard work and time, providing a smooth run of the experiments and also for their repeated kind words of support. Without their hard work, none of this would have been possible. Also to Emma Revill for her hard work and support.

Last, but not least, a huge thank you goes to my mother and father - their endless support is always so uplifting. I cannot thank them enough for continually believing in me and for picking me back up during those times where faith in myself was lost. You are my inspiration, I love you both very much.

Abbreviations

ADT	Androgen deprivation therapy
AF-1/2	Activation function 1/2
ALA	Aminolevulinic Acid/Aminolevulinate
ALAS1/2	Aminolevulinic Acid/Aminolevulinate Synthase 1/2
APS	Ammonium persulphate solution
AR	Androgen receptor
ARE	Androgen response element
BBS	BES-buffered saline
BES	N,N-bis[2-Hydroxyethyl]-2]aminoethanesulfonic acid
BPH	Benign prostatic hyperplasia
BSA	Bovine serum albumin
CRPC	Castration resistant prostate cancer
CTD	C-terminal Domain
CSC	Cancer stem cell
CZ	Central zone
CV	Crystal violet
DBD	DNA binding domain
ddH2O	Double distilled water
DHT	Dihydrotestosterone
DMEM	Dulbecco's Modified Eagle Medium
DMSO	Dimethyl Sulphoxide
EDTA	Ethylenediaminetetraacetic
EtOH	Ethanol
Ferr	Ferrostatin-1
FET/TET	Fused in sarcoma (FUS)/Translocated in Liposarcoma (TLS), Ewings Sarcoma, TATA-binding protein-associated factor (TAF)
FMZ	Fibromuscular zone
FUS	Fused in Sarcoma
GnRH	Gonadotropin releasing hormone
HAT	Histone acetyltransferase
HCl	Hydrochloric acid
HEPES	4-(2-hydroxyethyl)-1-piperazineethanesulfonic acid

HDAC	Histone deacetylase
HGPIN	High Grade Prostatic Intraepithelial Neoplasia
HOTAIR	Hox Transcription Antisense Intergenic RNA
HSP	Heat shock protein
IPTG	Isopropyl-beta-D-thiogalactopyranoside
kDa	Kilodaltons
KOH	Potassium hydroxide
LB	Luria broth
LBD	Ligand-binding domain
LH	Luteinising hormone
LHRH	Luteinising hormone releasing-hormone
LiCl	Lithium chloride
LncRNA	Long noncoding RNA
$MgCl_2$	Magnesium chloride
$MnCl_2$	Manganese chloride
Na_2HPO_4	Disodium hydrogen phosphate
NAD	Nicotinamide adenine dinucleotide
NaOH	Sodium hydroxide
NEAT1	Nuclear Enriched Antisense Transcript 1
Nec	Necrostatin-1
NES	Nuclear export signal
NLS	Nuclear localisation sequence
NTC	Non-Targeted Control
NTD	N-terminal domain
PBS	Phosphate buffered saline
PBS-T	PBS-Tween
PCa	Prostate cancer
PEG-800	Polyethene glycol 8000
PIA	Prostatic Inflammatory Atrophy
PIC	Protease inhibitor cocktail
PIN	Prostatic Intraepithelial Neoplasia

PSA	Prostate-specific antigen
PSG	Penicillin-Streptomycin-Glutamine
PZ	Peripheral zone
RIPA	Radioimmunoprecipitation assay
RPMI	Rosewell Park Memorial Institute
SA	Succinylacetone
SDS	Sodium dodecyl sulphate
SHBG	Sex hormone-binding globulin
SOC	Super optimal broth with catabolic repressor
SR	Steroid receptor
TAE	Tris-acetate-Ethylenediaminetetraacetic
TBS	Tris-buffered solution
TAU1/5	Transactivation unit
TEMED	Tetramethylethylenediamine
TF	Transcription factor
TLS	Translocated in Liposarcoma
TZ	Transitional zone
UGS	Urogenital sinus

Contents

List of Figures

List of Tables

Chapter 1: Introduction

1.1 The Prostate Gland and Associated Diseases

1.1.1 The Structure and Function of the Prostate Gland

The prostate is a male accessory reproductive gland involved in producing seminal secretions, essential for fertility. Multiple accessory glands of the reproductive system contribute towards the ejaculate volume, with 30% originating from the prostate (Aneck-Hahn *et al.*, 2007). The prostate is situated within the subperitoneal cavity, inferior to the bladder and anterior to the rectum (Figure 1.1.1a). The base of the prostate is situated immediately below the bladder, narrowing to a point known as the apex. The human prostate surrounds the urethra and consists of a fibromuscular stroma and glandular tissue which are encased within a fibrous "capsule". For many years, there was unanimity amongst scientists as to whether a true capsule was present. Some believed there existed a fibromuscular band surrounding the organ instead (Ayala *et al.*, 1989). Currently, it is thought that a combination of these structures exists but an intact, complete capsule is absent. Indeed, the prostate possesses a capsule along its lateral dorsal side, whereas the ventral lateral side is surrounded by thick smooth muscle (Antonioli *et al.*, 2004; Blana *et al.*, 2004).

Multiple different cell types are found within the prostate including epithelial, fibromuscular and stem cells (Kumar and Majumder, 1995). The epithelial group can be further subdivided into three main categories including the luminal, basal and neuroendocrine cells (Wang *et al.*, 2009). Prostatic secretions from the luminal cells contain factors which are crucial for spermatozoa function and survival such as enzymes, zinc, citrate, calcium and prostate-specific antigen (PSA) (Franz *et al.*, 2013; Rodriguez-Martinez *et al.*, 2011). Neuroendocrine cells are distributed throughout all prostatic zones and may contribute to the regulation of growth and differentiation of surrounding epithelial cells via paracrine signalling (Dutt and Gao,

2009; Parimi *et al.*, 2014). Stem cells are located in prostatic ducts throughout the basal cell layer (Lawson *et al.*, 2010).

The prostate is divided into four distinct regions: the fibromuscular stroma (or fibromuscular zone [FMZ]), transitional (TZ), peripheral (PZ) and central zone (CZ) (Figure 1.1.1b), whereby the latter two contain glandular tissue and are involved in producing prostatic secretions. The FMZ, the most anterior zone of the prostate, comprises both muscle and connective tissue (Sah *et al.*, 2015). The TZ surrounds the urethra, superior to the verumontanum and accounts for the smallest region of the prostate at approximately 5% of the total mass (Aaron *et al.*, 2016). The PZ, around 70% of prostatic mass, lies most dorsally of the exocrine organ (Franz *et al.*, 2013)). The central zone (CZ) surrounds the ejaculatory duct and accounts for approximately a quarter of prostate mass (Bhavsar and Verma, 2014). From a coronal plane, the CZ is situated towards the base of the prostate, ventral to the peripheral zone and tapers towards the verumontanum (seminal colliculus) (Vargas *et al.*, 2012) (Figure 1.1.1b). The vermontanum is in close proximity to the juncture by which the ejaculatory duct merges with the urethra (Bhavsar and Verma, 2014). The ejaculatory duct is continuous with the vas (ductus) deferens which passes through the seminal vesicles from the epididymis and enters the prostate (Cohen *et al.*, 2008).

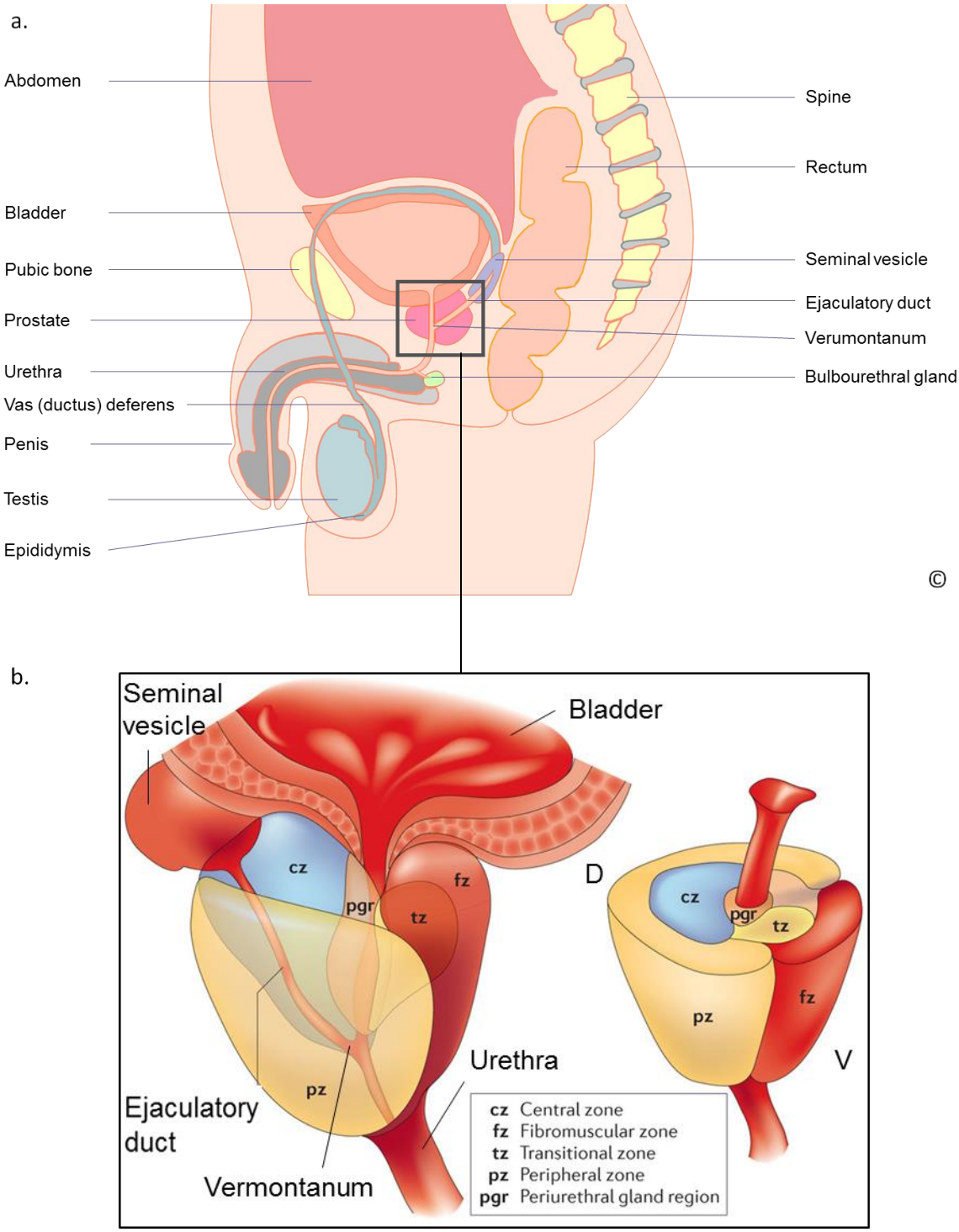

Figure 1.1.1: Schematic of the male reproductive system and prostate anatomy. a. Sagittal plane of the male reproductive system. b. Prostate gland anatomy. D, Dorsal; V, Ventral. NOTE: These schematics are not to scale. (Figure 1b Adapted from (Verze *et al.*, 2016).

1.1.2. Foetal Development of the Prostate Gland

The development of the prostate commences in the foetus at approximately 10 weeks of gestation in humans and originates from the urogenital sinus (UGS) (Marker *et al.*, 2003). The UGS is derived from the cloaca (from the posterior end of the hindgut). It is composed of endodermal epithelia and mesenchyme (Ricke *et al.*, 2005). The latter continuously expresses the androgen receptor (AR) and has the capacity to undergo prostatic morphogenesis if depicted by the presence of circulating androgens produced by the foetal testes (Ricke *et al.*, 2005). Before this occurs, the UGS is ambisextrous. The continual presence of androgens is important to sustain branching extension and its rate. Dysfunctional ARs during development leads to impeded prostatic induction while androgens in the presence of a female UGS leads to prostatic budding and branching (Toivanen and Shen, 2017). This therefore demonstrates the necessity of androgens and a functional AR for the development of the prostate. Prostatic organogenesis occurs within four stages: prostatic induction – induced via the presence of androgens thus determining prostatic fate, budding – the urogenital sinus epithelia invades the surrounding urogenital sinus mesenchyme, branching – leads to the formation and maturation of a ductal network and distinct zones within the prostate and finally canalisation – lumen formation and discreet cell types fully differentiate (Toivanen and Shen, 2017). Via paracrine signalling, mesenchyme and epithelial cells communicate to regulate branching morphological processes. These signalling events are depicted by the presence of the AR as well as multiple growth factors including sonic hedgehog, fibroblast growth factor and transforming growth factor-β families, among others (Murashima *et al.*, 2015) (Figure 1.1.2). Reproduction, development of male characteristics, well-being as well as the function of the prostate are dependent upon androgens and their receptor (the AR) throughout a male's lifetime. Prostatic growth and development continue until sexual maturation at puberty (Brooke and Bevan, 2009; Marker *et al.*, 2003).

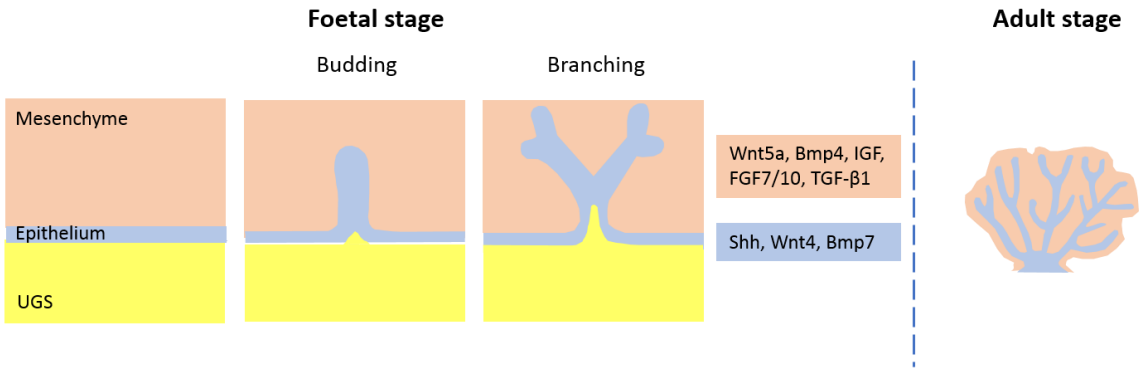

Figure 1.1.2: Schematic of prostatic foetal branching within the urogenital sinus during development. The prostate gland develops from the urogenital sinus (UGS). Epithelial cells undergo differentiation and buds invade the mesenchyme of the UGS. Elongation of prostatic ducts and a branching morphogenesis is observed. Orange and blue boxes depict some signalling molecules present within the urogenital epithelia and mesenchyme respectively. The adult prostate contains multiple lobes and distinct zones.

1.1.3 Testosterone and Androgen Biosynthesis

1.1.3.1. Testosterone is Regulated by The Hypothalamus-Pituitary-Gonadal Axis

Testosterone is a steroid hormone which is the principal circulating androgen in males. It is produced in both the testes and adrenal glands through multiple enzymatic steps. The majority of testosterone is synthesised in the former by Leydig cells which are located in the interstitial compartment, outside the seminiferous tubules, within the testis (Chen *et al.*, 2015). Testosterone production and spermatogenesis are tightly regulated via the hypothalamus-pituitary-gonadal axis. Further, gonadotropin releasing hormone, also known as luteinising hormone releasing hormone (LHRH), is released by the hypothalamus in a pulsatile fashion (regulated by testosterone levels) into the anterior pituitary gland via the hypophyseal portal system (Fraietta *et al.*, 2013). The presence of LHRH in the anterior pituitary gland causes luteinising hormone and follicle stimulating hormone release. The former directly acts upon membrane receptors on Leydig cells to promote testosterone release into the blood, thereby creating a negative feedback loop with the hypothalamus-pituitary gonadal axis (Fraietta *et al.*, 2013) (Figure 1.1.3). Follicle stimulating hormone stimulates Sertoli cells to promote spermatogenesis (Sanderson, 2006).

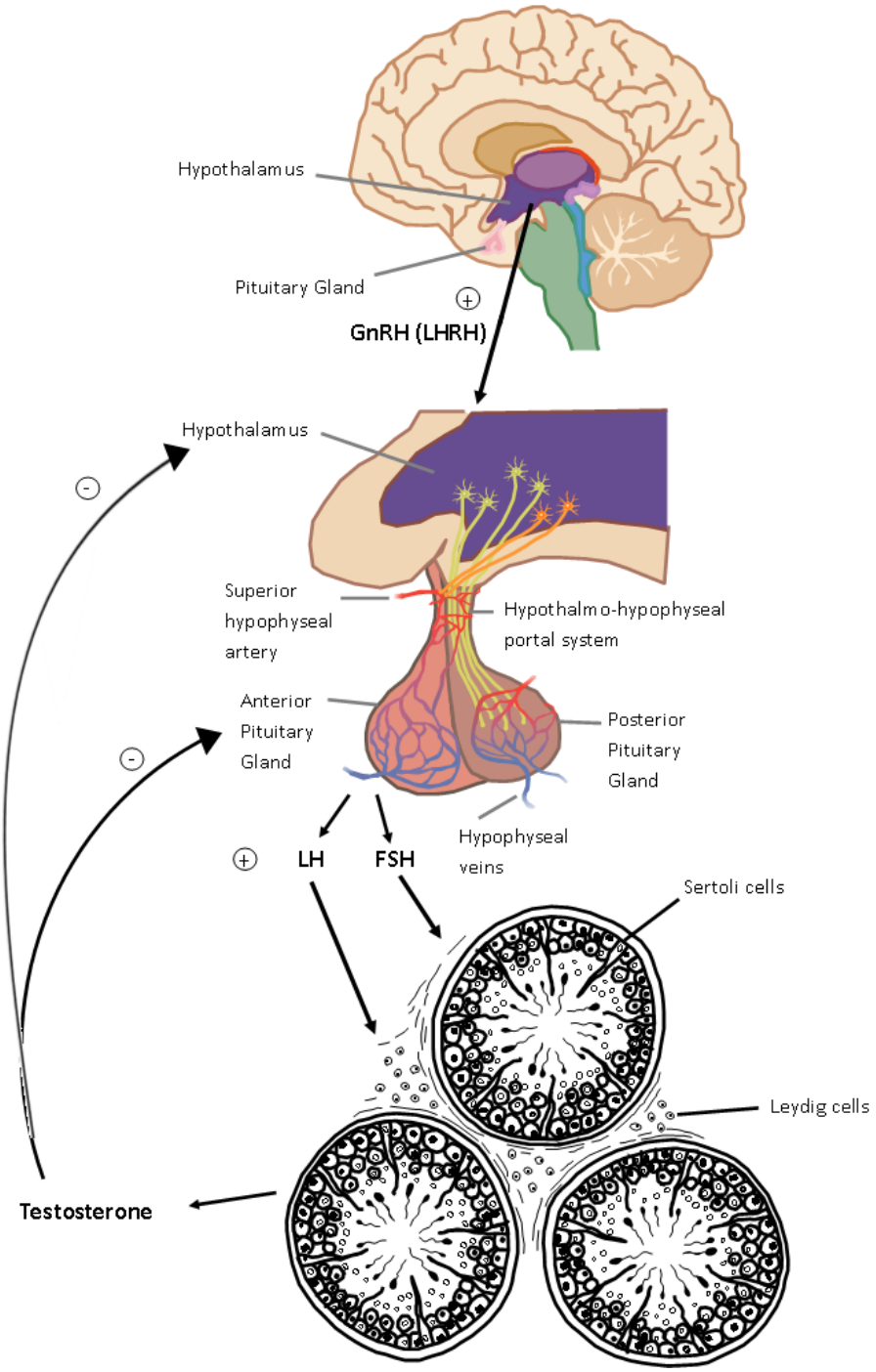

Figure 1.1.3. Schematic of the male hypothalamus-anterior pituitary gland axis. a. Gonadotropin releasing hormone (GnRH) is released from the hypothalamus and transported to the anterior pituitary gland via the hypophyseal portal system. The hypophyseal portal system is composed of blood vessels via which hormones are transported from the hypothalamus to the pituitary gland without entering the circulatory system. The presence of GnRH within the anterior pituitary gland leads to the release of luteinising hormone (LH) and follicle stimulating hormone (FSH) which both target Leydig and Sertoli cells within the testes respectively. This leads to testosterone release which instigates negative feedback activity at the level of both the anterior pituitary gland and the hypothalamus. Cross section of the testis shows Leydig cells are located within the interstitium.

1.1.3.2. Androgen Biosynthesis

Once LH binds its receptor on Leydig cells, androgens are converted from cholesterol via cyclic adenomonophosphate (cAMP) signalling. Cholesterol is produced *de novo* from acetic acid, found in intracellular cholesterol stores or sourced from low-density lipoproteins in the blood (Miller and Auchus, 2011). The innermost layer of the adrenal cortex, the zona reticularis, also acts as a source of weak androgens known as dehydroepiandrosterone (DHEA) and DHEA-sulphate (DHEAS) (Bird, 2012). There exist three pathways by which testosterone and dihydrotestosterone (DHT) can be synthesised. DHT is a more potent androgen which has a higher affinity for the AR than testosterone (Grossmann *et al.*, 2001). Known as the classical pathway, adrenal DHEA is altered by 3β-hydroxysteroid dehydrogenase (*HSD3B1*) to Δ^4-androstene-3. This acts as a substrate for reduction to testosterone via multiple 17β-hydroxysteroid dehydrogenase isoforms. Testosterone can then be reduced to DHT by 5α-reductase. This is also known as the delta-5 pathway (Mostaghel, 2013). This is thought to be the primary pathway in normal prostatic cells, though a previous study by Chang *et al*., (2011) demonstrated that this may not occur in CRPC cells and testosterone production is bypassed. This evasion of producing testosterone is known as the alternative pathway, whereby Δ^4-androstene-3, produced from the inactive precursor DHEA, is converted into 5α-androstane-3, 17-dione (adione) by 5α-reductase then subsequently into DHT (Chang *et al.*, 2011). Also, from cholesterol, pregnenolone is constructed into progesterone by 3β-hydroxysteroid dehydrogenase. By 5α-reductase, progesterone is converted into 5α-dihydroprogesterone, then into allopregnanolone via 3α-hydroxysteroid dehydrogenase. 17α-hydroxylase/17,29-lyase then converts it into androsterone which acts as a substrate for reduction by 17β-hydroxysteroid dehydrogenase into 3α-androstanediol. Subsequent oxidisation into DHT is carried out by 3α-hydroxysteroid dehydrogenase. This is known as the delta-4 pathway or “backdoor pathway” (Penning, 2014) (Figure 1.1.4).

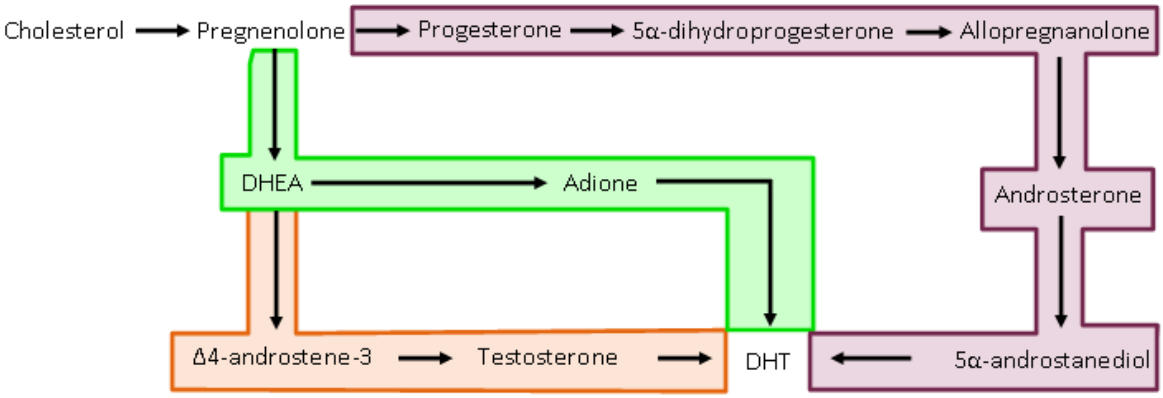

Figure 1.1.4: Testosterone biosynthesis pathway in Leydig cells. Testosterone is derived from cholesterol in one of three ways. The classical pathway is highlighted in orange, the "backdoor" pathway in purple and the alternative pathway in green. DHEA, dehydroepiandrosterone; DHEAS. DHEA-sulphate; DHT, dihydrotestosterone

Testosterone enters the circulation to affect target organs such as the bone (Mundy, 2002), lungs (Liu *et al.*, 2011) and liver as seen in mouse models (Soff *et al.*, 1995). The majority of testosterone is transported in circulation bound to carrier proteins such as albumin or sex hormone-binding globulin (SHBG) (Tan *et al.*, 2014). Testosterone bound to these proteins prevents diffusion and thus renders it inactive (de Ronde *et al.*, 2005). The free form of steroid hormones is bioactive and can diffuse directly into cells (de Ronde *et al.*, 2005; Tan *et al.*, 2014). Testosterone diffuses into the cell where it is often locally converted into dihydrotestosterone (DHT) by the enzyme 5α-reductase.

1.1.4 Prostate Diseases

Frequently, the prostate gland is subject to develop diseases such as prostatitis, benign prostatic hyperplasia (BPH), prostatic inflammatory atrophy (PIA), prostatic intraepithelial neoplasia (PIN) and prostate cancer (PCa), which can preclude a high quality of life for men of all ages.

1.1.4.1 Prostatitis

Prostatitis involves inflammation of the prostate and can occur at any age. Approximately 25% of men will be diagnosed with prostatitis within their lifetime. Typically, symptoms include voiding issues, pain and occasionally, sexual dysfunction. There are four types of prostatitis whereby two include acute and chronic bacterial pathogenesis from the urinary tract (less than 10% of cases). The remaining two are non-infectious and include chronic pelvic pain syndrome and asymptomatic inflammation. The non-infectious causes are not yet well understood (Lipsky *et al.*, 2010).

1.1.4.2 Benign Prostatic Hyperplasia

Benign prostatic hyperplasia (BPH) is a commonly occurring disease of ageing men which involves enlargement of the prostate gland. From histological dissection analyses, BPH can be evident from the age of 40 (Untergasser *et al.*, 2005). However, more than 50% of BPH incidence occurs between the ages of 51-60 and 90% by 85 years of age (Nickel *et al.*, 2011). Hyperplasia of prostatic glandular and stromal cells in the TZ surrounding the urethra is caused by DHT. This overgrowth often engenders urethral narrowing and eventual obstruction, consequently causing issues with micturition including hesitancy, weak flow and partial bladder voiding (Nickel *et al.*, 2011).

1.1.4.3 Prostatic Inflammatory Atrophy

It is well established that there is a close association between inflammation and carcinogenesis. Approximately a quarter of cancers are linked with inflammation. In prostatic inflammatory atrophy (PIA), inflammation causes amplified proliferation with no subsequent apoptosis in comparison with normal prostatic epithelia (Woenckhaus and Fenic, 2008). PIA affects the glands of the prostate, decreasing their volume. Two subsets of PIA patterns have been identified: focal and diffuse. Focal PIA occurs primarily in the PZ and affects the glands in patches, with proliferating cells surrounded by normal appearing tissue. Diffuse PIA is associated with a decrease in circulating androgens which affects the whole prostate simultaneously (De Marzo *et al.*, 2003). PIA commonly occurs in the PZ of the prostate and appears to be linked with PCa as these lesions can transition into malignant epithelia (De Marzo *et al.*, 2003). Therefore, it is thought that PIA could be a precursor for PCa.

1.1.4.4 Prostatic Intraepithelial Neoplasia

Prostatic intraepithelial neoplasia (PIN) is defined as novel epithelial growth which occurs within ducts or acini in the PZ of the prostate (Brawer, 2005). PIN can be graded from 1-3 whereby 1 has no link towards malignant behaviour whereas both grades 2 and 3 are known as high-grade PIN (HGPIN) which is associated with PCa (Joniau *et al.*, 2005). HGPIN is therefore thought of as an intermediate stage between benign and cancerous issue states. There is also evidence that PIA may act as a progenitor for PIN and consequently, PCa (Sciarra *et al.*, 2008).

1.1.4.5 Prostate Cancer and Risk Factors

1.1.4.5.1 Prostate Cancer

Prostate cancer (PCa) is the most frequently occurring malignancy in older men. Approximately 40,000 are diagnosed with this disease and more than 10,000 die each year in the United Kingdom alone (Schreiber *et al.*). Associated risk factors which cause men to be more susceptible to develop PCa include certain genetic stimuli, family history, ethnicity, age and diet (Lane *et al.*, 2017) whereby the penultimate has the greatest influence. PCa can occur within all zones of the prostate but the majority occur within the largest peripheral zone. Androgen hormone and its receptor are vital for prostate function and growth (Brooke and Bevan, 2009). Dysregulation and mutations in this essential steroid receptor are becoming frequently more associated with PCa development.

1.1.4.5.2 Prostate Cancer Risk Factors

1.1.4.5.2.1 Age

Age is a significant risk factor for the development of PCa whose intimate relationship could be explicated by the ageing population and slow growing tissue and thus disease development

(Abate-Shen and Shen, 2000). This means a tumour is more detectable with age. Another explanation involves diminished immunosurveillance, a mechanism by which abnormal tumour cells are detected by the immune system. Immune senescence augments with increasing age (Foster *et al.*, 2011). PCa occurrence is most frequently observed between the ages of 70-74. However, as incidence drops after 80 years of age, it highlights the complexity of underlying mechanisms as it does not follow the theory that immune senescence is linked to increasing cancer incidence. It is therefore thought that these older individuals age successfully without disease occurrence as they may have a genetic predisposition to a weaker inflammatory response (Foster *et al.*, 2011).

1.1.4.5.2.1 Genetics and Family History

There is strong evidence that genetic inheritance can predispose an individual towards developing PCa, especially those whose immediate family members have been diagnosed with the disease. Though, despite this knowledge and years of extensive, ongoing studies, it has continually proved challenging to identify penetrant PCa related genes. This is thought to be potentially due to the high proportion of patients with sporadic disease and genetic heterogeneity associated with PCa (Cooney, 2017). However, through genome-wide association studies, multiple single nucleotide repeats (SNPs) have been identified which can be associated with PCa risk and a subset linked to advanced metastatic PCa (Ahn *et al.*, 2011; Bao *et al.*, 2012; Xu *et al.*, 1998). Loci in which they can be located include 8q24, 17q as well as prostate relevant genes: KLK3, LMTK2 and MSMB (Di Lorenzo *et al.*, 2010; Haiman *et al.*, 2007). Rare mutations in *BRCA2* have also been found which add to risk of PCa development (Pritchard *et al.*, 2016) and also in noncoding DNA regions such as a promoter (Hua *et al.*, 2018). Although not strong evidence, genetic analysis of certain genes involved in the androgen synthesis pathway demonstrated the presence of certain SNPs puts individuals at a higher susceptibility to PCa (Cooney, 2017). To date, less than 100 genetic variants have been recognised which explains only a third of familial cases. However, some of these could

be tag SNPs which could “hide” other less common penetrant coding mutations (Cooney, 2017).

1.1.4.5.5.4 Ethnicity

It appears that high PCa risk and aggression is linked with short poly-Q (CAG) repeats within the N-terminal domain of the AR (Roney *et al.*, 2010). This short-length allele is found within different ethnicity groups, for example African-Americans have fewer CAG repeats compared with Asians. The AR with short-length poly-Q regions are thought to engage in overstimulated transcriptional activity due to its higher affinity with androgens, leading to increased cell proliferation (Nelson and Witte, 2002), potentially explaining their susceptibility to the disease. However, the tolerance of the CAG repeat length which is identified as “short” and “long” is varied and appears rather subjective (Nelson and Witte, 2002). In addition, the difference amongst ethnicities and PCa development is multifactorial and may also be linked to environment, diet, androgen levels and other genetic factors (Nelson and Witte, 2002).

1.1.4.5.5.5 Androgens

It is well known that androgens can influence PCa development. Both low or high serum androgens exposed long-term can increase likelihood of PCa. Banach-Petrosky *et al*. (2007), demonstrated low levels of androgen exposure over 7 months accelerated PCa development in Nkx3; Pten mutant mice (a transgenic model of PCa) in comparison to those exposed to normal-range and castrated levels (Banach-Petrosky *et al.*, 2007). They suggested this may be due to advantageous genetic selections which promotes tumorigenic survival in these conditions, for example an increase in AR and potentially AR co-factor expression (Zhou *et al.*, 2015). As androgen levels decrease with as men get older, this mechanism could be related to PCa incidence and age. High androgen serum levels would suggest an overstimulation of the AR leading to PCa. However, this could be inconsistent as serum levels

of androgens, sub- or supraphysiological, do not reflect those in the prostatic microenvironment (Zhou *et al.*, 2015).

1.1.4.5.5.6 Endocrine Disruptor Compounds

There are other environmental factors which pose a minor increased risk of developing PCa. These include endocrine disruptor compounds, sexually transmitted diseases and smoking. Humans are exposed to a plethora of chemicals within their daily environment and diet. Some agents have hormone-like properties and can interfere with endocrine biosynthesis and signalling, giving rise to development and reproductive system abnormalities (Diamanti-Kandarakis *et al.*, 2009). Examples of endocrine disruptors include dichlorodiphenyltrichloroethane (DDT) in pesticides, bisphenol A (BPA) in plastics and phytoestrogens in natural plant products such as soy (Hess-Wilson and Knudsen, 2006). Endocrine disruptors can exert their effects via NRs (Diamanti-Kandarakis *et al.*, 2009). Of note, mutant AR (AR-T877A) found frequently in CRPC patients can be activated by BPA in the absence of androgens (Wetherill *et al.*, 2005).

1.1.4.6 Castrate-Resistant Prostate Cancer

Initially, patients with early stage PCa will respond to treatment, their tumour is known to be hormone-sensitive, however, 10-20 % of tumours can develop resistance to the lack of hormone presence as well as antiandrogens (Brooke *et al.*, 2015; Kirby *et al.*, 2011). This advanced stage of the disease is known as castrate-resistant prostate cancer (CRPC) whereby relapse is highly aggressive and lethal for the patient as well as incurable. Prostate Specific Antigen (PSA) (section 1.1.7) levels are closely monitored in patients undergoing treatment therefore CRPC is diagnosed when there is a continuous rise of PSA in serum despite the patient undergoing androgen deprivation therapy (ADT) (section 1.1.9) (Hotte and Saad, 2010). The time by which an androgen-sensitive tumour develops into CRPC is

approximately 2 years (Moeller *et al.*, 2018). Unfortunately, therapeutics which inhibit testosterone do not target adrenal glands, and thus weak androgens remain in circulation which possibly could stimulate PCa cells and aid disease progression. One such mechanism proposed for castrate-resistance is *de novo* synthesis of androgens. Multiple research groups have demonstrated that despite castration, intracellular levels of androgens are still at sufficient levels to activate WT AR (Zhou *et al.*, 2015). There is also evidence of amplification of the *AR.* As a result, present efforts are focussed into understanding mechanisms by which a high-grade tumour can become resistant to ADT as well as the identification of novel PCa therapeutic strategies through targeting the AR.

1.1.5 Androgen Receptor Mutations in Prostate Cancer

Altered AR activity has been associated with both PCa and CRPC. This has been potentially correlated with somatic and germline genetic mutations as well as gene duplication (Koochekpour, 2010). Several point mutations such as missense, silent, deletion and insertion (positioned within coding regions) have been demonstrated by Jiang *et al.*, 2010. They used circulating tumour cells from 35 patients with advanced PCa and found that 57% of the patients acquired point mutations (Jiang *et al.*, 2010). Point mutations can lead to promiscuous ligand and co-factor binding (Brooke and Bevan, 2009). Generally, AR mutations can lead to hypersensitive AR, gene overexpression and promiscuous ligand binding (Koochekpour, 2010).

1.1.6 Androgen Receptor Splice Variants

Alternative mRNA splicing of the AR leads to a truncated protein, frequently at the carboxy terminus. These mutants remain constitutively transcriptionally active despite lacking the LBD. These are known as AR splice variants (AR-V) of which multiple occur. The most common splice variant seen in driving CRPC disease progression is AR-V7 (Figure 1.1.5). AR-Vs can

arise from stop codons within transcribed intronic regions, namely, cryptic exons (Lu and Luo, 2013). A ligand-independent transcription factor develops resistance to ADT and is thought to have implications in CRPC due to its frequent expression at this metastatic stage of the disease (Li *et al.*, 2013). Splice variants are always found in the presence of fully transcribed AR but never alone.

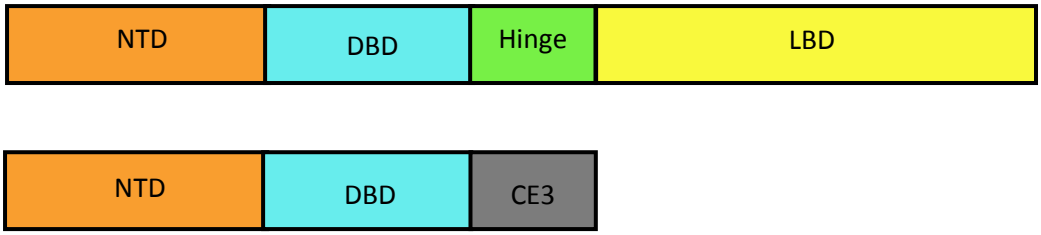

Figure 1.1.5: Androgen receptor slice variant Androgen Receptor-Variant 7 (AR-V7). Known structure of both androgen receptor (AR) full length (Top) and AR-V7 (Bottom). C, C-terminal domain; CE3, Cryptic exon 3; DBD, DNA binding domain; LBD, ligand binding domain; NTD, N-terminal domain,

1.1.7 Prostate Specific Antigen

Prostate specific antigen (PSA) is a 33 kDa serine protease produced by predominantly by epithelial cells of the prostate. PSA is an essential component of seminal fluid where its role is required for liquefication of coagulate (Stephan, 2011). PSA is produced only in prostatic tissue, but it is not solely related to the presence of PCa as it is also elevated in hyperplasia, prostatitis and inflammation. PSA presence in the blood can aid PCa diagnosis

1.1.8 Gleason Grading System

The Gleason Grading system was developed in the 1960's-1970's. It is based on PCa tissue features at different stages of the disease observed using haematoxylin and eosin tumour histology slices and a score from 1-10 (Chen and Zhou, 2016). Patterns differ dramatically as PCa progresses, which is reflected in the number i.e. the higher the pattern number, the poorer the prognosis for the patient. For example, a ranking of 1 indicates uniform, distinct gland structure and a score of 5 states that glands are fused (Chen and Zhou, 2016) (Figure 1.1.6). Due to identification of novel growth pattern variations and a change in needle biopsy techniques, the Gleason System was altered in 2005 to incorporate these factors. Indeed, biopsies were taken from multiple sites which frequently contained different Gleason Patterns. Therefore, primary and secondary (most and second common) patterns were combined to give a new score (e.g. 5 + 4 = 9). This system also no longer assigned patients with a total Gleason score of less than 6, as the grade was frequently higher at surgery (Gordetsky and Epstein, 2016). Again, this system was revised in 2014 and adopted by the World Health Organisation in 2016 due to continued confusion surrounding the scores given to patients. For instance, a score of 7 (i.e. 3 + 4 = 7 and 4 + 3 = 7) are not homogenous, with the latter engendering a much worse prognosis (Berney *et al.*, 2016). Therefore, based on Gleason patterns and scores, the current Prognostic Group system was created to provide patients with a clearer understanding of disease outcome and to avoid misperception. The five groups,

numbered I to V (whereby I refers to Gleason score 6), aims to reduce fear and overtreatment of low-grade tumours by more accurately discriminating between prognostics.

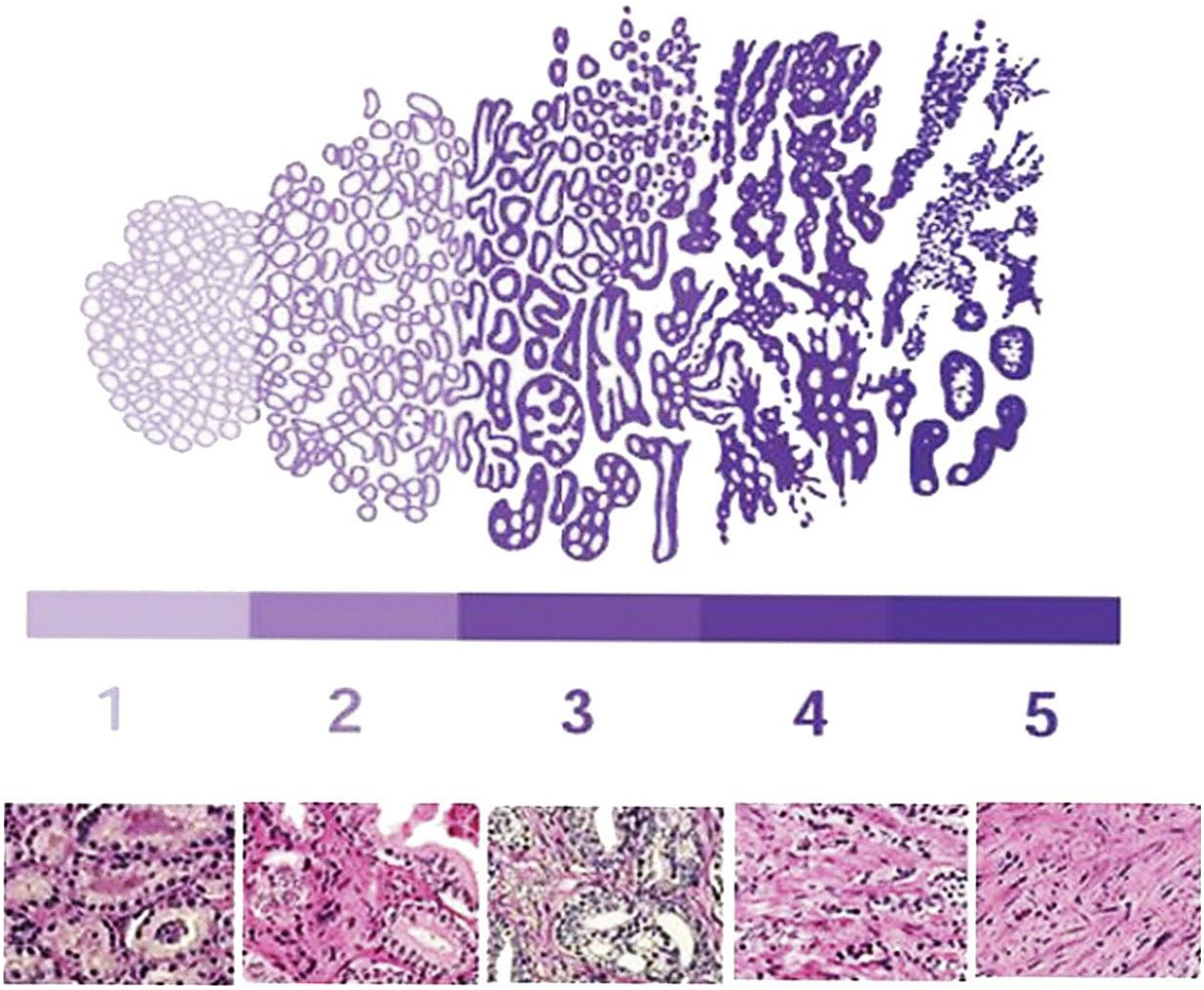

Figure 1.1.6: Gleason grading system schematic for prostate cancer. The numbers represent the Gleason score with 5 being a worse diagnosis. Uniform distinct glands fuse as prostate cancer disease progresses (Harnden *et al.*, 2007)

1.1.9 Current Prostate Cancer Therapies and Surveillance

For PCa detection, often the preferred routine methods involved a digital rectal examination and a PSA check. However, it is thought that this method is not accurate as detection of prostatic irregularities differed greatly between assessors (Zheng *et al.*, 2012). Additionally, the correct determination of PCa stage in the patient is essential for disease management. Thus ultrasound and magnetic resonance imaging can also be used for diagnosis (de Rooij *et al.*, 2016). Men diagnosed with localised, slow-growing PCa are not always treated instantaneously and treatment options are dependent upon the patients' health, the Gleason grade and presence of metastasis. Multiple management strategies are in place which monitor tumour progression including active surveillance and watchful waiting. Men are placed onto these programmes when their cancer is localised and slow growing to avoid unnecessary treatment, thus circumventing any unpleasant side effects (Prostate Cancer UK, 2019). When required, there are multiple therapies available to men with PCa which aim to both control and/or cure the cancer. Treatments include prostatectomy, cryotherapy (freezing of tumour cells), radiation, chemotherapy and brachytherapy (radioactive source planted directly into the tumour). The way by which the patient is treated is dependent upon their suitability for surgery, i.e. health and/or age. If the disease progresses further to a localised, organ-confined advanced PCa or a metastatic CRPC stage, treatment switches to either physical or chemical castration and antiandrogens, (Evans, 2018). Chemical castration is a type of hormone therapy which involves the use of luteinising hormone releasing hormone (LHRH) analogues to block androgen production via the hypothalamus-pituitary-gonadal axis (Kluth *et al.*, 2014). Initially, this treatment promotes a spike in LH levels followed by a surge in testosterone for 1-2 weeks after introducing treatment. This may aid cellular growth and thus further PCa progression in patients within this time (Kluth *et al.*, 2014). Although administration is continuous, along with the risk of worsened disease within this 1-2 week period, LHRH analogues are frequently still the preferred option. It is reversible, as effective as physical

castration and prevents any detrimental psychological issues associated with orchiectomy (Kluth *et al.*, 2014).

Testosterone is produced in both the testes and the adrenal glands (90-95% and 5-10% respectively) (Perlmutter and Lepor, 2007). LHRH agonists supress testosterone production within the testes but do not affect adrenal androgen precursor production which can be converted into testosterone and DHT by prostatic cells. Antiandrogens block AR signalling by directly binding to the AR. ADT was therefore often combined with antiandrogens, together to function as a maximal androgen blockade (MAB) (Perlmutter and Lepor, 2007). However, it has been shown that LHRH therapies without use of a MAB treatment are just as efficient as LHRH inhibitor combined with antiandrogens with fewer side effects, so this method is no longer necessary (Cheng *et al.*, 2017). However, eventually hormone therapeutics fail as cancers become androgen-independent. Enzalutamide is dispensed to patients at this advanced stage as it competitively binds to the AR at the ligand binding domain. This drug inhibits AR translocation and DNA binding as well as blocking recruitment of its co-regulators (Beer *et al.*, 2014). Also used is a cytochrome p450 (*CYP17A1*) enzyme inhibitor: Abiraterone. This enzyme is involved in the production of androgens (Petrunak *et al.*, 2014). Therefore, this inhibitor can block any *de novo* androgen production leading to apoptosis (Dueregger *et al.*, 2014).

1.2 The Androgen Receptor

1.2.1 The Androgen Receptor and its Structure

Nuclear receptors are one of the most abundant superfamilies of proteins which currently consists of 48 members (Burris *et al.*, 2012; Robinson-Rechavi *et al.*, 2003). Steroid receptors (SRs) are a subclass of nuclear receptors (NRs) to which the AR belongs. SRs are transcription factors (TFs) which are activated upon ligand binding (Burris *et al*, 2013). The *AR* gene is localised on chromosome Xq11-12 and encodes a protein of 110 kDa. This

receptor plays vital roles in cellular proliferation and differentiation which is especially important in male reproductive organ development and survival throughout a man's lifetime (Burris *et al.*, 2012). AR structure consists of four main domains: The N-terminal domain (NTD), DNA-binding domain (DBD), hinge region and the ligand-binding domain (LBD) (Brooke and Bevan, 2009) (Figure 1.1.7).

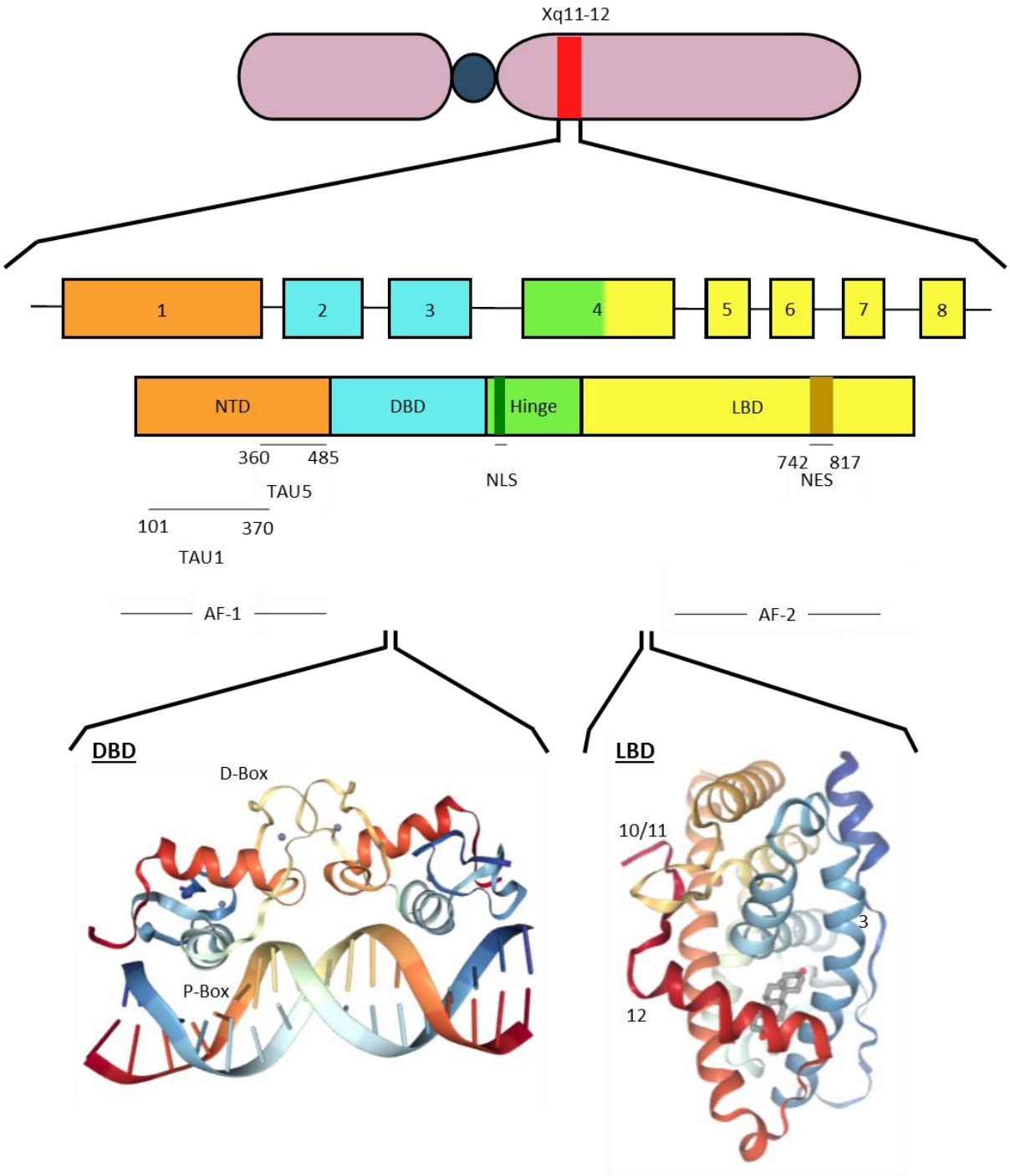

Figure 1.1.7: Schematic of *Androgen Receptor* gene and protein structure. a. The *androgen receptor* is located on the X chromosome at position q11-12. b. The *androgen receptor* consists of 8 exons. c. Structure of the androgen receptor protein which contains 4 main domains: The N-terminal domain, DNA binding domain, the hinge domain and ligand binding domain, The N-terminal domain contains activation function 1 which consists of TAU 1 and TAU 5. The hinge region contains the nuclear localisation sequence and the ligand binding domain contains the nuclear export sequence. Crystallography images were generated using PDB. DBD and LBD codes were 1R4I and 4OEA respectively. AF-1, activation function-1; NES, nuclear export sequence; NLS, nuclear localisation sequence; NTD, N-terminal domain; DBD, DNA binding domain, LBD, ligand binding domain; Tau, Transactivation unit.

1.2.1.1 The N-terminal Domain

The NTD is an intrinsically disordered region of the AR which contains the modular activation function-1 (AF-1). AF-1 consists of two distinct transactivation units (TAU), TAU1 (101-360 amino acids) and TAU5 (370-494 amino acids) (Bevan *et al.*, 1999; Heemers and Tindall, 2007) (Figure 1.1.7). The majority of AR activity occurs via these motifs (van der Steen *et al.*, 2013). Flexibility within the NTD is essential for AR activity as it is required for protein interactions (Myung *et al.*, 2013). The NTD has high polymorphic variability and a diverse number of CAG (glutamine, Q) repeats within exon 1 has been identified (Nelson and Witte, 2002). This is thought to be associated with PCa risk (Section 1.1.5.5.2). The NTD can also bind to the LBD and other AR co-factors which facilitates transcription initiation via AF-1 (Pietri *et al.*, 2016).

1.2.1.2 DNA-Binding Domain

The DBD (coded by exons 2 and 3) (Figure 1.1.7) is the most highly conserved region of SRs, consisting of approximately 80 amino acid residues (Claessens *et al.*, 2008). It contains two zinc fingers that both comprise specialised, distinct motifs which co-ordinate and bind to the major groove of DNA at target sites. One finger contains the proximal box (P-box) region which recognises the androgen response element (ARE) and the other contains a distal box (D-box) region which mediates and stabilises DNA binding (Pietri *et al.*, 2016). AREs contain hexameric inverted repeats which lie on the same strand. These are separated by a distinct three base pair spacer known as IR3 (Shaffer *et al.*, 2004). There are also specific response elements which are unique to the AR. The ARE is a motif found within promotors or enhancers of AR targeted genes (Wilson *et al.*, 2016). Indeed, IR3 in the AR is known as ADR3 which distinguishes the ARE from other steroid receptor response elements. This consequently allows definitive gene activation and prevents unambiguous, nonspecific binding with other response elements (Shaffer *et al.*, 2004).

1.2.1.3 The Hinge Region

The hinge region (exon 4) acts as a flexible bridge which connects the DBD and LBD (Figure 1.7). It contains a nuclear localisation sequence (NLS) that allows its passage into the nucleus via importin α (Claessens *et al.*, 2008) (Figure 1.1.7). It can undergo posttranslational modifications such as acetylation and methylation to further control AR activation/inhibition respectively (van der Steen *et al.*, 2013).

1.2.1.4 The Ligand Binding Domain

At the carboxyl terminus of the AR, the LBD (exons 4-8) interacts with specific steroidal ligands known as androgens, namely, testosterone and DHT (Figure 1.1.7). There are eleven α-helices and four short β-sheets which together form the LBD tertiary structure (Tan *et al.*, 2014). The LBD contains two essential surfaces that interact with AR co-factors: activation function-2 (AF-2) and binding function-3 (BF-3), as well as a ligand binding pocket (Nadal *et al*, 2016). It is thought that co-activator interactions with AF-2 are regulated by BF-3 (Nadal *et al.*, 2017). AF-2 facilitates transcriptional activity of the AR via interactions with co-factors (Pietri *et al.*, 2016; Tan *et al.*, 2014). Maximum steroid receptor activity commonly requires synergistic co-operation between AF-1 and AF-2, albeit they can function independently. This co-operation occurs via direct amino/carboxy terminal interactions or by binding of co-factors, individually or simultaneously, to either activation functions (Kumar and McEwan, 2012). A nuclear export signal is also found in this region (amino acids 742-817) (Figure 1.1.7).

1.2.2 Androgen Receptor Signalling Cascade

The AR is located within the cytoplasm, bound to a complex of proteins which maintain it in an inactive state while also holding the receptor in the correct conformation for high affinity ligand binding (Brooke and Bevan, 2009; De Leon *et al.*, 2011; Massard and Fizazi, 2011)

(Figure 1.1.8). Some principal proteins include co-chaperone heat-shock proteins (HSP): HSP90, HSP70 and HSP56 (De Leon *et al.*, 2011). Upon ligand binding, these HSPs dissociate, the AR homodimerize, and is phosphorylated. Posttranslational modifications occur throughout the signalling cascade. For example, phosphorylation at residue S81 (NTD) in response to hormone presence retains the AR in the nucleus and prevents degradation (Koryakina *et al.*, 2014). The phosphorylated homodimer translocates into the nucleus where it interacts with an array of co-factors (co-repressors and co-activators) and its AREs to orchestrate target gene transcription and regulation, promoting proliferation and repressing apoptosis (Sukocheva *et al.*, 2015) (Figure 1.1.8).

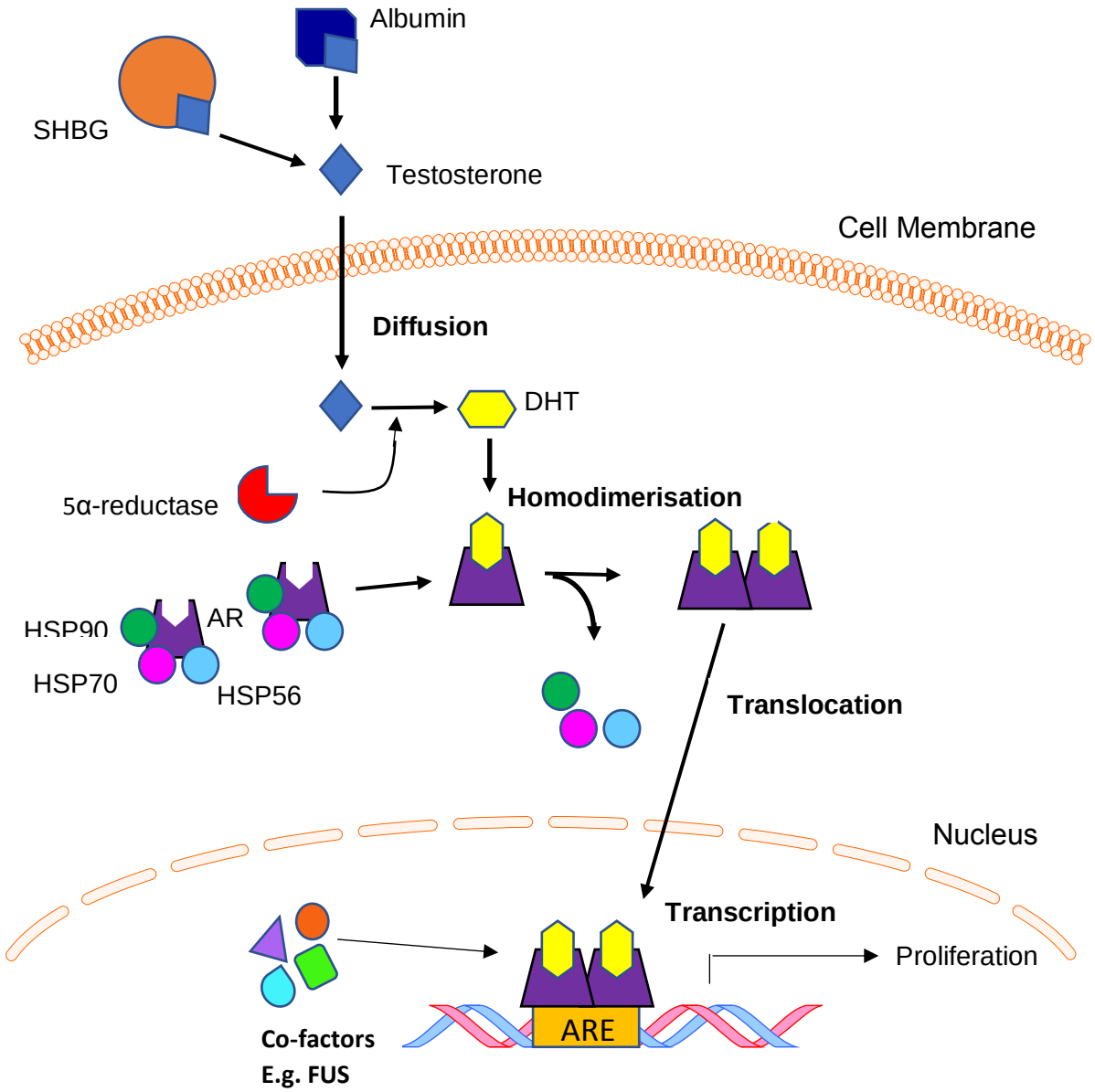

Figure 1.1.8: Schematic of the Androgen Receptor signalling cascade. Testosterone is released from its chaperone either albumin or sex hormone binding-globulin (SHBG) and diffuses into its target cell. Testosterone is converted into dihydrotestosterone (DHT) by 5α-reductase. The cytoplasmic androgen receptor (AR) is held in the correct conformation for ligand binding by heat shock proteins (HSPs), namely HSP90, HSP70 and HSP56. DHT binds to the receptor and HSPs dissociate. ARs homodimerize and translocate into the nucleus where they bind specific regions of DNA known as androgen response elements (AREs). AR target genes are transcribed leading to proliferation and cell survival. AR activity is regulated by co-factors e.g. Fused in Sarcoma (FUS) which can act to co-activate/co-repress transcription.

1.2.3 Androgen Receptor Co-factors

Co-factor proteins can interact either directly or within a complex to alter transcriptional activity, namely via promotion (co-activators) or inhibition (co-repressors) of receptor activity (Edwards and Bartlett, 2005). It is thought that the former type of co-regulator has implications in CRPC and can act as drug targets for PCa (Chang and McDonnell, 2005).

1.2.3.1 Androgen Receptor Co-activators

Co-activators interact with the AR to promote and enhance its activity. They can alter C and NTDs and frequently possess or are able to recruit proteins with histone acetyltransferase (HAT) activity, aiding transcriptional activation by relaxing heterochromatin arrangements. The first described co-activators of SRs belong to the p160 family, one of which includes SRC-1/NCoA-1 (Meijer *et al.*, 2000). Many SRC proteins can interact with the AR via its NTD or LBD mediated by LXXLL motifs (otherwise known as the N-box) only in the presence of ligand (Dubbink *et al.*, 2004). Other co-activators include AR-associated proteins ARA70, ARA55 and ARA54 (Grossmann *et al.*, 2001) and cyclic adenosine monophosphate (cAMP) response element-binding protein-binding protein (CREB) binding protein (CBP). CBP possesses HAT activity and acts as a docking site for other transcriptional proteins, bridging them with AR-bound DNA (Heemers and Tindall, 2007). In addition, Haile *et al.*, (2011) demonstrated that a protein known as Fused in Sarcoma (FUS) can act as a co-activator of the AR by binding via its DBD.

1.2.3.2 Androgen Receptor Co-repressors

Co-repressors act as suppressors of AR-mediated gene transcription whose mechanism of action is just as varied as co-activators. Mechanisms include chromatin modifications via histone deacetylase (HDAC) activity consequently arranging DNA more tightly, modification

of C/NTD interactions, blocking co-activator binding or blocking either AR translocation into the nucleus or preventing AR-DNA interactions (Burd *et al.*, 2006) (Figure 1.1.9). Moreover, FUS has been identified as a co-repressor of the AR (Brooke *et al.,* Unpub.*)*.

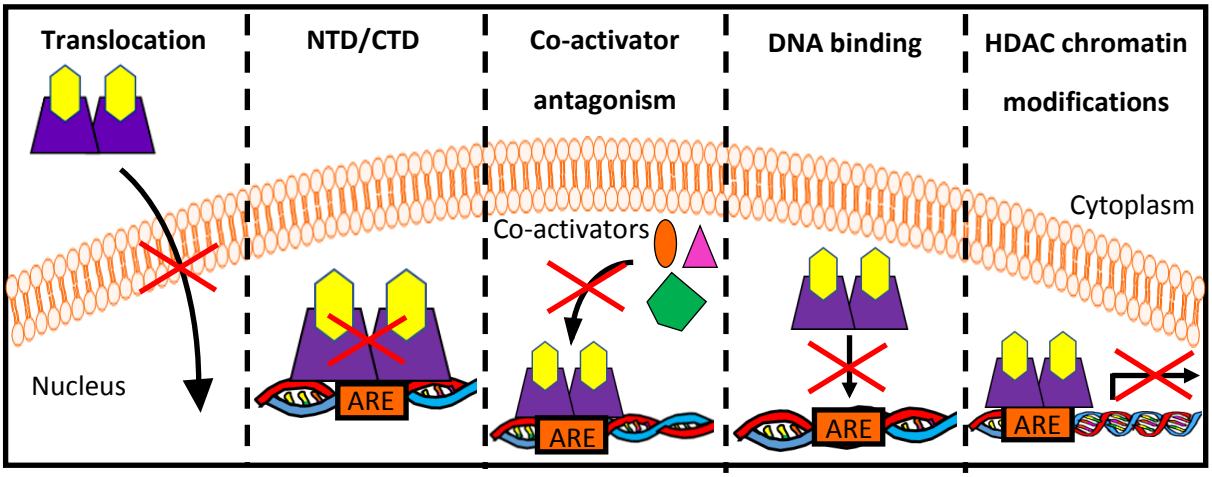

Figure 1.1.9 Androgen Receptor co-repressor mechanisms. In prostatic tissues, androgen receptor signalling can be repressed for a variety of reasons through multiple different mechanisms. These mechanisms include preventing translocation from the cytoplasm to the nucleus, interference of N-terminal domain and C-terminal domain interactions, competition with co-activators, prevention of DNA binding and modifying DNA into heterochromatin using histone deacetylase (HDAC) enzymes to thwart transcription. ARE, androgen response element.

1.3 Fused in Sarcoma

1.3.1 Fused in Sarcoma and its Structure

FUS (also known as Translocated in Liposarcoma (TLS)) is a member of the FET/TET family of RNA binding proteins which comprises FUS/TLS, Ewings sarcoma (EWS) and TATA-binding protein-associated factor (TAF) due to their structural similarities (Chau *et al.*, 2016). FUS is expressed ubiquitously and is primarily located in the nucleus, though mutants can accumulate within the cytoplasm (Lagier-Tourenne and Cleveland, 2009). This is well-known to occur in Amytrophic Lateral Sclerosis leading to motor neuron degeneration (Ederle and Dormann, 2017). FUS is involved in multiple cellular processes such as gene expression, for example splicing and transcriptional regulation (Dormann *et al.*, 2010). The multifunctional FUS protein has been seen to bind to RNA (Zinszner *et al.*, 1997), DNA (Tan *et al.*, 2012) and proteins (Haile *et al.*, 2011). FUS was first discovered in a malignant myoxoid liposarcoma within an oncogenic fusion protein complex with CCAT-enhancer-binding homologous protein (CHOP) (Rabbitts *et al.*, 1993). Translocations between chromosome 12 and 16 is responsible for the formation of this chimera (Rabbitts *et al.*, 1993). FUS is encoded by the *FUS* gene located on chromosome 16p11 and is made up of 15 exons totalling 526 amino acids giving a molecular weight of 75 kDa (Baechtold *et al.*, 1999; Lashley *et al.*, 2011; Rabbitts *et al.*, 1993). It characterises multiple domains such as a serine, tyrosine, glutamine and glycine (SYQG) rich NTD, three tripeptide repeat arginine-glycine-glycine rich regions (RGG), an RNA recognition motif (RRM), a cysteine2/cysteine2 zinc finger motif at the C-terminus and a very conserved C-terminal domain (CTD) extreme (Ederle and Dormann, 2017; Lagier-Tourenne and Cleveland, 2009) (Figure 1.1.10). The SYQG, RRM and zinc finger domains are linked via a flexible linker (Iko *et al.*, 2004).

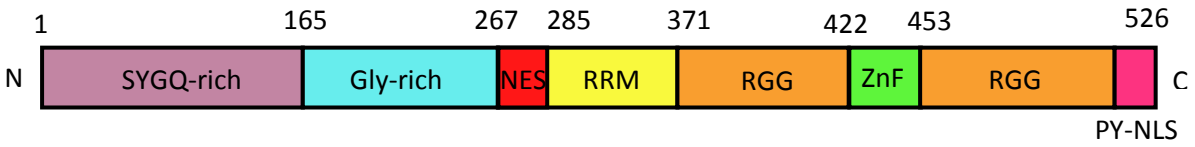

Figure 1.1.10: Schematic of Fused in Sarcoma domain structure. The N-terminal domain contains the serine, tyrosine, glycine and glutamine (SYGQ) (amino acids 1-165) rich region which plays roles in transcriptional activation, a glycine rich region (amino acids 165 - 267), an RNA recognition motif (RRM) (amino acids 285 - 371) that contains a nuclear export signal (NES) (amino acids 267 - 285) within its domain, a zinc finger (ZnF) (amino acids 422 - 453) flanked by two arginine, glycine, glycine (RGG) trinucleotide repeats (amino acids 371 – 422 and 453 – 526) all important in RNA binding and finally the C-terminal domain contains a proline-tyrosine nuclear localisation sequence (PY-NLS) essential for nuclear import (adapted from (Dormann *et al.*, 2010)). Amino acid numbers taken from (Ozdilek *et al.*, 2017)

1.3.1.1 The Serine, Tyrosine, Glutamine and Glycine (SYQG) Rich Region

The NTD domain consists of 165 amino acids and is thought to be intrinsically disordered (Monahan *et al.*, 2017; Yang *et al.*, 2014). Mutations within this domain can instigate aggregation, consequently giving rise to proteinopathies. Serine, tyrosine, glutamine and glycine constitute approximately 80% of the NTD (Yang *et al.*, 2014). Through the formation of truncated FUS constructs, Yang *et al*, 2014 demonstrated that the SYQG region mediates chromatin binding. Additionally, they showed that chromatin binding and therefore the SYQG rich region was also essential in transcriptional activation which agrees with previous studies which stated that FUS is able to regulate gene transcription (Dhar *et al.*, 2014; Tan *et al.*, 2012). A possible mechanism of protein expression regulation by FUS is via the potential presence of FUS response elements in the promoter regions of FUS targeted genes in single stranded DNA motifs (Tan *et al.*, 2012). Chromatin binding may be facilitated by zinc fingers and the RRM (Yang *et al.*, 2014).

1.3.1.2 Glycine and Arginine-Glycine-Glycine Rich Regions

The Glycine and RGG rich regions (also known as an RGG box) flank the RRM and are predicted to be unstructured. RGG boxes are often targets for arginine methylation which appears to alter the ability to form hydrogen bonds with RNA targets (Dammer *et al.*, 2012). RGG boxes are responsible for both RNA and protein-protein interactions. A recent study by (Ozdilek *et al.*, 2017) demonstrated that FUS appears to mediate RNA interactions via its RGG box as opposed to its well folded RRM and zinc fingers.

1.3.1.3 The RNA Recognition Motif

The RRM is a common domain required for nucleic acid binding in eukaryotes. FUS contains a KK loop which is not present in most RRMs which commonly contain positively charged and

aromatic amino acids instead. These conserved lysine residues are essential in DNA/RNA binding along with other positively charged residues (Liu *et al.*, 2013). Liu *et al.*, 2013, also demonstrated that mutating the KK loop significantly altered the ability of FUS to bind to nucleic acids. A study by Zinszner *et al*., (1997) showed that FUS can undergo nucleo-cytoplasmic shuttling which occurs via a nuclear export sequence (NES) and acting as an RNA chaperone. The NES is located within the RRM (Yamashita *et al*., 2012). The zinc finger, together with the RRM and RGG rich domains appear to be responsible for binding to DNA/RNA (Liu *et al.*, 2013).

1.3.1.4 Extreme C-terminal Domain

The extreme CTD contains the essential nuclear localisation sequence (NLS) on exon 15 (Yamashita *et al.*, 2012). Mutations within these regions can cause FUS accumulation in the cytoplasm, acting as a FUSopathy i.e. a disease caused by aggregation of FUS protein (Liu *et al.*, 2013). The NLS, more specifically known as a proline and tyrosine NLS (PY-NLS), is essential for FUS nuclear transport by transportin (Dormann *et al.*, 2010). FUS lacking a CTD was not transported into the nucleus (Dormann *et al.*, 2010; Zinszner *et al.*, 1997).

1.3.2 Fused in Sarcoma in Prostate Cancer

FUS has implications in several cancers, including PCa. In 2011, Brooke *et al*. suggested that FUS can act as a tumour suppressor due to its role in cyclin D1 regulation and apoptosis. Indeed, they demonstrated that patients were less likely to have tumour metastasis and had better prognosis if FUS was highly expressed and that low FUS levels may aid tumour progression (Brooke *et al.*, 2011). They also state that there is an inverse correlation of FUS levels with Gleason grade. However, later that year, Haile *et al.,* (2011) challenged these findings by demonstrating that transcriptional activity of the AR increased upon FUS overexpression and that when FUS levels were depleted via knockdown experiments, LnCAP

cell proliferation also decreased. They concluded that FUS acts as a co-activator of the AR in PCa. It is predicted that perhaps FUS can indeed function as both types of co-factor in AR regulation depending upon the stage of PCa. In unpublished findings by Brooke *et al.*, they showed, in patient tumour samples, a rekindling of FUS expression in high grade tumours. This means that in advanced PCa, FUS could be acting as a co-activator thus aiding tumour progression due to potential promiscuous mutations of the AR or alterations in FUS regulatory effects.

1.4 Long Noncoding RNA

1.4.1 Long Noncoding RNA and its Formation

Not only do co-factors interact with nuclear receptors, lncRNA can also interact and regulate their activity (Gutschner and Diederichs, 2012). The majority of DNA within the human genome is transcribed (85%) (Fang and Fullwood, 2016), less than 2 % encodes for exons which engender proteins (Bhat *et al.*, 2016). The prevalence of noncoding regions within DNA is essential for cellular functions and processes. Noncoding RNA can be divided into two distinct groups: small (sncRNA) and long (lncRNA). sncRNAs, some of which include micro RNA, small interfering RNA and piwi-interacting RNA, are powerful regulators of gene expression (Choudhuri, 2010). LncRNAs are described as transcripts, 200 nucleotides or longer, which include antisense, intergenic and enhancer RNAs (Boon *et al*., 2016). These transcripts also play essential, diverse roles in epigenetics and gene expression. For example, mRNA splicing, chromatin remodelling as well as potentially modifying protein synthesis by acting as microRNA sponges (Ding *et al.*, 2017; Michalik *et al.*, 2014). Examples of lncRNA include Hox Transcription Antisense Intergenic RNA (HOTAIR) and Nuclear Enriched Abundant Transcript 1 (NEAT1) (Boon *et al.*, 2016). LncRNAs are processed like messenger RNA as they are transcribed by RNA polymerase II, mostly contain polyadenylated tails, a 5' 7-methylguanosine (m^7G) cap and are spliced (Geisler *et al.*, 2012; Guttman *et al.*, 2009).

Polymerase II recognises conserved promoter loci at histone 3 with a trimethylated lysine (H3K4me3) (Guttman *et al.*, 2009). Certain lncRNA also appear to be tissue specific, such as BC200 associated with brain tissue and Prostate Cancer Associated 3 (PCA3) in PCa (Gibb *et al.*, 2011; Misawa *et al.*, 2017).

1.4.2 Long Noncoding RNA has Implications in Cancer

Due to the essential roles multifunctional lncRNA transcripts play throughout the body, aberrant function and expression of lncRNA can have implications in cancer development and progression (Gibb *et al.*, 2011). The first lncRNA linked with cancer was PCA3 and prostate-specific transcript 1 (PCGEM1) due to their anomalous expression, with the former currently used as a PCa biomarker. NEAT2 (also known as metastasis-associated lung adenocarcinoma transcript 1, MALAT1) appears to play a role in the proliferation of breast, colon and hepatocellular cancer, though its precise role is yet to be fully elucidated (Huarte, 2015). LncRNA can be either overexpressed or inhibited to aid tumour progression depending upon its role within the cell. For instance, PR-lncRNA-1 promotes apoptosis and is thus downregulated in colorectal cancer, whereas Antisense Noncoding RNA in the INK4 Locus (ANRIL) is upregulated in PCa as it stimulates cell proliferation (Huarte, 2015). LncRNA expression can also be altered as a result of amplification or deletion. For example, Focally Amplified Long noncoding RNA in Epithelial Cancers (FALEC) acts as an oncogene by repressing expression of a cell cycle inhibitor and hence is frequently found to be amplified in epithelial cancers (Huarte, 2015). Examples of lncRNAs in cancer can be seen in table 1.

1.4.2.1 Hox Transcript Antisense Intergenic RNA Regulates Androgen Receptor Activity

HOTAIR is localised on chromosome 12q13.13 amongst the *HOXC* gene locus, accounting for around 2.2 Kb of this region. This lncRNA plays essential roles in recruitment of specific proteins required for histone modification, acting as a scaffold for protein docking as well as

acting as a microRNA sponge (Bhat *et al.*, 2016; Ding *et al.*, 2017). Dysregulation of these essential processes can give rise to tumorigenesis. HOTAIR was one of the first lncRNAs associated with cancer metastasis. In breast cancer, for example, this lncRNA is associated with metastasis and poor survival rates and has been found to be overexpressed up to 2000 fold compared with normal breast tissue (Gupta *et al.*, 2010). Gupta *et al*., (2010) also demonstrated that direct HOTAIR injections into murine mammary fat pads with severe combined immunodeficiency moderately augmented primary tumour growth.

HOTAIR can interact with and regulate AR activity, especially in advanced PCa (Chu *et al.*, 2012). It binds to the AR NTD and blocks E3 ubiquitin ligase interaction consequently preventing degradation, enhancing AR activity. HOTAIR overexpression leads to increased cell proliferation and metastasis. This transcript also aids PCa progression by driving AR activity even in the absence of androgen and may mediate androgen-independent transcription, leading to CRPC (Misawa *et al*., 2017). For this reason, HOTAIR has been proposed as a novel therapeutic target for PCa.

Table 1.4.2.1: Examples of long noncoding RNAs which have implications in prostate cancer

lncRNA	Role in cancer	Other cancer sites	Expression in PCa	Mechanism	Reference
HOTAIR	Promotes metastasis	Breast, prostate, colon	Upregulated	Enhances androgen receptor activity by preventing its degradation	(Misawa *et al.*, 2017)
MALAT1	Associated with epithelial-mesenchymal transition (EMT), promotes cell growth, invasion and migration	Prostate, breast	Upregulated	Increases LPHN2 and ABCA1 proteins (important factors associated with EMT) Acts as a sponge to sequester miR-1	(Chang *et al.*, 2018; Zhan *et al.*, 2018)
NEAT1	Androgen deprivation resistance	Prostate, breast, lung, rectal, colon, stomach, kidney, liver, oesophageal, uterine etc.	Upregulated	Drives oncogenic proliferation by promoting epigenetic alterations and transcription	(Li *et al.*, 2017; Misawa *et al.*, 2017)
PCA3	Promotes malignant cell growth	Prostate	Highly upregulated	Downregulates PRUNE2 (tumour suppressor gene in PCa)	(Salameh *et al.*, 2015)
PCAT18	Affects cell proliferation, migration and invasion	Prostate	Upregulated	Affects AR signalling although exact mechanism is not clear	(Zhan *et al.*, 2018)
PCGEM-1	Promotes cell proliferation	Prostate	Upregulated	Enhances androgen receptor transcription and c-myc activation	(Huarte, 2015)
SChLAP1	Promotes cell proliferation and metastasis	Prostate	Upregulated	Downregulates miR-198 and thus promotes the MAPK1 pathway	(Li *et al.*, 2018)

1.5. Prostate Cancer and Metabolism

1.5.1 The Androgen Receptor Regulates Metabolism

The AR is key for the up- or downregulation of an array of genes involved in different cellular processes and it is recognised to be a main driver in PCa progression. Brooke *et al.,* (2015) found that proteins involved in protein synthesis and metabolism were downregulated upon bicalutamide treatment on LNCaP cells. Ultimately, proteins which are upregulated in the presence of androgen include those involved in anabolic and metabolic pathways, the cell cycle, glucose transformation, lipid synthesis, ATP synthesis and gene transcription, consequently leading to cellular growth (Barfeld *et al.*, 2014; Brooke *et al.*, 2015) These genes are known to be androgen-dependently regulated.

1.5.2 Normal Metabolism in Somatic Cells

To maintain homeostasis, cells require energy. This energy can be used to make essential components as well as to grow and divide. Glucose, a major source of energy, is fundamental for multiple different pathways. These include the serine biosynthesis pathway required for amino acid generation, the hexosamine pathway for protein glycosylation, glycogenesis for the storage of glucose, the pentose phosphate pathway for ribonucleotide production, glycolysis amongst others (Hay, 2016). Glycolysis consists of various enzymatic steps which gives rise to pyruvate and 2 molecules of ATP (Kim and Dang, 2006). Pyruvate can be transported into the mitochondria for use in the Krebs cycle. These reactions produce NADH and ATP which can be utilised in other cellular processes. NADH can also be utilised in the electron transport chain within the inner membrane of the mitochondria in normoxic conditions to drive ATP synthesis (Fernie *et al.*, 2004) (Figure 1.2.1). One molecule of glucose can produce up to 36 molecules of ATP (Kim and Dang, 2006). In hypoxic conditions however, glucose is converted into lactic acid and consequently the Krebs cycle ceases. This process

known as anaerobic glycolysis and is utilised in tissues following an intense occurrence of exercise, for example (Kim and Dang, 2006).

1.5.3 Metabolism in Cancerous Tissues

The uncontrolled cell division observed in cancer cells eventually leads to an avascular phase and consequently hypoxic conditions. Glycolysis is upregulated for the continuation of ATP synthesis (Cairns *et al.*, 2011). Eventually, in cancerous cells, metabolism switches to enhance the glycolysis reaction even in the presence of high oxygen levels. This event is known as The Warburg Effect or aerobic glycolysis (Kim and Dang, 2006; Kroemer and Pouyssegur, 2008). This, in turn means that there is an increase in glucose uptake and lactate formation (Figure 1.2.1). Cancer cells can utilise both glucose (as a source of carbon molecules) as well as the intermediates produced within aerobic glycolysis for anabolic reactions to produce other macromolecules necessary for growth and division. Such macromolecules include amino acids, lipids and proteins (Zheng, 2012). Moreover, too high a production of ATP would lead to inhibition of phosphofructokinase-1, a rate-limiting step and pyruvate kinase-1 leading to complete inhibition of glycolysis (Zheng, 2012). Additionally, the advantageous acidic microenvironment caused by the production of lactate promotes invasion and metastasis (Vaupel, 2010; Zheng, 2012) (Figure 2.2).

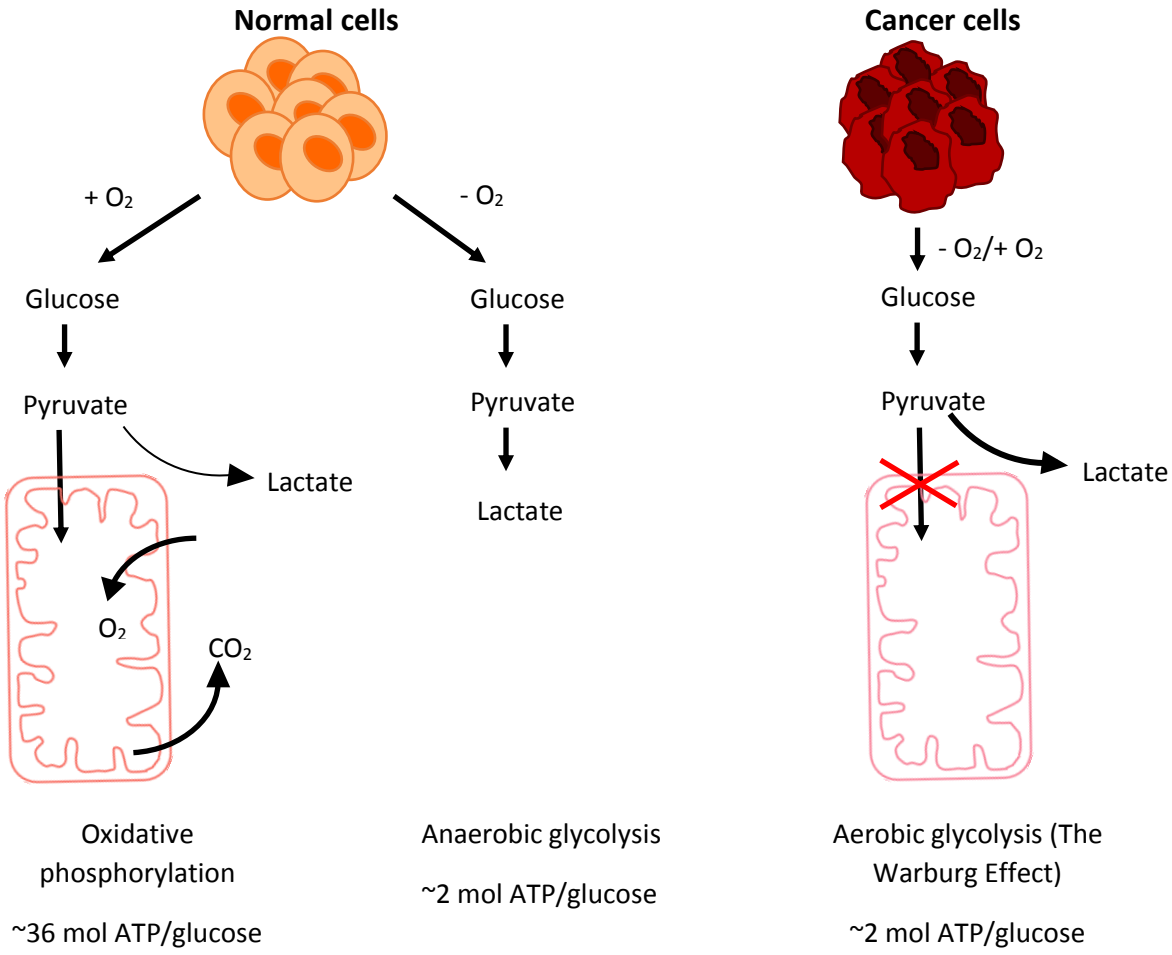

Figure 1.2.1: Glucose metabolism switch in cancer cells. Glucose can be used as a source of energy for cells glucose is converted into pyruvate via glycolysis. In the presence of oxygen (normoxic) in non-cancerous cells, this pyruvate can enter the Krebs cycle where substrates produced are required for oxidative phosphorylation. In the absences of oxygen (hypoxia) cells use the process of anaerobic glycolysis (fermentation) to produce lactate and ATP. This is not such an efficient means of ATP production. In cancer, both in the presence and absence of oxygen, cells show preference to using glycolysis due to the intermediate products produced. This is known as aerobic glycolysis.

1.5.4 Metabolism in Normal Prostate Tissue

Prostate cell metabolism is highly unique and is altered compared to other cells of the body to compensate for the large amounts of citrate required in prostatic secretions. Pyruvate is generated via glycolysis which undergoes decarboxylation to form acetyl-CoA. Citrate is produced in the mitochondria from the condensation reaction between oxaloacetate and acetyl-CoA (Costello and Franklin, 2006; Cutruzzolà *et al.*, 2017). Usually, this would be followed by oxidation within the Krebs cycle to reproduce oxaloacetate. However, in prostate cells, citrate is the end-product of the glucose metabolic pathway as opposed to a respiratory intermediate (Costello and Franklin, 2006). This is achieved via inhibition of the enzyme, mitochondrial acotinase (m-acotinase), which performs the first step in citrate production. This blockage is due to high levels of zinc which accumulate in prostatic tissues via zinc transporters Zrt- and Irt-like Proteins (ZIP) of which there are three subtypes ZIP1, ZIP2 and ZIP3 (Cutruzzolà *et al.*, 2017). ZIP proteins are part of the SLC39 family of zinc transporters (Franz *et al.*, 2013). Rishi *et al.*, (2003) interestingly reported that the zinc transporters: ZIP1 and ZIP2 are downregulated in Afro-American men in comparison to Gleason score-matched white individuals. This could be linked somewhat to the high susceptibility of cancer in this racial group (Rishi *et al.*, 2003). Furthermore, to compensate for the essential inhibition of the Krebs cycle, prostate cells increase glycolysis reactions for their survival and for the maintenance of high citrate production (Cutruzzolà *et al.*, 2017). Although this may appear an inefficient means of ATP production, the amount obtained from this process is sufficient due to the low respiring characteristics of prostatic tissue (Costello and Franklin, 2006).

1.5.5 Alteration of Metabolism in Prostate Cancer Cells

Depleted zinc levels has been proposed as a potential biomarker for PC as healthy prostate cells have higher levels (Costello and Franklin, 2006). Levels are significantly diminished or even to an undetectable level, in malignant stages of disease. High Gleason scores and poor

prognosis are also correlated with low zinc levels (Franz *et al.*, 2013). This depletion is due to a downregulation of ZIP1, ZIP2 and ZIP3 in PCa compared to normal or BPH cells. ZIP1 is located on epithelial cells within the basolateral membrane whereas ZIP2 and ZIP3 are found on the apical membrane. ZIP1 is the major transporter of zinc within the prostate, obtaining zinc from the blood whereas, it is postulated that both ZIP2 and ZIP3 are involved in the reabsorption of zinc from prostatic fluids (Franz *et al.*, 2013). Negligible zinc levels within the prostate leads to reactivation of the truncated Krebs cycle, switching from an energy inefficient to an energy efficient state due to escalated energy demands. To further support energy pressures, PCa cells corrupt surrounding fibroblasts through IL-6 secretions. This switches on the Warburg Effect in fibroblasts and leads to a cancer-associated fibroblast (CAF) phenotype. Lactate production and secretion from this switch can be utilised as a substrate for cancer cells. Therefore, the exposure of CAFS to PCa cells promotes oxidative phosphorylation (Cutruzzolà *et al.*, 2017). Unlike other cancers, the Warburg Effect in PCa cells is switched on only at advanced metastatic stages of disease (Cutruzzolà *et al.*, 2017) (Figure 1.2.2).

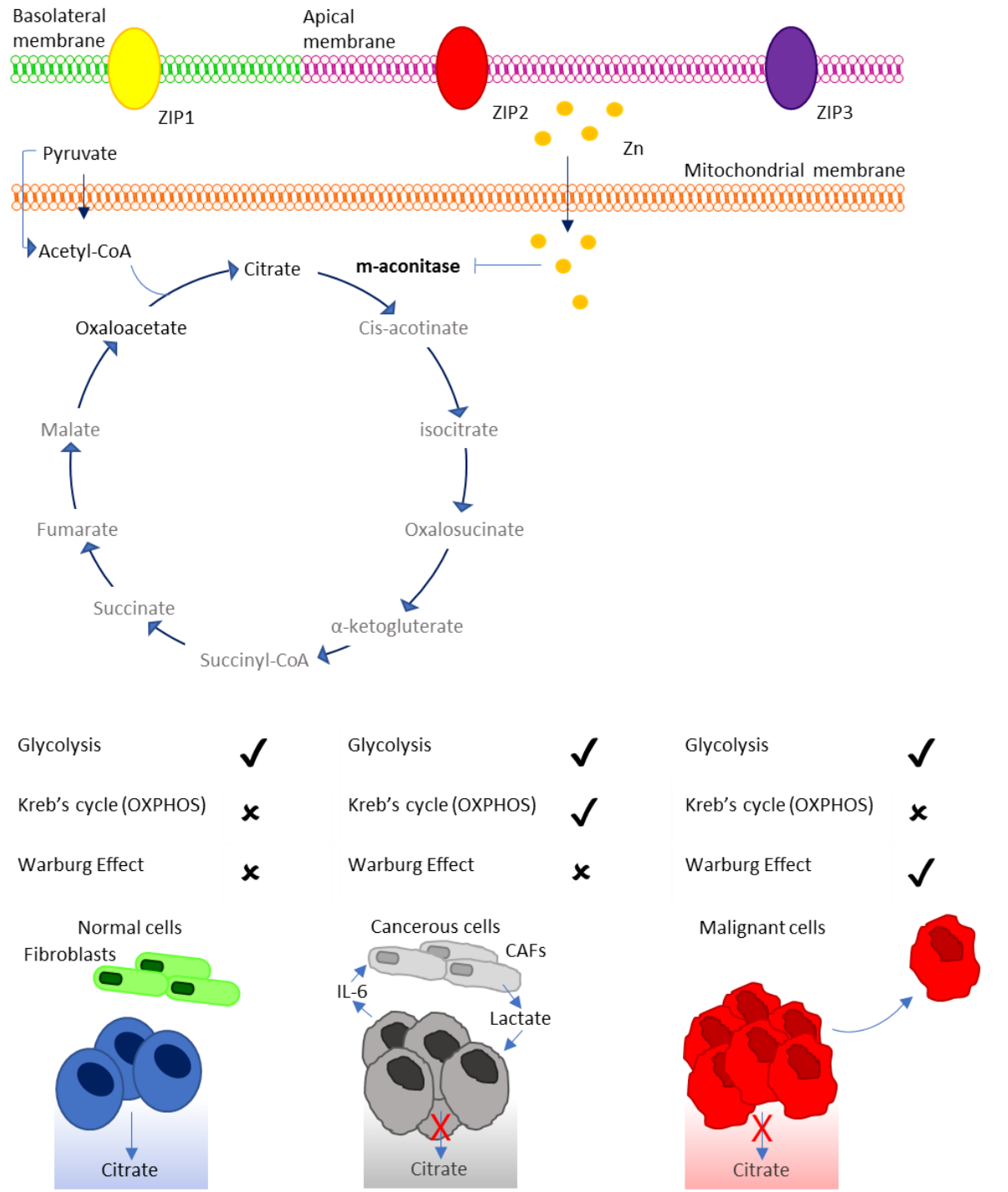

Figure 1.2.2: Metabolic alterations in prostate cancer progression. In normal prostate tissues, the Krebs cycle in truncated to produce citrate required for prostatic secretions. This is due to high levels of zinc, an important characteristic of healthy prostate tissue, which inhibits the enzyme mitochondrial aconitase (m-aconitase). Zinc is transported into cells by ZIP proteins ZIP1, ZIP2 and ZIP3. In prostate cancer (PCa), ZIP proteins become downregulated and the complete Krebs cycle is restored. Therefore, both zinc and citrate levels are decreased in PCa tissues. Secretions of IL-6 cause neighbouring fibroblasts to become cancerous, secreting lactate into the microenvironment. This can be utilised by PCa cells for anabolic metabolism. At advanced stages of disease, PCa switch to the Warburg Effect and eventually metastasise to other parts of the body.

1.5.6 The Importance of Haem and its Biosynthesis

Haem is an iron-containing macromolecule and is the most abundant commonly used metalloporphyrin in the biosphere (Poulos, 2014). It is ubiquitous throughout the body and plays multiple vital roles. This includes electron transfer within the mitochondria (cytochromes) essential in the process of respiration, enzymes such as catalases and is recognised for its role in oxygen transfer and storage within haemoglobin and myoglobin respectively (Layer *et al.*, 2010). Haem (Figure 1.2.3a) can be produced in one of two pathways known as C_4 and C_5 (Shemin pathway). Generally, humans and other non-photosynthetic organisms utilise the latter pathway. In the Shemin pathway, haem biosynthesis commences with the condensation of succinyl-CoA and glycine to form 5-aminolevulinic acid (ALA) in the mitochondria (Layer *et al.*, 2010). This single catalytic step is performed by 5-aminolevulinic acid synthase (ALAS). The sequential five steps are catalysed in the cytosol before the final three steps occur in the mitochondria (Figure 1.2.3b).

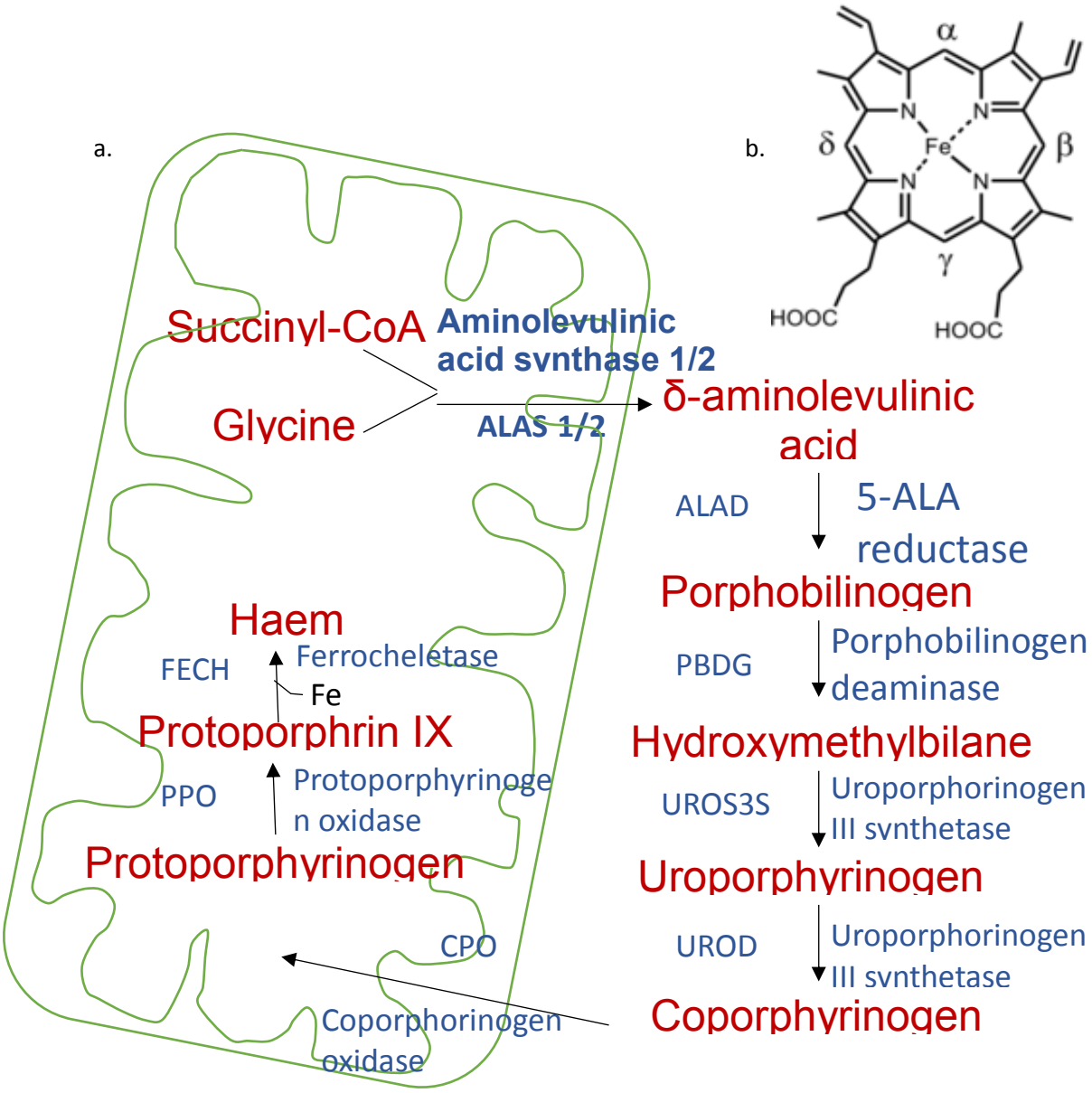

Figure 1.2.3: The structure of haem and its synthesis pathway in mammalian cells. a. The haem synthesis pathway occurs in both the mitochondria and cytosol. Succinyl-CoA and glycine are converted to δ-aminolevulinic acid by 5-aminolevulinic acid synthase (ALAS) (bold) in the first catalytic step of haem production. The first and final three steps occur within the mitochondria while the remainder is performed within the cytosol. Products used within the pathway are depicted in red and enzyme names and their capitalised abbreviations in blue (Adapted from Ajioka *et al*., 2006). b. The skeletal structure of haem (Gisk *et al.*, 2010).

1.5 7 Aminolevulinic Acid Synthase, ALAS

5-aminolevulinic acid synthase (ALAS) performs the irreversible primary step in the haem synthesis pathway whereby succinyl-CoA and glycine undergo condensation to form 5-aminolevulinic acid (ALA). This rate-limiting step can be carried out by two different isoforms: ALAS-1 (ALAS-H) and ALAS-2 (ALAS-E) whereby the former is ubiquitously expressed and the latter is expressed only in erythrocytes (Ajioka *et al.*, 2006). Using somatic cell hybrid and *in situ* hybridisation techniques, *ALAS1* was located on chromosome 3p21 and *ALAS2* on the X chromosome (Bishop *et al.*, 1990). The molecular weight of precursor and mature ALAS1 is 71 kDa and 65 kDa, respectively and ALAS2 is 65 kDa and 60 kDa respectively (Munakata *et al.*, 2004). The precursor of ALAS is synthesised in the cytoplasm before being imported into the mitochondria to mature as a functional enzyme. ALAS is located in the mitochondria where it performs its activity as a homodimer. Although these isoforms are regulated differently, to initiate reactions they both necessitate pyridoxal 5-phosphate (PLP) as a co-factor. More specifically, PLP forms a covalent bond with the enzyme via a Schiff Base complex with lysine-313 which then reacts with glycine and succinyl-CoA to form ALA, CO_2 and CoA (Hunter and Ferreira, 1999). Previous studies demonstrated that mutagenesis of this specific lysine to alanine or histidine formed a dysfunctional enzyme (Ferreira *et al.*, 1993), demonstrating the importance of this residue in enzymatic activity.

Both isoforms of mature mammalian ALAS also contain a haem regulatory motif (HRM), also known as a CP motif as it consists of core cysteine and proline residues. In the ALAS1 precursor protein, three HRMs have been identified (CP 1, CP2 and CP3). CP1 and CP2 are located within the pre-sequence of the precursor protein which together aid translocation into the mitochondria (Figure 1.2.4). Once imported, the pre-sequence is catalytically removed (Kubota *et al.*, 2016). CP3 is located toward the N-terminus and remains in the mature enzyme. It is thought that this motif binds haem when it is at high levels. Dependent on haem levels, CP3 then recruits ClpXP for its degradation thus a negative feedback inhibition loop is established (Kafina and Paw, 2017; Kubota *et al.*, 2016). Haem can also bind to the immature

protein which hinders its translocation into the mitochondria and consequently lacks complete folding. This makes it susceptible to protein degradation via the proteasome, although this process is not fully understood (Franken *et al.*, 2011).

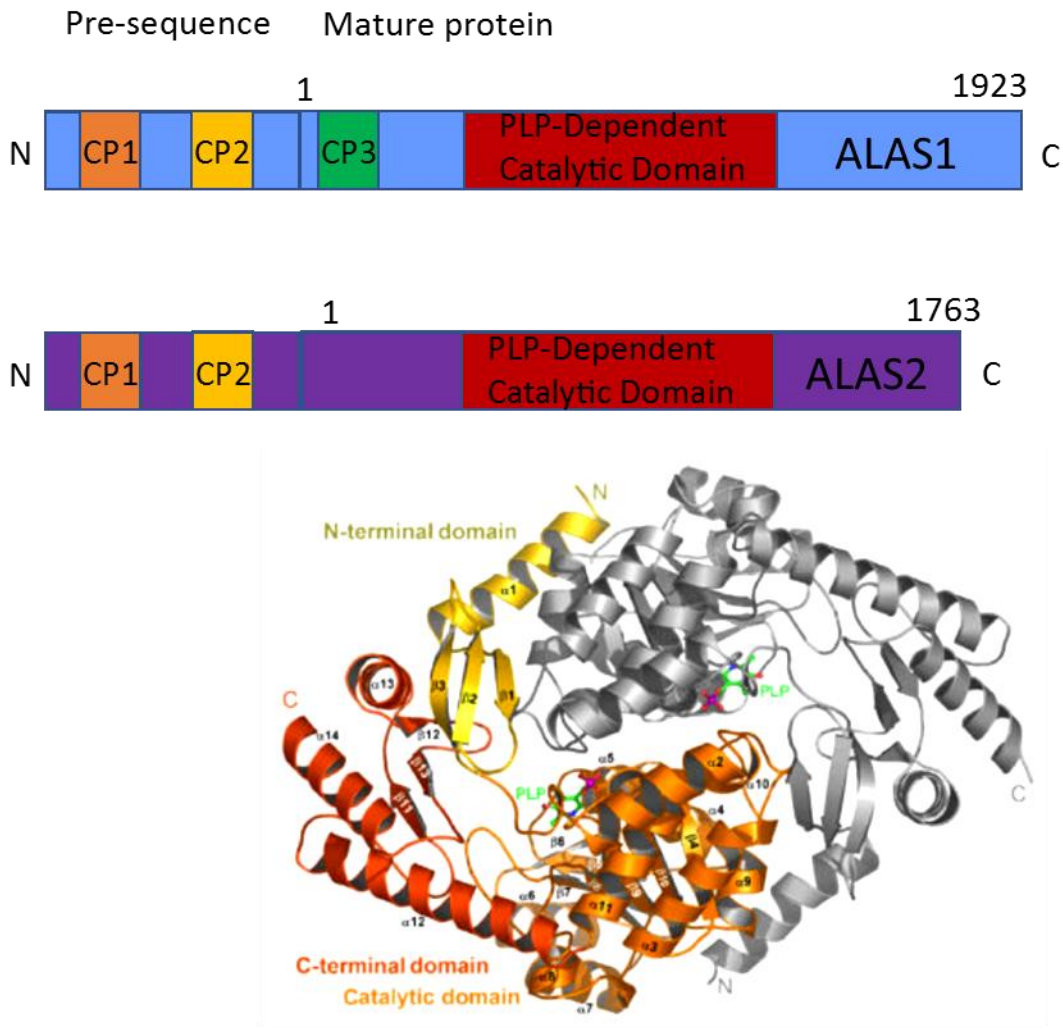

Figure 1.2.4: *Aminolevulinate synthase (ALAS)* gene and protein structure. a. Human ALAS1 and ALAS2 contain a PLP-Dependent Catalytic Domain and consists of 1923 and 1763 bp respectively. The precursor proteins of ALAS1 consists of 640 amino acids b. The ribbon structure of the *R. capsulatus* ALAS homodimer. The N-terminal domain is coloured in yellow, the catalytic domain in light orange and the C-terminal domain in dark orange (Astner *et al.*, 2005).

1.5.8 Cellular Death Pathways

1.5.8.1 Apoptosis

Apoptosis (or programmed cell death PCD) involves a tightly controlled series of morphological and biochemical events (Dwyer *et al.*, 2012; Kaufmann *et al.*, 1993). PCD is a vital process and improper control can lead to diseases, such as autoimmunity, syndactyly and a variety of cancers (Elmore, 2007). Apoptosis can be subdivided into two pathways: extrinsic and intrinsic. The former is triggered via death receptors which leads to procaspase-8 activation to caspase-8 whereas the intrinsic pathway involves the internal stresses such as unrepairable DNA damage, executed via the mitochondria and B-cell lymphoma-2 (Bcl-2) (Elmore, 2007; Youle and Strasser, 2008) (Figure 1.2.5). Caspases are proteolytic enzymes which target aspartic acid residues, although recognition of cleavage sites differs amongst caspases depending upon neighbouring amino acids. It is thought that the cell is committed to die upon caspase activation as this step is irreversible. The best characterised examples of ligands and their death receptors are Fatty acid synthase Ligand (FasL)/Fatty acid synthase Receptor (FasR) and Tumour Necrosis Factor alpha TNF-α/ Tumour Necrosis Factor Receptor 1 (TNFR1). Different adaptor proteins are recruited upon ligand binding to the receptors. Fas-associated death domain (FADD) is recruited in response to FasR activation and TNFR Type 1-Associated Death Domain (TRADD) which recruits RIP and FADD in response to TNFR1 initiation. FADD then forms a complex with procaspase-8, dimerising at death effector domains (DED), altogether forming the death-inducing signalling complex (DISC). This leads to autocatalysis of procaspase-8 to caspase-8, known as an initiator caspase. Caspase-8 can cleave BH3 Interacting Domain Death Agonist (BID), which can heterodimerase with pro-apoptotic protein Bcl-2 Associated X protein (Bax) (Kantari and Walczak, 2011). This demonstrates cross-talk between the intrinsic and extrinsic apoptotic pathways. Caspase-8 will also lead to activation of executioner or effector caspases (such as caspase-3) which implement the final stage of apoptosis. Ultimately these series of events

lead to DNA fragmentation, nuclear and cytoskeletal degradation, protein cross-linking demonstrating classic apoptotic body characteristics (also known as blebs).

1.2.7.2 Necrosis

Necrosis is an unprogrammed form of cell death. There are multiple ways by which necrotic cell death can be triggered which depends upon the circumstances of the cell. These include cellular stress, damage to organelles, proteins and DNA, mechanical damage, extreme heat and cold, together causing a loss of functionality of the cell (Zong and Thompson, 2006). This can be mediated by ROS, calcium ion uptake, non-apoptotic protease activation and/or ATP bioenergetic collapse through enzymatic destruction of co-factors (Schiffer *et al.*, 2018; Zong and Thompson, 2006). Typical characteristics of necrosis include organelle failure, irreversible plasma membrane breakdown, cytoplasm swelling and non-specific degradation of DNA (Schiffer *et al.*, 2018). Often, as cytoplasmic contents leak into the extracellular space, necrosis is concomitant with triggering the inflammatory response (Rock and Kono, 2008). Usually distinct phases of cell death are observable: initiation, propagation and execution, however in necrosis these stages are not very well defined (Festjens *et al.*, 2006).

2.7.3 Necroptosis

Necrosis is a recognisable form of unprogrammed cell death which generally is the result or cause of disease. Apoptosis was later established and is driven by a specific molecular mechanism within the cell which “program” cellular death. These means of cellular demise remain distinguished pathways. It is now believed that there is a programmed form of necrosis namely, necroptosis (Galluzzi and Kroemer, 2008). Necroptosis is triggered by a variety of diseases such as inflammatory bowel disease, myocardial infarction and pancreatitis, amongst others (Linkermann and Green, 2014). Activated receptors such as death receptor TNFR1 and Toll-Like Receptor (TLR) as well as other inter- and intracellular triggers, can

induce necrosome formation. This form of cellular death is caspase-independent and requires inhibition of caspase-8 to occur (Figure 1.2.5). Activated TNFR1 ultimately triggers the Nuclear Factor Kappa Light Chain of B Cells (NF-κB) signalling pathway via NF-κB Essential Modulator (NEMO) and the inactivation of anti-apoptotic protein: Receptor Interacting Protein Kinase I (RIPK1) through polyubiquitination. Adaptor protein TRADD binds to the FADD adaptor to which pro-caspase 8 associates. Normally, pro-caspase 8 initiates its own activation upon homodimerization. However, in necroptosis, procaspase-8 appears to form a complex with both cFLIP and FADD via the DED (Micheau *et al.*, 2002). cFLIP is a structurally similar protein to caspase-8 but lacks protease activity. The presence of cFLIP prevents full cleavage to initiate caspase-8 activity, ultimately thwarting the trigger of cell death via apoptosis (Micheau *et al.*, 2002). Once the procaspase-8-cFLIP heterodimer is formed and/or there is a loss of caspase-8 function within the cell, RIPK1 arranges a complex with RIPK3 which together cause formation of the necrosome (Figure 1.2.5). The key characteristics of necroptosis include dysfunctional mitochondria, permeabilization of the plasma membrane, cell swelling and release of intracellular contents into the extracellular space (Giampietri *et al.*, 2014).

2.7.4 Ferroptosis

Ferroptosis was recently discovered unintentionally in 2012 by Dixon *et al.* who demonstrated that cells which express oncogenic RAS mutants are targeted for cell death initiated by erastin via a non-apoptotic means. Ferroptosis is a distinct form of regulated cell death which differs both biochemically and morphologically from apoptosis and necroptosis (Xie *et al.*, 2016) (Figure 1.2.5). Ferroptosis is characterised by a diminished cytoplasmic volume, increased density of the mitochondrial membrane, accumulation of ROS, namely membrane lipid peroxides, propagated by the presence of intracellular iron. Cysteine and cystine are vital compounds required for the synthesis of glutathione. Glutathione, utilised by Glutathione Peroxidase 4 (Gpx4), is a fundamental antioxidant whose role is to protect cells from lipid peroxide (L-OOH) ROS by neutralising them into lipid alcohols (Agbor *et al.*, 2014; Banjac *et*

al., 2007; Fanzani and Poli, 2017). Cysteine is carried into the cell via a specialised membrane-bound cystine/glutamate antiporter, system x_c^- (Dixon and Stockwell, 2013). Cystine is the predominant oxidised form found within the extracellular space, cell culture medium and plasma. Glutamate is released extracellularly as cystine is taken up by the cell simultaneously by a ratio of 1:1 (Lewerenz *et al.*, 2013). Erastin can inhibit system x_c^- leading to an increased intracellular glutamate, a decrease in glutathione production thus exposing the cell to damaging lipid radicals as well as iron accumulation. Iron is transported from plasma by transferrin and is transported into cells via endocytosis by transferrin receptor 1 (TfR1) (Figure 2.5). Iron is reduced and can then be utilised by the mitochondria to make haem as well as throughout other processes. Excess intracellular iron is sequestered into ferritins for storage. However, in malignant tissues, often an augmentation of the iron pool is observed due to increased TfR1 expression which supports dysregulation within the cell such as the rise in metabolism levels, growth and angiogenesis (Fanzani and Poli, 2017). Resulting iron accumulation generates hydroxyl radicals from hydroperoxide via the Fenton Reaction (Fanzani and Poli, 2017; (Winterbourn, 1995). These hydroxyl ROS execute extreme membrane impairment by the oxidation of polyunsaturated fats (PUFAs) into lipid hydroperoxides (L-OOH). L-OOH can exert damaging effects by encouraging further ROS production as well as degrading into compounds able to cross-link proteins and DNA (Gaschler and Stockwell, 2017). This disruption leads to extensive damage throughout the cell and consequently, cell demise via ferroptosis.

2.8 Cell Death Induction by Anti-cancer Compounds

Many anti-cancer therapies target directly or indirectly cellular death pathways, principally apoptosis. The effect of initiating apoptosis to treat and circumvent cancer is generally considered a positive event. However, it can also be detrimental due to the pro-tumorigenic

effects it can promote, such as genomic instability caused by caspase enzymes in the absence of cell death and signals sent to neighbouring cells for stimulation to repopulate (Fitzwalter and Thorburn, 2017; Giampazolias *et al.*, 2017). It is known that mitochondrial outer membrane permeabilization (MOMP) is important for the release of cytochrome c, essential to activate caspase enzymes. These enzymes execute the process of apoptosis (Giampazolias *et al.*, 2017). However, MOMP can give rise to cell death in the absence of caspase enzymes, known as caspase-independent cell death (CICD). This is thought to be via TNF-dependent necroptosis (Giampazolias *et al.*, 2017). MOMP in the presence of CICD can the NF-κB pathway and enhance tumour reduction due to the engagement of the immune system (Giampazolias *et al.*, 2017).

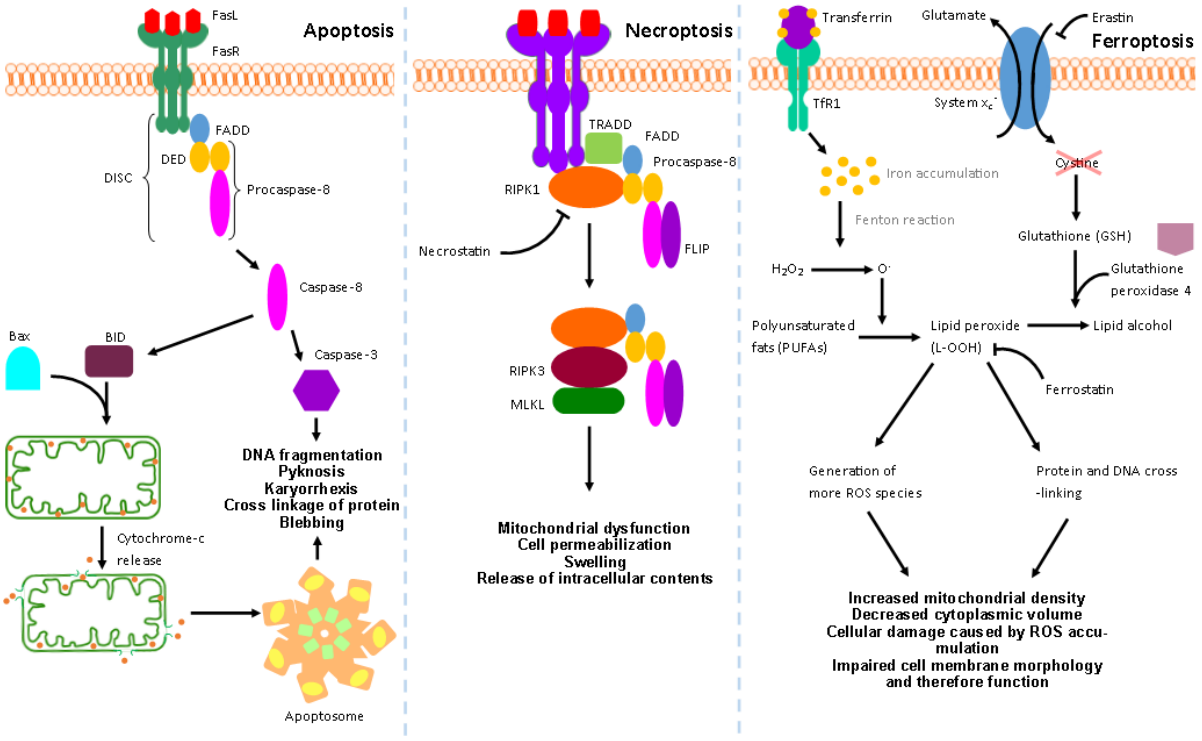

Figure 1.2.5. Schematic of cellular death signalling cascades. Apoptosis can be triggered in one of two ways – the intrinsic and extrinsic pathway. The former pathway involves the release of cytochrome c from the mitochondria and the formation of the apoptosome. The extrinsic pathway is triggered from extracellular signals and requires activation of caspase enzymes. The extrinsic pathway can also activate the intrinsic pathway simultaneously. Apoptosis via both pathways leads to blebbing, chromatin condensation (pyknosis), DNA fragmentation, fragmentation of the nucleus (karorryhexis). Necroptosis is caspase-independent and requires the presence of cFLIP to occur. Necroptosis leads to mitochondrial dysfunction, membrane permeabilization, cell swelling and release of intracellular contents. Ferroptosis is triggered when the system xc- is inhibited. It is essential for importing extracellular cysteine into the cell whilst releasing glutamate. This makes system xc- an antiporter. Cysteine is required for glutathione peroxidase 4 to convert damaging lipid peroxides into lipid alcohol. if this is prevented, the increase in reactive oxygen species causing damage within the cell, leading to an impaired membrane and cellular death.

1.6 Project Aims

1.6.1 Androgen Receptor Regulation

PCa is a devastating disease affecting many men around the world. In some cases, treatments eventually fail causing the disease to relapse with high aggression, making this disease incurable at this stage. It is thought that the androgen receptor (AR) is the main driver of disease, therefore it is important to characterise factors that regulate the AR to further understand its signalling and role in disease progression. One such co-factor includes Fused in Sarcoma (FUS) which could potentially act as both a co-repressor and co-activator of the AR at early and advanced stages of disease respectively. It is important to characterise the role of FUS and its potential role in disease progression. Another factor which can regulate the AR is lncRNA. A known lncRNA known to interact with the AR is Hox Transcript Antisense Intergenic RNA (HOTAIR). It is unclear how lncRNA interacts with the AR to regulate its activity. Understanding these individual interactions may give insight to novel therapeutic strategies in the future.

1. Investigate how FUS and lncRNA affect AR activity individually
2. To compare the activity of the un-tagged and biotin-ligase tagged androgen receptor, to ensure that they behave similarly in order to identify proteins at different phases of signalling using proximity-dependent biotin identification (BioID).

1.6.2 Project Aims: Prostate Cancer Metabolism

Alterations in multiple essential cellular processes is required to give rise to cancer. These changes are known as the Hallmarks of Cancer. The androgen receptor (AR) regulates a range of genes, some of which are fundamental in metabolic pathways. As AR dysregulation is known to be a main driver in prostate cancer, consequently metabolic pathways are altered too. One compound essential in respiration and hence metabolism is haem. Targeting haem synthesis promotes cell death, however the cell death mechanisms are not well understood and therefore this requires further investigation. 5-aminolevulinic acid synthase 1 (ALAS1) could be a potential target and no structure is available for the human form.

1. Validation of ALAS1 as a therapeutic target for prostate cancer
2. Elucidate specific cellular death mechanism using flow cytometry and inhibitors which target the death pathways
3. Explore effects of blocking haem production in the presence of reactive oxygen species, induced by hydrogen peroxide
4. To clone and express ALAS-1 and ALAS-2 full length as well as ALAS-1 and ALAS-2 truncations in preparation for structural studies

Chapter 2: Materials and Methods

2.1 Materials

2.1.1 All Reagents and their suppliers

Table 2.1.1 Reagents and their suppliers

Reagent	Supplier
4-(2-hydroxyethyl)-1-piperazineethanesulfonic acid (HEPES)	Sigma-Aldrich
6x DNA loading dye	ThermoFisher Scientific
Acrylamide	Sigma-Aldrich
Agarose	Fisher Scientific
Ammonium Persulphate Solution (APS)	Sigma-Aldrich
Ampicillin	Sigma-Aldrich
Bicalutamide	Sigma-Aldrich
Bovine Serum Albumin (BSA)	Sigma-Aldrich
Calcium chloride ($CaCl_2$)	Sigma-Aldrich
Crystal violet (CV) Stain	Sigma-Aldrich
Dimethyl sulphoxide (DMSO)	Sigma-Aldrich
Ethanol	Fisher Scientific
Ethylenediaminetetraacetic (EDTA)	Invitrogen™
Ethylene glycol-O,O'-bis)2-aminoethyl)-N, N, N',N'-tetracetic acid (EGTA)	Alfa Aesar ThermoFisher Scientific
Ethidium bromide	Sigma-Aldrich
Ferrostatin-1	Sigma-Aldrich
Gibco® OPTI-MEM™	ThermoFisher Scientific
Glycerol	Fisher Scientific
Glycogen blue	ThermoFisher Scientific
HALT™ phosphate inhibitor cocktail	Sigma Aldrich
Hydrogen peroxide	Sigma-Aldrich
IGEPAL® CA-630	Sigma-Aldrich
Isopropanol (propan-2-ol)	Fisher Scientific, VWR
Isopropyl-beta-D-thiogalactoside (IPTG)	Sigma-Aldrich
Kanamycin	Sigma-Aldrich
Lithium chloride (LiCl)	Sigma-Aldrich
Low-melt agarose	Fisher Scientific
Luria Broth (LB) Lennox Larger Granules	Fisher Scientific
LB Agar	Sigma-Aldrich
Magnesium chloride ($MgCl_2$)	Fisher Scientific
Manganese chloride ($MnCl_2$)	Sigma-Aldrich
Methanol	VWR
Mibolerone	Sigma-Aldrich
Molecular biology high grade water	Hyclone™ HyPure™
N-lauroylsarcosine sodium salt solution	Sigma-Aldrich
Necrostatin-1	Sigma-Aldrich
Phosphate Buffered Saline (PBS) (Dulbecco A) tablets	Oxoid
Potassium hydroxide	Fisher Scientific
RNAiMAX	ThermoFisher Scientific

Sodium chloride (liquid)	Alfa Aesar ThermoFisher Scientific
Sodium chloride (powder)	Sigma-Aldrich
Sodium deoxycholate	Sigma-Aldrich
Sodium dodecyl sulphate solution (powder)	Fisher Scientific
Sodium dodecyl sulphate solution (pure)	Sigma-Aldrich
Sodium hydroxide	Fisher Scientific
Sodium phosphate dibasic (Na_2HPO_4)	Sigma-Aldrich
Succinylacetone (SA)	Sigma-Aldrich
Tetramethylethylenediamine (TEMED)	Sigma-Aldrich
Tris base	Fisher Scientific
Triton X-100	Sigma-Aldrich
Tween®-20	Sigma-Aldrich
X-gal	Sigma-Aldrich

2.1.2 Kits

Table 2.1.2 Kits

Kit	Supplier
DC™ Protein Assay	Bio-Rad
Dual Glo® Luciferase Assay System	Promega
Fast Ion™ Plasmid Midi Advanced Kit	RBCBioscience
HiYield™ Gel/PCR Fragments Extraction Kit-300	RBCBioscience
HiYield™ Plasmid Mini Kit	RBCBioscience
Monarch® PCR and DNA Clean Up kit	New England BioLabs (NEB)
Monarch® Total RNA Miniprep Kit	New England BioLabs (NEB)
QIAEX® II Gel Extraction Kit	QIAGEN

2.1.3 Buffers, Media, Reagents, Solutions and Antibodies

2.1.3.1 General stock solutions

Table 2.1.3.1: General stock solutions

Name of Solution	Reagents and procedure	Sterilisation method	Storage
Ammonium persulphate solution (APS)		-	-20 ˚C
4-(2-hydroxyethyl)-1-piperazineethanesulfonic acid (HEPES)-KOH pH 7.5	11.915g HEPES in ddH2O. KOH was added until at the desired pH. The solution was then topped up to 50ml with ddH2O	Filter sterilisation (0.22 µm)	4 ˚C
2M Magnesium chloride ($MgCl_2$)	20.331g $MgCl_2$ in ddH2O made to 50ml volume	Autoclave	Room temperature
5M Lithium chloride (LiCl)	21.2g in 10ml of ddH2O	Filter sterilisation (0.22 µm	4 ˚C
Phosphate buffered saline (PBS)	1 tablet in 100ml de-ionised water	Autoclave	Room temperature
10% Sodium dodecyl sulphate (SDS)	10 g of SDS in 100 ml of ddH2O	Autoclave	Room temperature
1M Tris-Hydrochloric acid (HCl) pH	6.057g Tris base dissolved in some ddH2O. HCl is added until at the desired pH. This was then made up to 50ml with ddH2O.	Autoclave	Room temperature
1M Tris-Potassium hydroxide (KOH) pH	6.057g Tris base dissolved in some ddH2O. KOH is added until the desired pH is reached. This solution was then made up to 50ml with ddH2O.	Autoclave	Room temperature

2.1.3.2 Sodium dodecyl sulphate gel electrophoresis and western blotting

Table 2.1.3.2: Reagents for sodium dodecyl sulphate gel electrophoresis and western blotting

Name of solution	Reagents	Sterilisation method	Storage
Blocking buffer	1g Marvel™ semi skimmed dried milk powder in 20ml PBS-Tween	-	4 ˚C, kept for no longer than 24 hours
Bovine Serum Albumin (BSA)	Series dilutions from 0 – 10 (mg/ml)	-	4 ˚C
HALT™ phosphate inhibitor cocktail	-	-	4 ˚C or -20 ˚C
6x Loading dye	-	-	4 ˚C or -20 ˚C
PBS-Tween (PBS-T)	0.1 % Tween®-20 in PBS. E.g. 800 µl Tween®-20 in 800 ml PBS	-	Room temperature
Millipore Luminata™ Classico/Forte Western HRP Substrate	-	-	4 ˚C / Room temperature respectively
Molecular weight ladder (kilodaltons [kDa])	-	-	-20 ˚C
10% polyacrylamide (separation gel)	For one gel: 1.65 ml Acrylamide (1.875 ml Tris pH 8.9 1.375ml H_2O (purite) 50 µl 10 % SDS 50 µl 10 % APS 5 µl Tetramethylethylenediamine (TEMED)	-	Used immediately/4 ˚C for up to 4 weeks
12% polyacrylamide (separation gel)	For one gel: 2 ml Acrylamide (1.875 ml Tris pH 8.9 1.075 ml H_2O (purite) 50 µl 10 % SDS 50 µl 10 % APS 5 µl Tetramethylethylenediamine (TEMED)	-	Used immediately/4 ˚C for up to 4 weeks
Running buffer	30 g Tris 144.45 Glycine 5 g SDS Purite water to 1 L	-	Room temperature
Stacking gel for	425 µl Acrylamide (937.5 µl Tris pH 6.8 1.0875 ml H_2O (purite)		Used immediately/4 ˚C for up to 4 weeks

polyacrylamide gels	25 µl 10% SDS 25 µl 10% APS 2.5 µl TEMED		
1x Semi Dry Transfer Buffer	11.26 g Glycine 2.44 g Tris 200 ml Methanol Filled to 800 ml using purite water	-	4 ˚C
Tween®-20	-	-	Room temperature

2.1.3.3: Agarose gel electrophoresis

Table 2.1.3.3: Reagents for agarose gel electrophoresis

Type of gel	Reagents	Storage
1% agarose gel	0.75 g agarose in 75 ml 1x Tris-acetate-Ethylenediaminetetraacetic buffer + 4 µl ethidium bromide Agarose was dissolved by boiling	Used immediately/4 ˚C for up to 4 weeks
1Kb DNA ladder		
10x Tris-acetate-Ethylenediaminetetraacetic (EDTA) (TAE) buffer	48.4 g Tris base 11.4 ml Glacial acetic acid 3.7 g EDTA Deionised H_2O to 1 L	Room temperature
Ethidium bromide	-	Room temperature
1x TAE buffer	100 ml 10x TAE buffer in 900 ml purite water	Room temperature
10x FastDigest Green buffer		-20 ˚C

2.1.3.4 Bacterial cloning

Table 2.1.3.4: Reagents used in bacterial cloning

Solution	Reagents	Sterilisation method	Storage
Ampicillin	1 g ampicillin made up to 10 ml with ddH2O	-	-20 ˚C
Luria Broth (LB)	4 g Luria broth Lennox in 200 ml deionised water	Autoclave	Room temperature
LB agar	4 g in 200 ml H_2O	Autoclave	Room temperature
LB Ampicillin (LB Amp)	0.1 % ampicillin in LB e.g. 200 µl ampicillin in 200 ml LB	-	4 ˚C
LB amp + X-gal & isopropyl-beta-D-thiogalactopyranoside (IPTG)	4 µl of X-gal + 40 µl IPTG spread onto a set LB amp plate	-	4 ˚C
Super optimal broth with catabolic repressor (SOC)	-	Autoclave	Room temperature

2.1.3.5 Gibson Assembly

Table 2.1.3.5: Reagents required for the Gibson Assembly master mix

Solution	Reagents	Storage
1M DTT	11.6 mg DTT in150 µl water	-20 ˚C
5x ISO buffer	300 µl 1 M Tris-HCl pH 7.5 15 µl of 2 M $MgCl_2$ 6 µl 100 mM dGTP 6 µl 100 mM dATP 6 µl 100 mM dTTP 6 µl 100 mM dCTP 30 µl 100 mM NAD 30 µl 1 M DTT	-
100mM NAD	19.9 mg in 300 µl water	-
Gibson Assembly Master Mix	480 µl 5x ISO buffer 0.96 µl 10 U/µl T5 exo 30 µl 2 U/µl Phusion polymerase (New England Biosciences) 240 µl of 40 U/µl Taq ligase 1.049 ml water	-20 ˚C
Polyethene glycol 8000 (PEG-8000)	150 mg PEG-8000 in 600 µl water	Room temperature

2.1.3.6 Transfections

Table 2.1.3.6: Reagents used for transfections

Solution	Reagents	Sterilisation	Storage
2x BBS	5.33 g BES 14 ml 10 µM $NaCl_2$ 1.5 ml Na_2HPO_4 0.5 M NaOH to 6.95 pH Top up to 500 ml pure water	Filter Sterilised (0.22 µm)	-20 ˚C
Calcium chloride	138.75 g $CaCl_2$ 500 ml water	Filter Sterilised (0.22 µm)	-20 ˚C
Opti-MEM	-	-	4 ˚C
RNAiMax	-	-	4 ˚C

2.1.3.7 siRNA knockdown

Table 2.1.3.8: Reagents and siRNA used for knockdown

siRNA	Target region	Supplier	Storage
ALAS-1		MISSON ® esiRNA Sigma Aldrich	-80 ˚C
Non-Targeted Control (NTC)		MISSON ® esiRNA Sigma Aldrich	-80 ˚C
Opti-MEM™	-	ThermoFisher Scientific	4 ˚C
RNAiMAX	-	ThermoFisher Scientific	4 ˚C

2.1.3.8 Flow cytometry

Table 2.1.3.8: Buffers for flow cytometry

Buffer	Storage
DNA hypoploidy buffer	4 ˚C
Propidium iodide	4 ˚C

2.1.4 Antibodies

Table 2.1.4: Antibody information

Antibody	Type of antibody	Species raised	Manufacturer	Technique
Ab74272 (AR)	Polyclonal IgG	Rabbit	Abcam	ChIP
Ab (AR				Western blot
ALAS-E (D-4)	Monoclonal IgG	Mouse	Santa Cruz Biotechnologies	Western blot
ALAS-H (F-6)	Monoclonal IgG	Mouse	Santa Cruz Biotechnologies	Western blot
FUS	Polyclonal IgG	Mouse	ThermoFisher	Western blot
N-20 (AR)	Polyclonal IgG	Rabbit	Santa Cruz Biotechnologies	ChIP
α-tubulin	Monoclonal IgG1	Mouse	Sigma Aldrich	Western blot
Secondary mouse	Goat-anti-mouse	Goat	Sigma Aldrich	Western blot
Secondary rabbit	Goat-anti-rabbit	Goat	Sigma Aldrich	Western blot

2.1.5 Cell cultures and treatments

2.1.5.1 Cell line information

Table 2.1.5.1: Cell line information

Cell line	Cell type	Derived from	Media	Source
A549	Adenocarcinoma alveolar basal epithelia	58-year-old Caucasian male	DMEM	
22Rv1	Prostate Cancer	Human carcinogenic prostate epithelial CWR22 cells had induced regression and relapse after castration were xenografted and propagated in mice to form 22Rv1 cells.	RPMI	
BPH-1	Benign Prostatic Hyperplasia	Human prostatic epithelial cells obtained from a 68-year-old with benign prostatic hyperplasia. Cells were then immortalised using Simian virus 40 (SV40) Large T Antigen	RPMI	
C4-2	Advanced Prostate Cancer	Human epithelial prostate carcinoma cells, subline of LNCaP. Mixed with osteosarcoma fibroblast cells and inoculated in an athymic mouse.	RPMI	
C4-2b	Metastatic Prostate Cancer	Bone metastasis after transplantation of C4-2 cells into a nude mouse.	RPMI	
COS-1	Fibroblast	African Green Monkey kidney, SV40 transformed.	DMEM	

COLO-205	Colorectal adenocarcinoma	70-year-old Caucasian male derived from a metastatic site	RPMI
DU145	Metastatic Prostate cancer	Epithelial cells derived from the brain of a 69-year-old Caucasian male with metastatic prostate cancer.	RPMI
HEK293	Human embryonic kidney	Foetal derived cells with adenoviral transfection	DMEM
HL-60	Acute promyelocyticytf leukaemia	36-year-old female Caucasian	RPMI
K-562	Chronic Myelogenous Leukaemia	Derived from the blast crisis stage (final phase) of chronic myeloid leukaemia of a 53—year-old Caucasian woman	RPMI
L929	Mouse fibroblast	100-day-old male mouse subcutaneous normal adipose and areolar tissue	RPMI
LNCaP	Early-stage Prostate cancer	Prostatic cell line taken from a 50-year-old Caucasian male using a needle biopsy at his supraclavicular lymph node. Androgen sensitive	RPMI
MCF-7	Breast adenocarcinoma	Derived from metastatic site of 69-year-old Caucasian female	DMEM
PANC1	Pancreatic cancer	Epithelial ductal carcinoma derived from a male 56-year-old Caucasian	DMEM
PC3	Prostate cancer	Grade 4 adenocarcinoma derived from a 62-year-old Caucasian man	RPMI

PC3-GFP	Prostate cancer	PC3 stably transfected with green fluorescent protein (GFP)	RPMI
PNT1A	Normal Prostate Tissue	Post-pubertal normal prostatic cells from a 35-year-old immortalised with SV40	RPMI

2.1.5.2 Media and other cell culture reagents

Table 2.1.5.2: Media and other cell culture reagents

Media/Reagent	Supplier	Additives
Dulbecco's Modified Eagle Medium (DMEM)	Lonza	5ml Penicillin-Streptomycin-Glutamine (PSG) (10 %) 25ml Foetal calf serum (FCS) (10 %)
Hormone and phenol-red free Dulbecco's Modified Eagle Medium	Lonza	5ml Penicillin-Streptomycin-Glutamine (PSG) (10%) 12.5ml Stripped FCS (sFCS) (5 %)
Rosewell Park Memorial Institute (RPMI)	Lonza	5 ml PSG 25 ml FCS
Hormone and phenol-red free Rosewell Park Memorial Institute (stripped RPMI)	Lonza	PSG sFCS
Penicillin-Streptomycin-Glutamine (PSG)	Sigma Aldrich	-
Trypsin EDTA	Lonza BioWhittaker®	-

2.1.5.3 Cellular Treatments

Table 2.1.5.3: Cellular treatment reagents

Inhibitor	Dissolved in	Storage
Bicalutamide	Ethanol	-20 ˚C
Ferrostatin-1	DMSO	-20 ˚C
Hydrogen peroxide	ddH_2O	4 ˚C
Necrostatin-1	DMSO	-20 ˚C
Mibolerone	Ethanol	-20 ˚C
Succinylacetone	ddH_2O	-20 ˚C

2.2 Methods

2.2.1 Cell cultures

2.2.1.1 Cell cultures

Cells were cultured in their corresponding medium (Table 2.4.1) supplemented with 2 mM L-glutamine, 100 U/ml penicillin, 100 mg/ml streptomycin and 10 % FCS. For transfection experiments, COS-1 and HEK were seeded in phenol red-free media supplemented with 2% charcoal-stripped FBS. PC3 cells were plated at a seeding density of 1 x 10^4 cells per well in 12-well plates for inhibitory drug experiments and 2 x 10^5 in 6 well plates for small interfering RNA (siRNA) knockdown experiments. Cells were incubated at 37 ˚C and 5 % CO_2 in air.

2.2.1.2 Cell passaging

2.2.1.2.1 Adherent cells

Cells were passaged when they reached 70 % confluency. Media was removed and cells were washed with 1x PBS. Cells were detached from the flask through the addition of Trypsin-EDTA incubation at 37 ˚C for 2-5 minutes. The cells were resuspended in media and the desired volume was transferred into a new flask with warmed media

2.2.1.2.2 Suspension cells

Suspension cells were passaged once they reached 70 % confluence. Cells were re-suspended and centrifuged at 1500 rpm for three minutes. Supernatant was removed and 10 ml media was added to re-suspend the pellet. 0.5 – 1 ml of suspension was then transferred into a new flask with pre-warmed media.

2.2.1.3 Cell counts and plating

Cells were prepared as described in section 2.1.2.1. and diluted 1 in 10. 10 µl cells were loaded onto a haemocytometer and counted then averaged to give the approximate number of cells per ml. For plating COS-1 cells, cells in a confluent T75 flask were diluted 1:200 prior to seeding in a 24-well plate. Cells were viewed in an Optika or Leica inverted microscope at 4x – 10x objective

2.2.1.4 Freezing/defrosting cells

To freeze cells for storage in liquid nitrogen, cell suspensions (as described in sections 2.2.1.1 and 2.2.1.2) were collected and centrifuged for 3 minutes at 1500 rpm. Media was aspirated and cells were resuspended in freezing solution (10% DMSO in FCS). This was then transferred into a cryovial and wrapped in insulating materials for gradual freezing at -80 ˚C. After 24 hours, cells were transferred to liquid nitrogen.

To defrost cells from liquid nitrogen, stocks were rapidly defrosted at 37 ˚C. The suspension was diluted with warmed media and centrifuged at 1500 rpm for three minutes. The media was aspirated and cells resuspended in fresh media. Cell were then transferred to a new flask containing warmed media. 24 hours later, the media was removed and replaced with fresh media. Cells underwent two passages before being used for experiments to ensure adequate cell health.

2.2.2 Transfections and luciferase reporter assays

2.2.2.1 Calcium phosphate transfections

24-48 hours after plating COS-1, cells were transfected with multiple vectors including TAT-GRE-E1B-Luc, pSVAR, pdmLacZ-Bos-β-gal (or PR1_CMV for DualGlo® Renilla Luciferase Assays) and depending upon the objective of the experiment: pSG5-FUS/pEGFP-C1-FUS,

pSG5-MUT-FUS/pEGFP-C1-MUT-FUS (K510E), pcDNA3.1^{+}-HOTAIR, myc-BioID2-msc WT AR and/or PSG5 empty control. DNA was mixed prior to the addition of $CaCl_2$ and BES-buffered saline solution (BBS) 1:10 volumes respectively. An equal amount of total DNA was added to each treatment, with concentrations adjusted using pSG5 (empty) plasmid. Once BBS and $CaCl_2$ was added, the transfection mix was left to incubate for 15 minutes at room temperature before 100 µl was added dropwise to each corresponding well of the 24-well plate. Cells were incubated for 24 hrs and then washed 2 x with phenol red free media containing 2 % charcoal stripped FCS. Cells were then treated with ligand and left for a further 24 hrs.

2.2.2.2 Treatments following COS-1 transfection

Up to 24 hours following transfection, cells were washed twice and treated with stripped media with the addition of ethanol and mibolerone (0-1000 nM or 1 nM) (Sigma-Aldrich) (or mibolerone (1 nM) and bicalutamide (0-1000 nM) (Sigma-Aldrich) for antiandrogen experiments).

2.2.2.3 Luciferase reporter assays

2.2.3.3.1 Luciferase β-galactosidase dual reporter assay

24 hours following treatments (See section 2.10.1), wells were washed twice with 1 ml of PBS buffer and 60 µl of reporter lysis buffer added per well. This was followed by a freeze-thaw cycle at -80 ˚C for 15 minutes. For the β-galactosidase assay, 5 µl of the lysate from each well were then transferred into a 96-well white Opti-plate along with 50 µl of a 1:100 mix of Tropix® Galacton plus and Tropix® Galacto reaction buffer diluent respectively. After an hour on a shaker, 75 µl Tropix® accelerator II was aliquoted. For the luciferase reporter assay, 20 µl of lysate was transferred into a 96 well white Opti Plate, added to this was 20 µl of luciferase

substrate (luciferin). Plates were read on a FLUOstar Omega plate reader and luciferase data were normalised to β-galactosidase data.

2.2.3.1.2 Renilla luciferase assay

An alternative Dual Glo® (Promega) luciferase reporter assay was also used for some experiments. Cells were lysed in 50 µl of 1x passive lysis buffer and incubated at room temperature for 30 minutes. 20 µl of lysate and 20 µl of Dual-glo® was added to a 96-well Opti Plate. After 10 minutes of incubation, the plate was read. 20 µl StopandGlo® was then added and the plate was read on after 10 minutes using a FLUOstar Omega plate reader.

2.2.4 Protein preparation and sodium dodecyl sulphate polyacrylamide gel electrophoresis

Firstly, separating and stacking gels were prepared (Table 2.1.3.2), Cell lysates were prepared through the addition of lysis buffer (Promega Reporter lysis buffer) and a freeze-thaw cycle at -80 ˚C. Absorbance (280 nM) was measured using a NanoDrop. Alternatively, a DC™ protein assay (Bio-Rad) was used to determine protein concentrations. Cells were lysed by removing media from cells and adding 60 µl RIPA mixed with protease inhibitors added (HALT, 1:100 dilution). The assay was performed according to the manufacturer's instructions and the plate was read at 650 nm on a FLUOstar Omega plate reader. For both methods, the absorbance from known concentrations of BSA were utilised to generate a standard curve and protein concentrations calculated. Equal concentrations of protein (30 µg) were prepared for loading, with the addition of loading dye. Proteins were denatured by heating to 95 ˚C for 5 min and immediately transferred to ice for a minimum of 2 minutes followed by vortexing and centrifugation. Samples were separated at 100 volts for approximately 2 hours.

2.2.5 Protein transfer to PDVF membrane and western blotting

Proteins separated by SDS-PAGE were then transferred onto a PDVF membrane (Amersham™ Hybond™), activated by methanol. The transfer was left for 2 hours at 15 V. The membrane was blocked using 0.5 % milk powder (Marvel™) dissolved in 0.1 % mix of Tween®-20 (Sigma Aldrich) and PBS. The membrane was probed using polyclonal rabbit anti-AR ab74272 antibody (Abcam), mouse monoclonal anti-FUS (4H11) antibody (Santa Cruz Biotechnology), mouse monoclonal anti-ALAS1 (Invitrogen, Santa Cruz Biotechnologies) or mouse anti-ALAS2 (Invitrogen, Santa Cruz Biotechnologies) and mouse monoclonal anti-β-tubulin (Sigma-Aldrich). Secondary antibodies tagged with horseradish peroxidase were used for detection with Millipore Luminata™ ClProteins separated by SDS-PAGE were transferred onto a PVDF membrane (Amersham™ Hybond™), activated with methanol. The membrane was blocked using 5 % milk powder (Marvel™) dissolved in 0.1 % Tween®-20 PBS. The membrane was probed using polyclonal rabbit anti-AR ab74272 antibody (Abcam), mouse monoclonal anti-FUS (4H11) antibody (Santa Cruz Biotechnology), mouse monoclonal anti-ALAS1 (Invitrogen, Santa Cruz Biotechnologies) or mouse anti-ALAS2 (Invitrogen, Santa Cruz Biotechnologies) and mouse monoclonal anti-β-tubulin (Sigma-Aldrich). Secondary antibodies tagged with horseradish peroxidase were used for detection with Millipore Luminata™ Classico/Forte Western HRP Substrate by the ECL method and visualised on a Fusion FX chemiluminescence detection system.

2.2.6 Bacterial cloning

2.2.6.1 Cloning of plasmids used throughout the study

2.2.6.1.1 The Cloning of The Human Wild Type Androgen Receptor into myc-BioID2-mcs

The AR was cloned into myc-BioID2-mcs (a kind gift from from M. Metodiev, Essex University) in frame of BioID2 using PCR amplification and Gibson Assembly. Firstly, the AR insert was amplified from the pSVAR plasmid in PCRBio Ultra Mix. The initial PCR step was 95 ˚C for 15

seconds followed by cycling conditions of 95 ˚C for 15 seconds, 72 ˚C for 15 seconds and 72 ˚C for 3 minutes for a total of 35 cycles. This was followed by a final cycle at 72 ˚C for 5 minutes. The myc-BioID2-mcs vector was then amplified using One Taq HotStart Polymerase. Gibson assembly primers can be seen in Table 2.2.6.1.1. The PCR cycling parameters included an initial denaturation of 94 ˚C for 30 seconds, 35 cycles of 94 ˚C for 30 seconds, 70 ˚C for 30 seconds and 68 ˚C for 6 minutes and 20 seconds followed by a final inubation at 68 ˚C for 10 minutes. The insert and vector were purified using the Monarch PCR Clean-up Kit (5 µg) (New England Biolabs). The purified products were combined with Gibson assembly master mix and incubated for 1 hour at 50 ˚C. XL1-blue competent bacteria were slowly defrosted on ice and transformed using 2 µl of Gibson assembly mix (see section 2.2.6.5 for transformation method). Minipreps were performed using an RBC Bioscience HiYield™ Plasmid Mini Kit followed by restriction enzyme digestion (FastDigest ThermoFisher Scientific) and sequencing to distinguish positive clones.

Table 2.2.6.1.1 Gibson Assembly primers for Androgen Receptor in myc-BioID2-msc

Primer	**Primer Sequence (5'-3')**
Insert Forward	GAGCGGCCGCCACTGTGCTGGATATCTGCAATGGAAGTGCAGTTAGGG
Insert Reverse	TAGTCCAGTGTGGTGGAATTCTCACTGGGTGTGGAAATA
Vector Forward	GAATTCCACCACACTGGA
Vector Reverse	TGCAGATATCCAGCACAG

Table 2.2.6.1.2: Traditional cloning primers and their incorporated restriction enzyme sequence

Primer	**Restriction enzyme**	**Primer Sequence (5'-3')**
ALAS-1 FL Forward	NheI	GCTAGCATGGAGAGTGTTGTTCGCC
ALAS-1 T Foward	HindIII	GCTAGCATGGCAGCAGTACACTACCAACAG
ALAS-1 FL/T Reverse	HindIII	CCCAAGCTTGGGTCAGGCCTGAGCAGATACCAACT
ALAS-2 FL Forward	NheI	GCTAGCATGGTGACTGCAGCCATG
ALAS-2 T Forward	NheI	GCTAGCATCCACCTTAAGGCAACAAAG
ALAS-2 FL/T Reverse	HindIII	CCCAAGCTTGGGTCAGGCATAGGTGGTGACATA
HOTAIR Forward	NotI	GGGGTACCCCCCAGTTCTCAGGCGAGAGC
HOTAIR Reverse	KpnI	TTGCGGCCGCAATTTATATTCACCACATGTAAAACTTTATT

2.2.6.1.2 The cloning of HOTAIR into pcDNA3.1^{+}

HOTAIR was synthesised by TWIST Bioscience into plasmid p-twist31_Amp HOTAIR was then cloned into pcDNA3.1^{+} in frame with the T7 promoter using PCR amplification. Primers were designed using the OligoPerfect™ online tool (Invitrogen, ThermoFisher Scientific) with incorporated *NotI* and *KpnI* restriction sites.

2.2.6.1.3 The cloning of ALAS-1 and ALAS-2 truncated and full length into pET-28a^{+}

ALAS-1 was amplified using PCR from pCMV3_ORF-ALAS1 plasmid (Sino Biological Inc.) and ALAS-2 was amplified using cDNA obtained from K562 cells. Full length (amino acids 1-641) and a truncated version (amino acids 49-641) lacking the NTD were cloned for protein purification and X-ray crystallography techniques. pGEM-T Easy (Promega) was utilised as an intermediate vector before the inserts were transferred into the desired pET28a^{+} plasmid. Primers were designed using SnapGene® Viewer 4.1. The sequence of the cloning primers can be found in Table 2.2.6.1.2.

2.2.6.1.4 Agarose gel electrophoresis, gel extractions and PCR clean-ups

Following the PCR reactions, samples were loaded into a 1 % low-melt agarose gel with a 1 kb DNA ladder to ensure correct sizing of plasmid vector or insert. Gels were run at 70 mV. Bands were visualised using a Flowgen ultraviolet light box. Gel extractions were performed using a QIAEX® II Gel Extraction Kit or HiYield™ Gel/PCR Fragments Extraction Kit-300. PCR clean-ups were also performed using a Monarch® PCR and DNA Clean Up kit.

2.2.6.1.5 Restriction enzyme digestion and alkaline phosphatase reactions

Prepared DNA from PCR reactions and either gel extractions or PCR clean ups were utilised for restriction enzyme digestion reactions. FastDigest enzymes (ThermoFisher Scientific) were used and the digested DNA gel extracted using QIAEX® II Gel Extraction Kit or HiYield™ Gel/PCR Fragments Extraction Kit-300. FastAP Thermosensitive Alkaline Phosphatase reaction was performed to prevent plasmid re-ligation. Enzymes and kits procedures were followed according to the manufacturers' instructions.

2.2.6.1.6 pGEM-T Easy and plasmid ligations

Once DNA was purified from either a gel extraction or PCR clean-up, it was ligated into pGEM. An online tool (Promega) was used to calculate insert:vector ratio for ligation reactions. Usage information from the manufacturer was followed for the DNA ligase. This included 5 µl 2x Rapid ligation buffer, T4 DNA ligase, 1 µl pGEM®-T Easy vector (50 ng), PCR product, 1 µl T4 DNA ligase and RNAse free water to a final volume of 10 µl. This reaction was usually left overnight for maximal efficiency or incubated at room temperature for 1 hour.

2.2.6.1.7 Bacterial transformations

Ligation products were used to transform XL blue competent *Escherichia coli* (Promega). 50 µl of bacteria cells were incubated with 2 µl of the ligation reaction on ice for 30 minutes. Cells were then heat shocked at precisely 42 ˚C in a water bath for 45 seconds and placed immediately on ice for 2 minutes. To aid cell recovery, 450 µl SOC media was added and cells were left to incubate for 1 hour and a half for pGEM®-T Easy vectors and 1 hour for all other vectors, with shaking. Cells were pelleted, resuspended in 50 – 100 µl LB and spread onto a LB agar plate supplemented with the desired antibiotic (Table 2.2.6.5). For pGEM®-T Easy transformations, 40 µl X-gal (20 mg/ml) and 4 µl IPTG (200mg/ml) were spread onto LB agar

plates and left to soak into the agar for a minimum of 30 minutes before cell spreading. Plates were placed in an incubator at 37 ˚C overnight. Once the colonies were of a sufficient size, individual colonies (white if blue-white screening was performed) were carefully selected using a sterile tip and LB, containing the required antibiotic, inoculated. This was left to incubate overnight before DNA harvesting using a miniprep kit. Glycerol stocks were produced by mixing 800 µl of overnight cultured cells with 200 µl of glycerol and placed in -80 °C for storage.

Table 2.2.6.1.7: Plasmids and their antibiotic resistance

Plasmid	**Resistance**
Myc-BioID2-mcs	Kanamycin
pcDNA3.1^{+}	Ampicillin
pET28a^{+}	Ampicillin
pGEM®-T Easy	Ampicillin
pSVAR	Ampicillin

2.2.6.1.8 Mini preparations, DNA digestion and DNA sequencing

Bacterial cells prepared as described in the previous section were used for plasmid extraction. 4.5 ml of bacteria were centrifuged at 5000 rpm for 5 minutes and DNA was harvested using HiYield™ Plasmid Mini Kit. The kit was followed according to the manufacturer's instructions. To ensure the insert was successfully ligated, restriction enzyme digests (FastDigest – ThermoFisher Scientific) were performed and DNA separated on a 1 % agarose gel along with the uncut plasmid for comparison. Once confirmed, DNA was sequenced for further confirmation (SourceBioScience or Eurofins Scientific).

2.2.6.1.9 Midi preparations

Once sequencing was confirmed as correct, a midi preparation was performed to generate larger quantities of DNA for use in further experiments. Midi preparations (Kit: Fast Ion™ Plasmid Midi Advanced Kit) were carried out according to the manufacturer's guidelines.

2.2.6.1.10 Reverse-Transcriptase Polymerase Chain Reaction

RNA extraction of K562 cells was performed using Monarch RNA Extraction Kit (New England Biolabs). 250 ng of RNA was used for the reverse-transcriptase PCR (RT-PCR) reaction, 1 µl oligoDTs (10 mM) and double distilled water (to 12.5 µl), was incubated for 5 minutes at 65 ˚C. After this, 4 µl 5x reaction buffer, 0.5 µl RNAse riboblock inhibitor, 2 µl dNTP (10 mM) (ThermoFisher Scientific) and 1 µl reverse transcriptase (ThermoFisher Scientific) added. This was incubated for 5 minutes at 65 ˚C, 42 ˚C for 1 hour and 70 ˚C for 10 minutes. This cDNA was then used for further PCR and qPCR reactions.

2.2.6.1.11 Polymerase Chain Reaction

Usually, Polymerase Chain Reaction (PCR) reactions were carried out using the standard protocol for REDTaq ® DNA polymerase ReadyMix (Sigma Aldrich) for 35 cycles unless otherwise stated.

2.2.7 siRNA knockdown transfections

PC3 cells were seeded in a 6-well plate at a density of 2 x 10^5. 24 hrs after plating, 95 µl of Opti-MEM (ThermoFisher Scientific) was combined with 5 µl of either non-targeting control (NTC) or ALAS1 siRNA. In addition, 6.81 µl of RNAiMAX (Invitrogen ThermoFisher Scientific) was mixed with 293.19 µl of Opti-MEM. These mixtures were then combined to make a total volume of 200 µl and incubated for 15 minutes at room temperature before adding to the cells. Cells were harvested after 72 hours and expression levels measured using western blotting and qPCR techniques from protein lysates and RNA extractions respectively.

2.2.8 Cell treatments

2.2.8.1 Succinylacetone treatment of BPH-1 cells

Firstly, to investigate whether inhibiting haem synthesis would affect normal tissues, BPH cells were treated with SA (50 nM). After 6 days, cells were treated with ± H_2O_2 (0-500nM) and left to grow for a further 24 hours before preparation for flow cytometry and cellular death readings using propidium iodide and DNA hypoploidy assays.

2.2.8.2 Co-treatment of PC3 cells with succinylacetone, necrostatin-1 and ferrostatin-1

Cells were plated at a seeding density of 2 x10^3 per well in 96-well plates and left for 24 hours before treatment. Ferrostatin-1 (40 µM) or necrostatin-1 (10 µM) and a dose range of

succinylacetone were subsequently added to the cells. Cells were left to proliferate for 6 days before crystal violet staining procedures were performed (section 2.10).

2.2.8.3 Treatment of cells in preparation for flow cytometry analysis of cell death induced by succinylacetone

To highlight a primary cellular death pathway upon haem synthesis inhibition by SA, cells were plated in a 12-well plate at a seeding density of 40,000 $x10^5$ /ml with RPMI supplemented with 10 % FCS and PSG. Cells were left for 24 hours prior to treatments. PC3 cells were treated with DMSO, ± SA (100 nM), ± Necrostatin-1 (40 nM) and ± Ferrostatin-1 (10 nM). DMSO was used as a control. Cells were left for a further 6 days before harvesting for flow cytometry using propidium iodide and DNA hypoploidy assays using Accuri C6 software (section 2.9). Cells density was also assessed using crystal violet staining (Section 2.12).

2.2.8.4 Mimicking hypoxic conditions in cancer cells and treatment with succinylacetone in PC3 cells

To investigate the effects of ROS and haem inhibition on cellular survival, PC3 cells were treated with DMSO, or SA (100 nM)., Cells were incubated for 5 days before treatment with H_2O_2 (300 mM). Cells were left for a further 24 hours before harvesting for flow cytometric analysis.

2.2.8.5 Investigation of succinylacetone treatments on other cancerous cell lines

To elucidate whether targeting ALAD affects the proliferation of other types of cancer, a SA dose range was performed. Cells were plated in 96-well plates at a seeding density of 4000 $x10^5$ cells /ml and left for 24 hours before treatment. Cells were stained using the crystal violet technique after 6 days of incubation.

2.2.9 Flow cytometry assays

Flow cytometry was used to determine the levels of necroptosis and apoptosis using Accuri C6 software.

2.2.9.1 Determining necroptosis levels

To harvest, cells, media was collected in a 1.5 microcentrifuge tube. Cells were then washed using 200 µl PBS buffer, which was also collected into its corresponding tube. To detach the cells from the wells, 100 µl of trypsin was added and left to incubate for 3 minutes. 500 µl of the media and PBS collected as before was added to aid removal of cells in trypsin. After pipetting multiple times, the mixture was transferred back into its tube. 10 µl of propidium iodide (PI) was added and cells were lightly vortexed prior to reading on a flow cytometer.

2.2.9.2 Apoptotic measurements

Cells were prepared as mentioned in the previous section. Cells were then centrifuged at 1500-2000 rpm for 4 minutes and media was removed before being resuspended in 200 µl DNA hypoloidy buffer. Cells were vortexed lightly before being read on a flow cytometer.

2.2.10 Cell fixing and the crystal violet growth assay

The effect of treatments on cellular growth of adherent cells was determined using crystal violet assays. This included ALAS-1 knockdown following transfection using siRNA (Section 2.9), succinylacetone with necrostatin-1 or ferrostatin-1 (Sections 2.10.4 and 2.10.5) and growth assays of a variety of cells after treatment with a range of SA concentrations (section 2.10.7, Primarily, adherent cells were fixed using 2% paraformaldehyde (PFA). Cells were left at room temperature for one hour before being washed three times in distilled water. After the

plates were air-dried, 50 µl (for a 96 well plate), 100 µl (for a 12 well plate) or 300 µl (for a 6 well plate) of crystal violet dye (0.04 % in PBS) was added to the well and cells were left at room temperature for an hour. Plates were then washed again three times in distilled water. 100 µl of 10 % acetic acid was added to 96 well plates and left to incubate for one hour with shaking. Absorbance was read on a plate reader (FLUOstar Omega) at 590 nm wavelength.

2.2.11 Quantitative Polymerase Chain Reaction (qPCR)

A Monarch® Total RNA Miniprep Kit was used to obtain RNA following manufacturer's guidelines. This RNA was utilised to create cDNA (see section 2.2.6.1.10). The National Centre for Biotechnology Information (NCBI) nucleotide database was used as a basis for primer design. SnapGene Viewer version 4.1 and OligoPerfect (ThermoFisher) were used to aid design and predict melting temperatures. Primers were synthesised using Eurofins Genomics Germany and their sequences for qPCR experiments can be found in Table 2.2.14.1. Gene expression was analysed using SsoAdvanced™ Universal SYBR® Green Supermix (BioRad) and a LightCycler® 96 (Roche) instrument. qPCR experiments were performed in triplicates on the same plate along with endogenous control genes including L19 and KLK2. Cycling conditions for these experiments firstly started with a polymerase activation and cDNA denaturation step for 30 seconds at 95 °C followed by a two-step amplification including 15 seconds at 95 °C (denaturation) and 20 seconds at 60 °C (extension, annealing and plate read) for 35 cycles. These cycles were lastly proceeded by a melt curve analysis at 95 °C at a ramp rate of 0.5 °C increments. Data were analysed to calculate C_q values of the gene of interest.

Table 2.2.11: Quantitative Polymerase Chain Reaction primers

Target	**Primer Sequence (5'-3')**
ALAS-1 Forward	AAATGAATGCCGTGAGGAAAGA
ALAS-1 Reverse	CCCTCCATCGGTTTTCACACTA
ALAS-2 Forward	TGTCCGTCTGGTGTAGTAATGA
ALAS-2 Reverse	GCTCAAGCTCCACATGAAACT
Androgen Receptor Forward	CAGTGGATGGGCTGAAAAAT
Androgen Receptor Reverse	AAGCGTCTTGAGCAGGATGT
KLK2 Forward	TCGGCACAGCCTGTTTCAT
KLK2 Reverse	TGGCTGACCTGAAATACCTGG
L19 Forward	GCGGAAGGGTACAGCCAAT
L19 Reverse	GCAGCCGGCGCAAA

2.2.15 Protein expression in BL21(DE3) Cells

ALAS constructs were cloned into pET28a^{+} plasmid (see section 2.3.3). The cloning strategy was designed to ensure that the genes were in frame with the histidine (His)-tag at the 5' end. Recombinant DNA assemblies were expressed in BL21(DE3) *Escherichia coli* bacteria strain. Cells were incubated in LB with kanamycin (50 mg/ml) and left to grow to a density of 0.4 – 0.5 at 600 nm (WPA Biowave CO8000 Cell Density Meter). Once reached, cells were induced with the addition of 0.5 nM IPTG for either 4 hours at 37°C or overnight at 18 °C. Cells were harvested by centrifugation (5 minutes at 5000 xg) and pellets frozen at -20 °C. Bacteria were thawed and resuspended in 3 ml of PBS and sonicated (Bioruptor® Plus) (30 seconds on and 30 seconds off). Expression was verified using SDS-PAGE (10 % acrylamide) followed by Coomassie brilliant blue-G250 staining (Fisher Scientific UK).

2.2.16 Confocal microscopy

To investigate the localisation of the AR with FUS-wild type (WT) or Mutant (Mut)-FUS within the cell, COS-1 cells were seeded in 24 well plates on cover slips (ThermoFisher Scientific) at approximately 30 % confluency. Cells were transfected with pSVAR, pEGFP-FUS-WT and/or pEGFP-MUT-FUS using Turbofect Transfection Reagent (ThermoFisher Scientific). After 24 hours, cells were washed with stripped DMEM and treated with 1 nM mibolerone for 4 hours. Cells were washed 3 times in PBS and fixed using 4 % paraformaldehyde for 15 minutes. Wells were washed again 3 times in PBS. 0.1 % Triton X-100 was added and cells incubated for 10 minutes followed by a further 3 washes with PBS. Cells were then blocked with 1 % BSA (in PBS-T) followed by an hour incubation with rabbit polyclonal AR antibody (ab74272). The wells were again washed 3 times prior to blocking and incubation with secondary antibody (568 nm) for 1 hour. Finally, wells were washed in PBS 3 times and cover slips mounted onto glass slides (VWR, counterstained using DAPI and viewed using a Nikon Eclipse Ti Confocal Microscope.

2.2.17 Graph formation and statistical analyses

Graphs were created using Microsoft Excel. Two-Tailed paired T-tests were used to determine the significance between the data for individual experiments to a significance level of $p = <0.05$.

Chapter 3. Results – Androgen Receptor Regulation - Investigating the effect of FUS and HOTAIR on the AR

3.1 Optimisation of Conditions for Luciferase Reporter Assays

The AR is thought to be the principle driver of PCa and hence therapies often aim to target this signalling axis. Unfortunately, these therapeutics invariably fail and the disease progresses to the aggressive CRPC stage, but importantly, the AR appears to continue to drive tumour growth. Therefore, further understanding AR signalling may aid in the development of novel therapeutics, especially for CRPC. FUS is a multifunctional protein that has been shown to act as a tumour suppressor in PCa (Brooke *et al.,* Unpub.). Paradoxically it has also been demonstrated to act as a co-activator of the AR (Haile *et al.*, 2011). The role of FUS in PCa and AR signalling is unclear due to its apparent dual function which is not well understood. Some lncRNAs are also known to interact with the AR (Misawa *et al.*, 2017) but the effects of this type of RNA on AR activity are not completely recognised. Therefore, the role of FUS and lncRNA on AR function requires further characterisation.

Optimisation of the concentration of synthetic androgen, mibolerone was firstly performed using luciferase reporter assays. COS-1 cells were used as they are AR negative. Cells were transfected with plasmids encoding the AR (pSVAR), a luciferase reporter under the regulation of an androgen response element (TAT-GRE-E1B-LUC-1) as well as a control expression vector, β-galactosidase (PDM-Lac-Z-β-GAL). Results were normalised to β-galactosidase expression and the activity of the receptor in the presence of 1000 µM mibolerone was set as 100%.

A mibolerone dose range, using a final concentration of 0 – 1000 nM (Figure 3.1a), demonstrated that AR activity increased as mibolerone concentration increased and plateaued at 1 nM. It was therefore decided that 1 nM mibolerone would be used for all future experiments. AR expression was confirmed using western blotting (Figure 3.1b). The

immunoblot demonstrated that AR levels are barely detectable in the absence of mibolerone (ethanol) and expression and that levels increased as mibolerone concentrations increased.

Next, to optimise AR concentrations, a dose range of 0 – 200 ng pSVAR was transfected into COS-1 cells, exposed to either ethanol as a control or 1 nM mibolerone (Figure 3.1b). Maximal activity of the AR was seen when cells were transfected with 100 – 200 ng of psVAR, therefore 100 ng was selected for future experiments. AR expression was again confirmed using western blot analysis. As expected, no AR expression in the presence of mibolerone at all concentrations with the AR. At the highest concentration, AR was not expressed when cells were not transfected with pSVAR. At 50 and 100 ng pSVAR, AR was only visible when cells were treated with mibolerone. In contrast, AR was detectable in the presence and absence of mibolerone when cells were transfected with pSVAR, with levels noticeably higher when the cells were treated with hormone. From this dose range, pSVAR at 100 ng was selected for future studies.

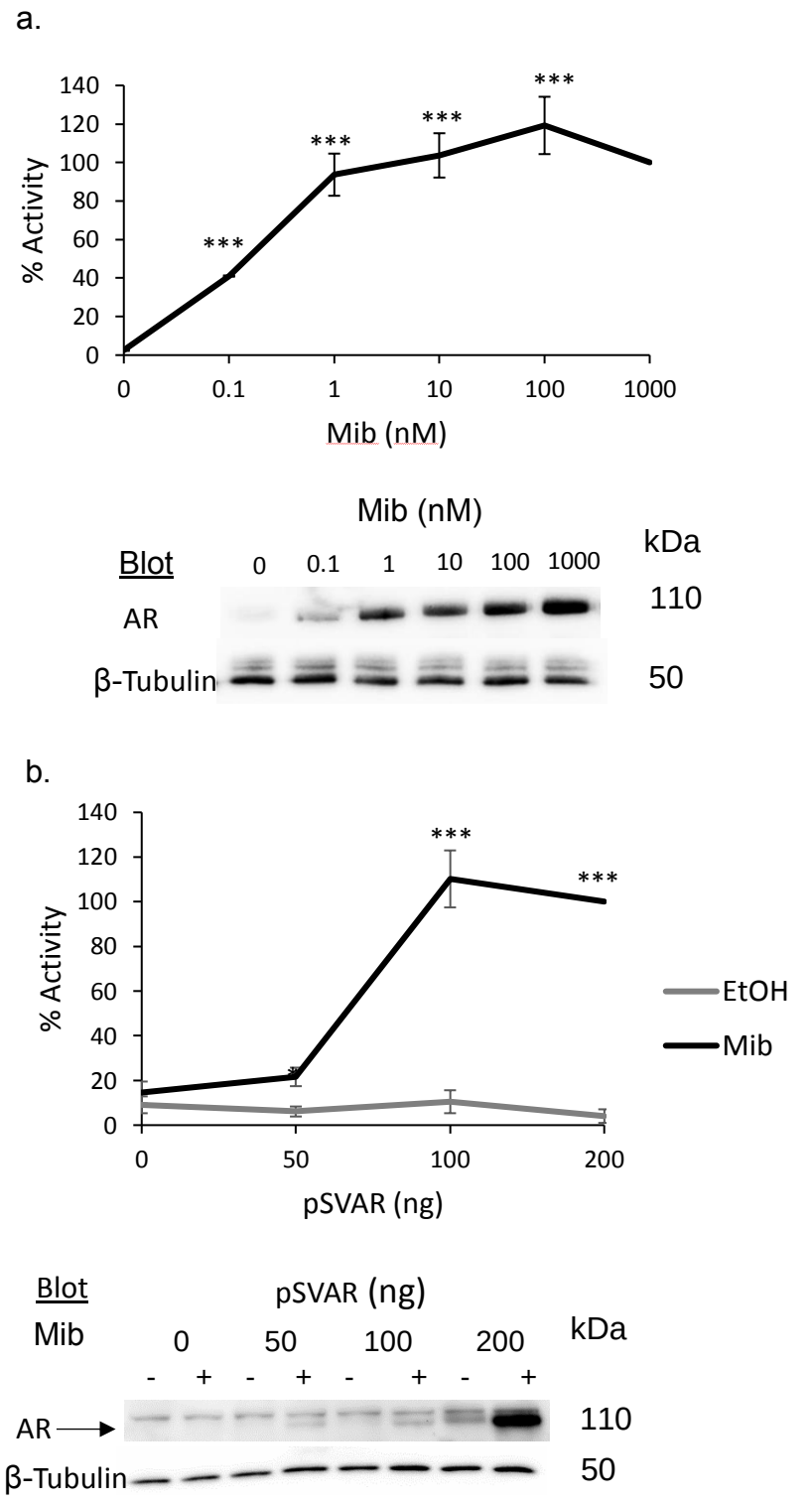

Figure 3.1: Optimisation of mibolerone and Androgen Receptor concentrations for COS-1 transfections. COS-1 cells were transfected with wild type human Androgen Receptor (AR) using the pSVAR plasmid, a luciferase reporter tagged to an Androgen Response Element (TAT-GRE-E1B-LUC) and β-galactosidase control expression vector (PDM-Lac-Z-β-GAL) ± FUS (PSG5-FUS). All treatments contained equal amounts of DNA, altered using empty PSG5 plasmid. Cells were plated in a 24-well plate and treated after 24 hours. Data from luciferase readings were normalised using the results from the β-galactosidase control assay. Statistical significance was calculated using T-Tests (* = P < 0.05, ** P < 0.005 and ***

= P < 0.005) a. (Left) Mibolerone dose range from 0 - 1000 nM. Averages of the mean ± standard error were calculated from four individual repeats. (Right) Western blot demonstrating AR expression. b. (Left) AR dose range from 0 – 200 ng. Averages of the mean ± standard error were calculated from three individual repeats. (Right) Western blot showing AR expression. Black arrow indicates location of AR. c. (Left) FUS dose range from 0 - 200 ng. Averages of the mean ± standard error were calculated from three individual repeats. (Right) Western blot showing successful FUS expression.

3.2 FUS Represses Androgen Receptor Activity

As described previously, FUS has been shown to interact with the AR and to act as a co-activator (Haile *et al.*, 2011) but it also appears to be a tumour suppressor in PCa (Brooke, *et al.,* Unpub.). The role that FUS plays within this disease and how the activity of the AR alters when it is present is not fully understood. To investigate the effects of FUS upon AR activity, luciferase assays were performed (Figure 3.2a and Figure 3.2b). COS-1 cells were transfected with plasmids encoding the AR (pSVAR), a luciferase reporter (TAT-GRE-EIB-LUC), β-galactosidase and a dose range of PSG5-FUS. In the presence of mibolerone, AR activity increased and this was significantly reduced when cells were transfected with 100 ng and 200 ng of pSG5-FUS (Figure 3.2b). To ensure FUS was successfully expressed, immunoblots were performed which demonstrated that levels were notably higher when cells were transfected with of pSG5-FUS. FUS therefore appears to be a repressor of AR activity.

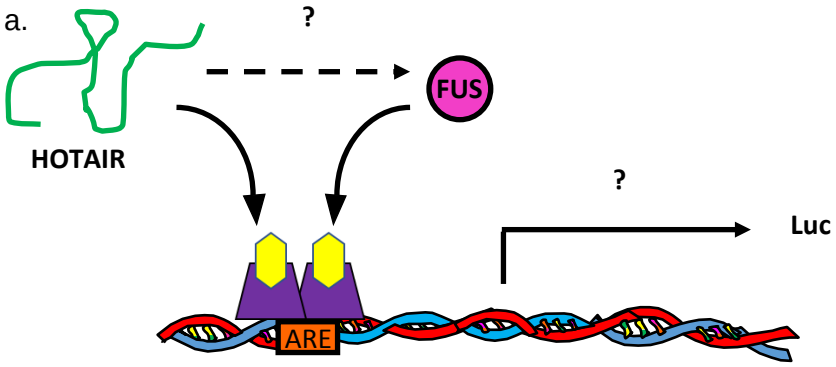

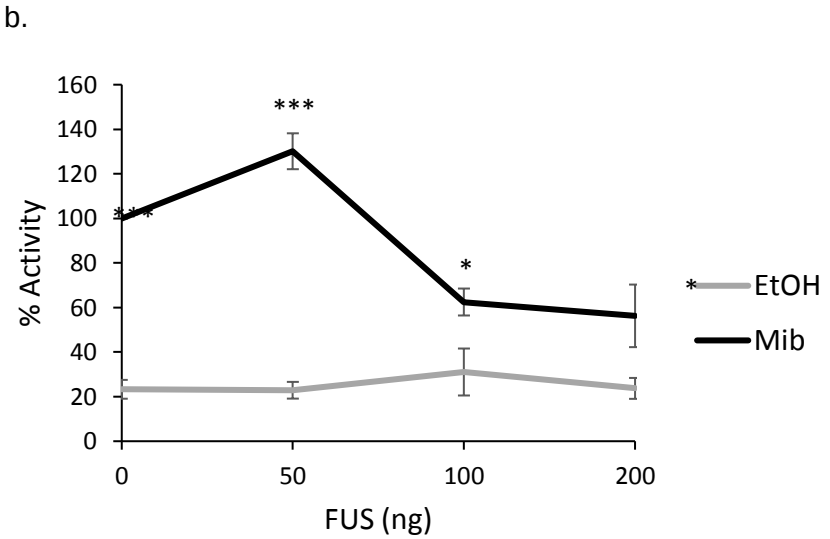

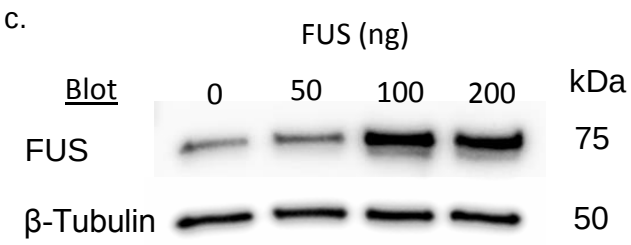

Figure 3.2: Fused in Sarcoma acts as an Androgen Receptor co-repressor. COS-1 cells were transfected with wild type human Androgen Receptor (AR) using the pSVAR plasmid, a luciferase reporter tagged to an androgen response element (TAT-GRE-E1B-LUC) and β-galactosidase control expression vector (PDM-Lac-Z-β-GAL) ± FUS (pSG5-FUS). All treatments contained equal amounts of DNA, altered using empty PSG5 plasmid. Cells were plated in a 24-well plate and treated after 24 hours. Data from luciferase readings were normalised using the results from the β-galactosidase control assay. Statistical significance was calculated using T-Tests (* = $P < 0.05$, ** $P < 0.005$ and *** = $P < 0.005$). c. (Left) FUS dose range from 0 - 200 ng. Averages of the mean ± standard error were calculated from three individual repeats. (Right) Western blot showing successful FUS expression.

3.3 The Effect of a Fused in Sarcoma Mutant on Androgen Receptor Activity and Localisation Within The Cell

Results from Figure 3.2 demonstrated that FUS represses AR activity and its expression has been found to be inversely correlated with the Gleason Grade (Brooke *et al.*, 2011). To investigate if FUS expression is lost in CRPC, Brooke *et al.,* (Unpub.) performed immunohistochemistry on PCa samples which were therapy sensitive and therapy resistant. Surprisingly, FUS levels were elevated in CRPC, but the protein was found to be partially cytoplasmic as well as nuclear (Brooke et al., Unpub.). Therefore, it was hypothesised that altered localisation of FUS may reduce its repressive activity upon AR signalling, contributing to CRPC progression. To investigate this, a mutation (K510E) was introduced into the FUS NLS (Figure 3.3a) using site-directed mutagenesis and the mutation was verified by sequencing (Figure 3.3b and Figure S1.1). This mutation was selected as it is a naturally occurring mutation in amyotrophic lateral sclerosis and it has been previously shown to interact weakly with transportin, thus creating a partially cytoplasmic protein (Niu *et al.*, 2012).

To investigate if the K510E mutation affected FUS localisation, COS-1 cells were transfected with pSVAR, pEGFP-C1-FUS-WT or pEGFP-C1-FUS-K510E. Cells were left for 48hrs post-transfection and treated with 1 nM mibolerone. Fixed cells were probed with a primary antibody specific for the AR followed by a fluorescently labelled secondary antibody. Slides were counterstained with DAPI and visualised using fluorescent microscopy (Figure 3.3c). Empty GFP was found to be partially nuclear and partially cytoplasmic. As expected, GFP-FUS-WT was nuclear. The FUS K510E mutant was found to be nuclear and partially cytoplasmic. The AR in the presence of WT FUS or mutant FUS remained nuclear in both cases and the receptor appeared to colocalise with both forms of FUS in the nucleus.

FUS-K510E mimics the localisation of FUS in CRPC. To see if the varied cellular localisation of FUS altered AR activity, luciferase reporter assays were performed. COS-1 cells were transfected with an AR expression plasmid (pSVAR), a luciferase reporter under the regulation of an androgen response element (TAT-GRE-E1B-LUC-1), PSG5-FUS-WT or PSG5 –FUS-

K510E and a β-galactosidase expression vector (PDM-Lac-Z-β-GAL). Results were normalised to β-galactosidase expression. WT and mutant FUS repressed AR activity to similar levels, demonstrating that the K510E mutation did not affect the ability of FUS to repress AR activity (Figure 3.3d).

a.

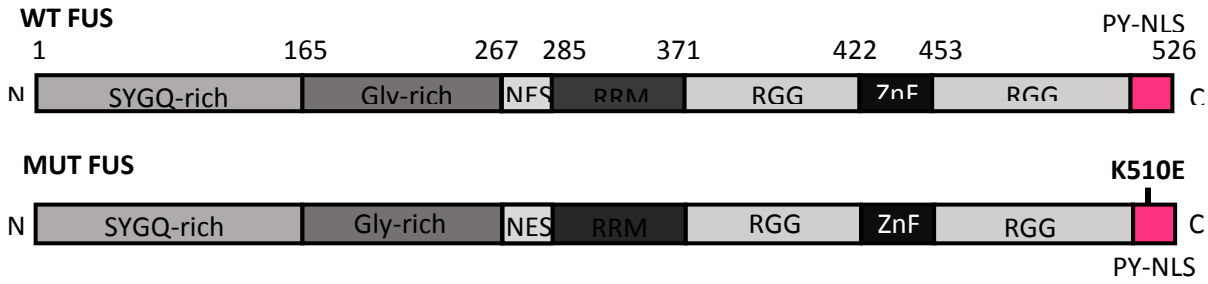
WT FUS
1
165
267
285
371
422
453
PY-NLS
526
N
SYGQ-rich
Gly-rich
NES
RRM
RGG
ZnF
RGG
C
MUT FUS
K510E
N
SYGQ-rich
Gly-rich
NES
RRM
RGG
ZnF
RGG
C
PY-NLS

b.

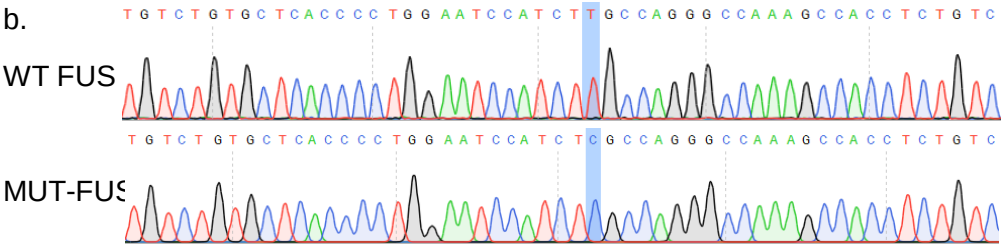
WT FUS
MUT-FUS

c.

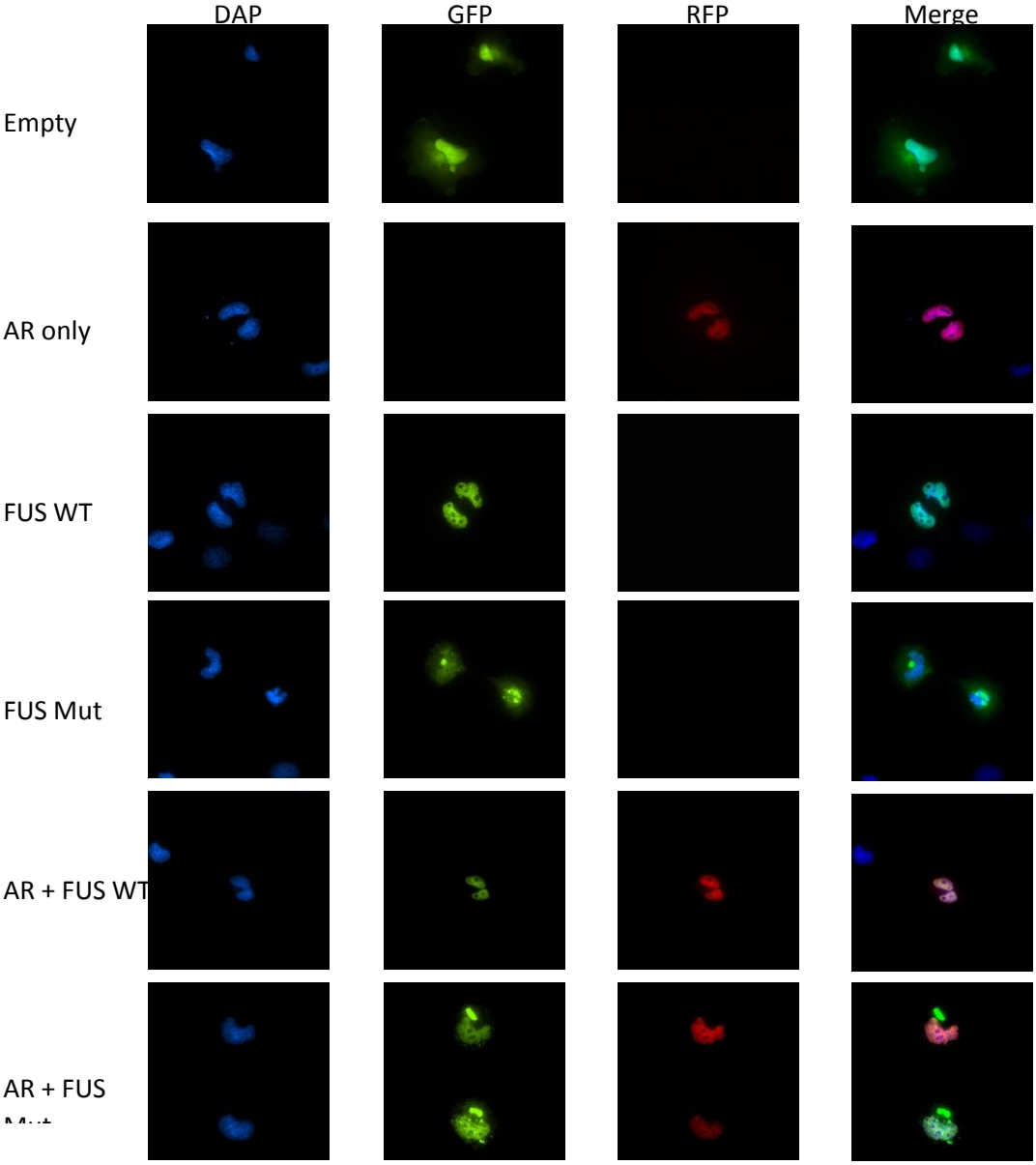
DAP
GFP
RFP
Merge
Empty
AR only
FUS WT
FUS Mut
AR + FUS WT
AR + FUS

d.

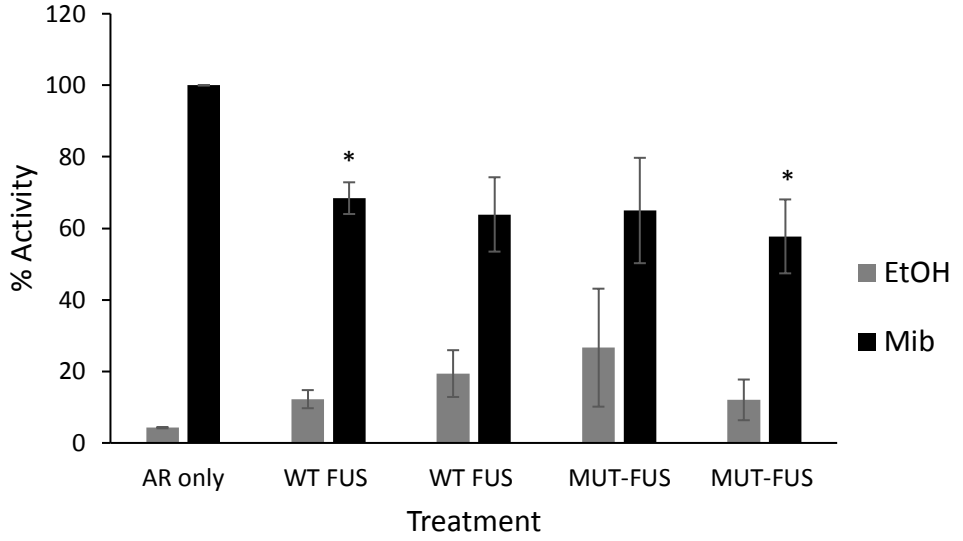

AR	+	+	+	+	+
FUS	0	50	100	0	0
FUS-Mut	0	0	0	50	100

Figure 3.3: Fused in Sarcoma mutant (K510E) effects on the transcriptional activity of the wild type Androgen Receptor. a. Schematic of WT FUS and FUS mutant (K510E). Mutation was introduced to into the nuclear localisation sequence towards to C-terminal domain. b. Chromatogram demonstrates base mutation (highlighted in blue) within MUT-FUS. c. Localisation of mutant FUS using fluorescence microscopy in the presence of mibolerone. COS-1 cells were transfected with GFP-FUS or GFP-mutant-FUS (K510E) PSG5 plasmid ± pSVAR, a luciferase reporter tagged to the Androgen Response Element (TAT-GRE-E1B-LUC) and β-galactosidase (β-gal) reporter (PDM-Lac-Z-β-GAL). All conditions were transfected with equal amounts of DNA, altered using empty PSG5 plasmid. Cells were treated with ethanol and mibolerone (Mib) (1 nM) for 2 hours. d. AR activity in the presence of WT or mutant FUS measured using luciferase reporter assays. COS-1 cells were transfected with either 50 ng or 100 ng of GFP-FUS or mutant FUS (K510E) PSG5 plasmid, WT AR (pSVAR), a luciferase reporter tagged to the Androgen Response Element (TAT-GRE-E1B-LUC) and β-galactosidase (β-gal) reporter (PDM-Lac-Z-β-GAL). All conditions were transfected with equal amounts of DNA, altered using empty PSG5 plasmid. Cells were treated with ethanol and mibolerone (Mib) (1 nM) for 24 hours. Data from luciferase readings were normalised using the results from the β-gal assay. Averages of the mean ± SE from four separate experiments were calculated and paired two-tailed T-tests were performed to measure statistical significance (* = $P < 0.05$, ** = $P < 0.005$ and *** = $P < 0.0005$) between AR only and the FUS treatments at the. Cells were plated in a 24-well plate in hormone-depleted DMEM.

3.4 Optimisation of Hox Transcript Antisense Intergenic RNA and its Effect on Androgen Receptor Activity.

HOTAIR has been found to be overexpressed advanced stages of PCa (Vance *et al.*, 2013) and we wanted to observe the effects on AR activity. This was also useful for optimisation experiments for future crosstalk experiments with FUS.

Firstly, HOTAIR was synthesised by TWIST Bioscience and cloned into their shuttle vector (pTWIST31_Amp-HOTAIR) (Figure S1.2). The gene was synthesised with NotI and KpnI restriction enzyme sites 5' to 3' respectively for preparation of cloning into pcDNA3.1^{+} (Figure 3.4a). The plasmid was digested with NotI and KpnI. HOTAIR was then gel extracted and ligated into pcDNA3.1^{+}, digested with the same restriction enzymes. Successful insertion was verified using a diagnostic digest (Figure 3.4b) cut with XmaI (in HOTAIR gene) and NheI (in pcDNA3.1^{+} plasmid) due to the similar sizes of the shuttle vector and HOTAIR. This digestion gave rise to bands of approximately 3,100 bp and 4,500 bp. Successful cloning was then confirmed using sequencing.

Following successful cloning, luciferase reporter assays were performed to investigate the effect of HOTAIR upon AR activity (Figure 3.4c). COS-1 cells transfected with AR (pSVAR), an androgen response element (TAT-GRE-E1B-LUC-1), HOTAIR (pcDNA3.1^{+}-HOTAIR) as well as a β-galactosidase (PDM-Lac-Z-β-GAL) expression vector. Luciferase data were normalised to β-galactosidase expression and an equal amount of DNA was added to each treatment using PSG5 (empty) plasmid. The presence of HOTAIR decreased AR activity with T-tests indicating a significant difference at 400 ng ($P < 0.005$).

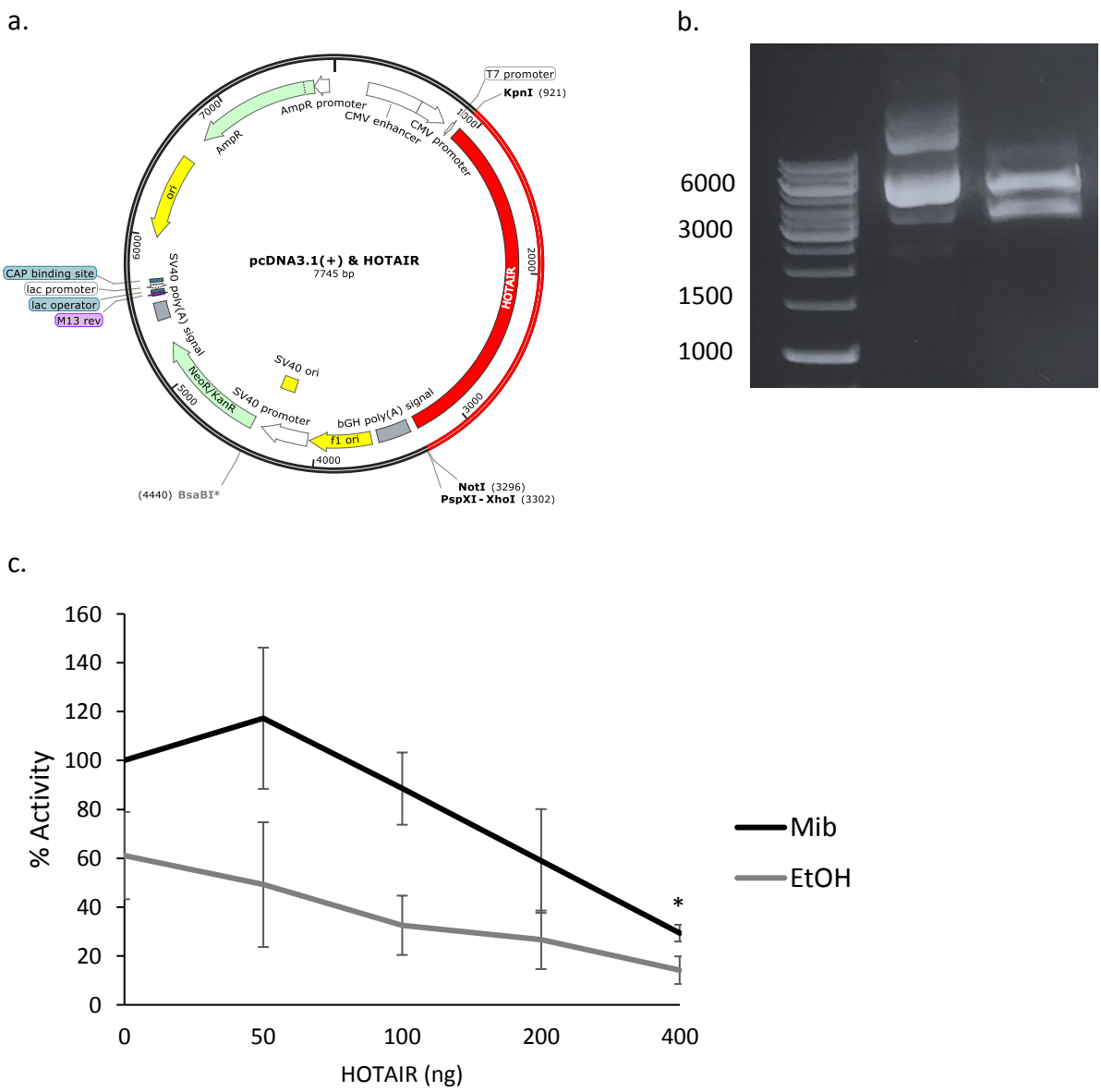

Figure 3.4: Cloning of Hox Transcript Antisense Intergenic RNA (HOTAIR) into pcDNA3.1+ and optimisation of HOTAIR concentrations for COS-1 transfections. a. HOTAIR was cloned into pcDNA3.1^{+}. This construct was designed using SnapGene Viewer Version 4.1. b. COS-1 cells were transfected with wild type human androgen receptor using the pSVAR plasmid, a luciferase reporter tagged to the androgen response element (TAT-GRE-E1B-LUC) and β-galactosidase (β-gal) reporter (PDM-Lac-Z-β-GAL). All conditions were transfected with equal amounts of DNA, altered using empty PSG5 plasmid. Cells were treated 24 hours after plating and data from luciferase readings were normalised using the results from the β-gal assay. Averages of the mean ± SE from four separate experiments were calculated and paired two-tail T-tests were performed to measure statistical significance between mibolerone concentrations (* = P < 0.05, ** = P < 0.005 and *** = P < 0.0005). Cells were plated in a 24-well plate and kept in an incubator in hormone-depleted DMEM

3.5. Proximity Dependent Biotin Identification-Androgen Receptor

The AR interacts with an array of cellular proteins during its signalling cascade (Davey and Grossmann, 2016). To further understand these interactions during different stages of signalling, the Proximity Dependent Biotin Identification (BioID) technique will be used to investigate receptor interactions. Indeed, this technique exploits a biotin ligase which is expressed within a cell, fused with a protein of interest (Le Sage *et al.*, 2016). When a protein interacts with the fusion protein, the promiscuous biotin ligase biotinylates it, allowing it to be identified by methods such as mass spectrometry (Le Sage *et al.*, 2016). Using this technique, transient protein-protein interactions with the AR could detect novel therapeutic targets for PCa. To facilitate this, the WT AR was cloned into the myc-BioID2-mcs plasmid (henceforth referred to as BioID-AR (Figure 3.5a)) utilising the pSVAR plasmid as a template using Gibson Assembly. Digestion of the BioID-AR plasmid using restriction enzymes NotI and BamHI was performed to confirm successful cloning (Figure 3.4b). This resulted in bands of approximately 6,150 bp and 2,800 bp, representing the plasmid backbone and AR insert respectively. Successful cloning was then confirmed using sequencing.

It is possible that the fusion of the AR to the BioID enzyme could affect receptor activity. To verify that the behaviour of BioID-AR was the same as unfused AR, luciferase reporter assays were performed. COS-1 cells were transfected with pSVAR or BioID-AR, an androgen responsive luciferase reporter plasmid (TAT-GRE-E1B-LUC-1) as well as a control expression vector, β-galactosidase (PDM-Lac-Z-β-GAL). Firstly, a mibolerone dose range (0 – 1000 nM) (Figure 3.5c). The activity of both receptors was enhanced by mibolerone, but BioID-AR was more sensitive to lower concentrations of androgen (1 and 10 nM). Next, the antiandrogen, Bicalutamide which is known to repress AR activity (Osguthorpe and Hagler, 2011) by acting as an antagonist was tested. BioID-AR behaved in a similar manner to WT AR with Bicalutamide decreasing receptor activity (Figure 3.5d). These results demonstrated therefore that BioID-AR appears to behave similarly to the untagged receptor.

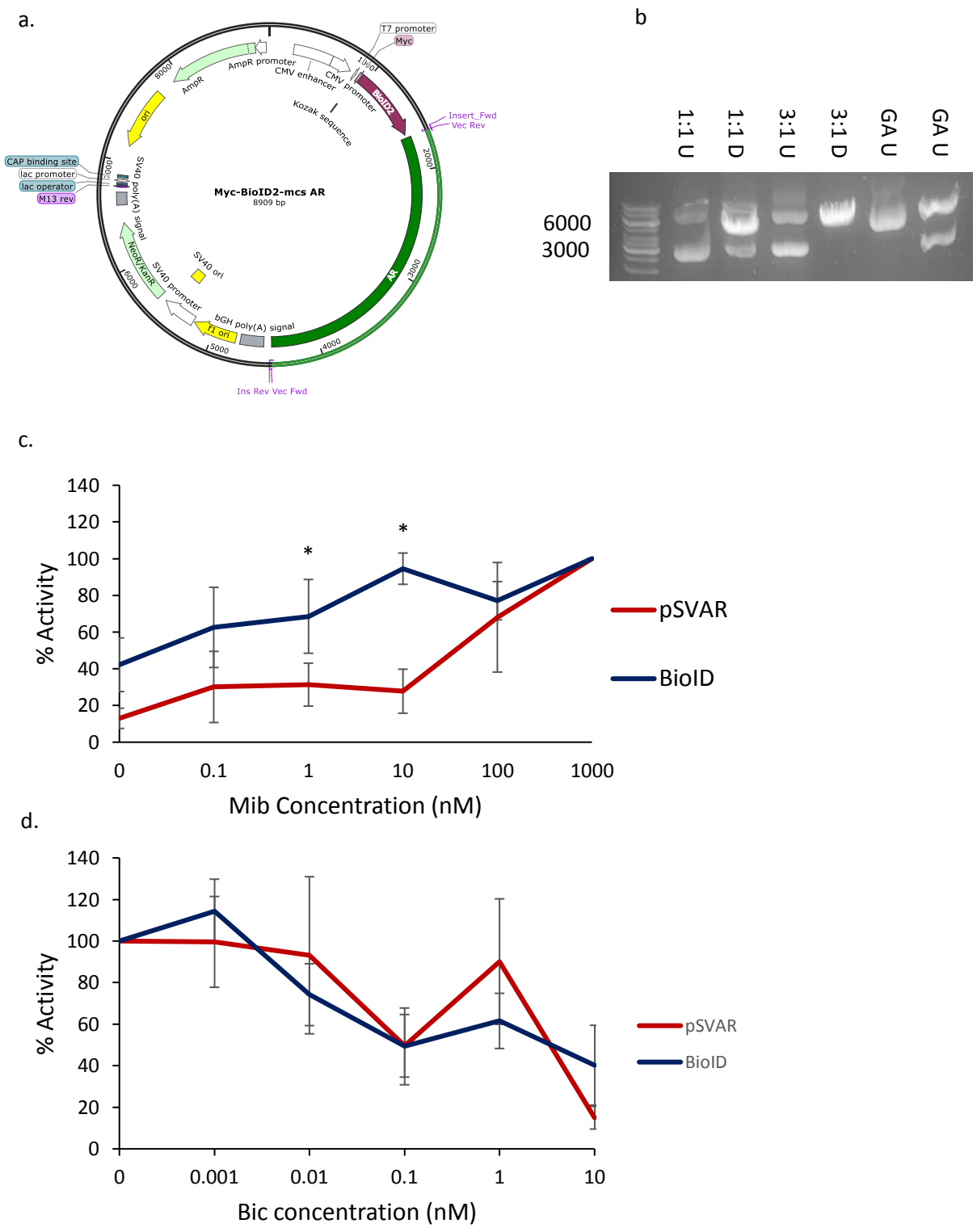

Figure 3.5: Formation and Characterisation of Proximity dependent Biotin Identification: myc-BioID2-mcs-Androgen Receptor in comparison with untagged Androgen Receptor (AR). a. Human WT AR was cloned into myc-BioID2-mcs for Proximity Dependent Biotin-Identification experiments. b. Successful cloning was confirmed using restriction enzyme digestion reactions with BamHI and NotI to produce a band of approximately 6,150 bp and 2,800 bp for the vector backbone and AR respectively.

COS-1 cells were transfected with AR using the pSVAR /myc-BioID2-mcs-AR (BioID-AR) plasmids, a luciferase reporter tagged to the Androgen Response Element (TAT-GRE-E1B-LUC) and β-galactosidase (β-gal) reporter (PDM-Lac-Z-β-GAL). All conditions were transfected with equal amounts of DNA. Cells were left for 24 hours before treatment and a further 24 hours before AR activity was measured. Data from luciferase readings were normalised using the results from the β-gal assay. Cells were plated in a 24-well plate and kept in an incubator in hormone-depleted DMEM. c. Mibolerone dose range. Cells were treated with a range of mibolerone (Mib) concentrations from 0 – 1000 nM. Averages of the mean ± SE from three separate experiments were calculated and paired two-tailed T-tests were performed to measure statistical significance (* = $P < 0.05$, ** = $P < 0.005$ and *** = $P < 0.0005$) between pSVAR and BioID-AR. d. Antiandrogen response. Cells were treated with mibolerone at 0.1 nM and an antiandrogen, bicalutamide from 0 – 10 nM. Averages of the mean ± SE from three separate experiments were calculated and paired two-tailed T-tests were performed to measure statistical significance. There were no significant differences between pSVAR and BioID-AR.

Chapter 4 – Results: Prostate Cancer Metabolism – Targeting the Haem Synthesis Pathway as a Novel Therapeutic

4.1 Inhibition of Haem Synthesis Reduces PC3 Proliferation and Induces Cell Death

The AR is a key driver of PCa and regulates essential genes required in fundamental processes such as the cell cycle and metabolism (Barfeld *et al.*, 2014; Brooke *et al.*, 2015). Metabolic reactions are increased in cancer cells to support their elevated cell growth and division (Kalyanaraman, 2017) and hence metabolism is a valid therapeutic target for the treatment of the disease. A previous study by Allafi *et al.,* (Unpub.) that used a siRNA screen to identify novel metabolic targets for PCa, identified that uroporphyrinogen III synthase (UROS), involved in the haem synthesis pathway, is an important regulator of proliferation and cell motility. Haem is an essential component of metabolism, for compounds such as cytochrome c and peroxidases (Zámocký *et al.*, 2015) and a number of these haem-containing factors have been shown to be up-regulated in cancer and to drive proliferation (Hooda *et al.*, 2013). Further validation of this pathway, as a therapeutic target, is therefore needed.

Succinylacetone is an irreversible inhibitor of aminolevulinic acid dehydratase (ALAD), the second step in the haem synthesis pathway (Bourque *et al.*, 2010). To investigate the effects of haem targeting upon PCa proliferation, PC3 were treated with a succinylacetone dose range (0 – 1000 µM) (Figure 4.3a). Cells were seeded in a 96-well plate at a density of 2×10^3 per well and treated after 24 hours. Cells were then incubated for 6 days, fixed and stained using 0.02% crystal violet stain. After solubilisation with 10% acetic acid, absorbance was read in an Omega plate reader. Succinylacetone was found to significantly reduce proliferation at 100-1000 µM and a concentration of 100 µM was selected for future experiments.

To see if succinylacetone induces cell death, flow cytometry was performed. Cells were plated in a 12-well plate at a seeding density of 2×10^4 and treated with 100 nM of succinylacetone or DMSO after 24 hours. After 6 days, cells were harvested, pelleted and stained with propidium iodide. Interestingly, cell death appears to be predominantly via

necrosis/necroptosis (28.75 % cell death) as opposed to apoptosis (13.10 %) (Figure 4.3b and Figure 4.3c).

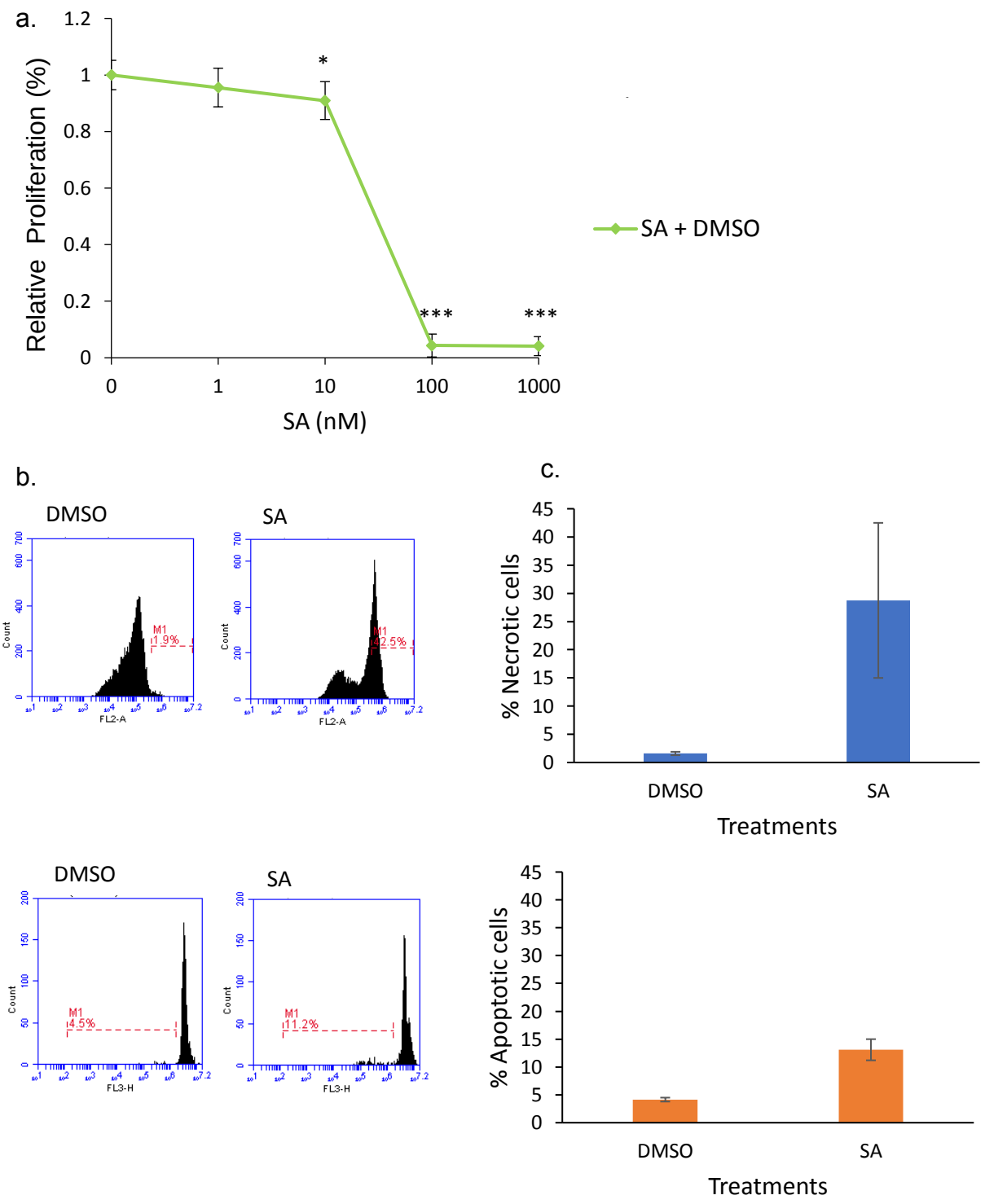

Figure 4.1: The effect of succinylacetone on PC3 cell proliferation and investigating the cell death pathway triggered. a.PC3 dose response curve to succinylacetone. PC3 cells were seeded in a 96-well plate at a seeding density of 2 x 10^3 and treated after 24 hours with 0 – 1000 nM succinylacetone. Cells were then incubated for 6 days before crystal violet assays were used to assess proliferation in response to different doses. b. Analyses of cell death (Top) necrosis and (Bottom) apoptosis using flow cytometry. PC3 cells were plated in a 12-well plate at a seeding density of 4 x 10^4 and treated as previously mentioned (Section 2.2.8.3). After 6 days, cells were harvested, pelleted and stained with propidium iodide. Accuri C6 software was used for analysis whereby only cells were gated and any debris was excluded.

(Top) Cells undergoing necrotic cell death. (Bottom) Cells undergoing apoptosis. c. Quantitative analyses of the results from Figure 4.1b. A two-tailed T-test demonstrated that there was no significant difference between DMSO and SA treatments.

4.2 Succinylacetone Promotes Necroptosis

Next, we sought to investigate which death pathway was triggered in in response to succinylacetone treatment. As previously demonstrated, cells predominantly via a non-apoptotic mechanism when haem synthesis is inhibited (Allafi *et al.*, Unpub). Therefore, we investigated caspase-independent cellular death mechanisms including necroptosis and ferroptosis. These pathways can be inhibited by necrostatin-1 and ferrostatin-1 respectively (Xie *et al.*, 2016). Concentrations of drugs used were taken from previous studies (Allafi *et al.,* Unpub.*)*.

PC3 cells were plated into a 96-well plate at a seeding density of 2 x 10^3. The succinylacetone dose range was repeated with the addition of 10 µM ferrostatin-1 or 40 µM of necrostatin-1 (final concentration) (Figure 4.2a). As seen previously, succinylacetone significantly inhibited PC3 proliferation at concentrations of 100-1000 µM. Ferrostatin-1 was unable to rescue this inhibition of proliferation. In contrast, necrostatin-1 was able to significantly reverse the effects of succinylacetone (Figure 4.4a and Figure 4.2b).

To further confirm and explore this, flow cytometry was performed to investigate the effects of necrostatin-1 and ferrostatin-1 upon SA-induced cell death. PC3 cells were seeded in 12-well plates at a density of 5 x 10^4. After 24 hours, cells were treated with 100 µM succinylacetone, 10 µM ferrostatin-1 and 40 µM of necrostatin-1 (final concentrations). After 6 days, cells were harvested, pelleted and stained with propidium iodide (Figure 4.2c and Figure 4.2d). As demonstrated previously, SA induced necrosis/necroptosis to a higher level than apoptosis. In agreement with the proliferation assays, the addition of ferrostatin-1 was unable to rescue this effect. The addition of necrostatin-1 reduced cell death from approximately 30% to 10%. The data therefore demonstrate the succinylacetone promoted necroptosis.

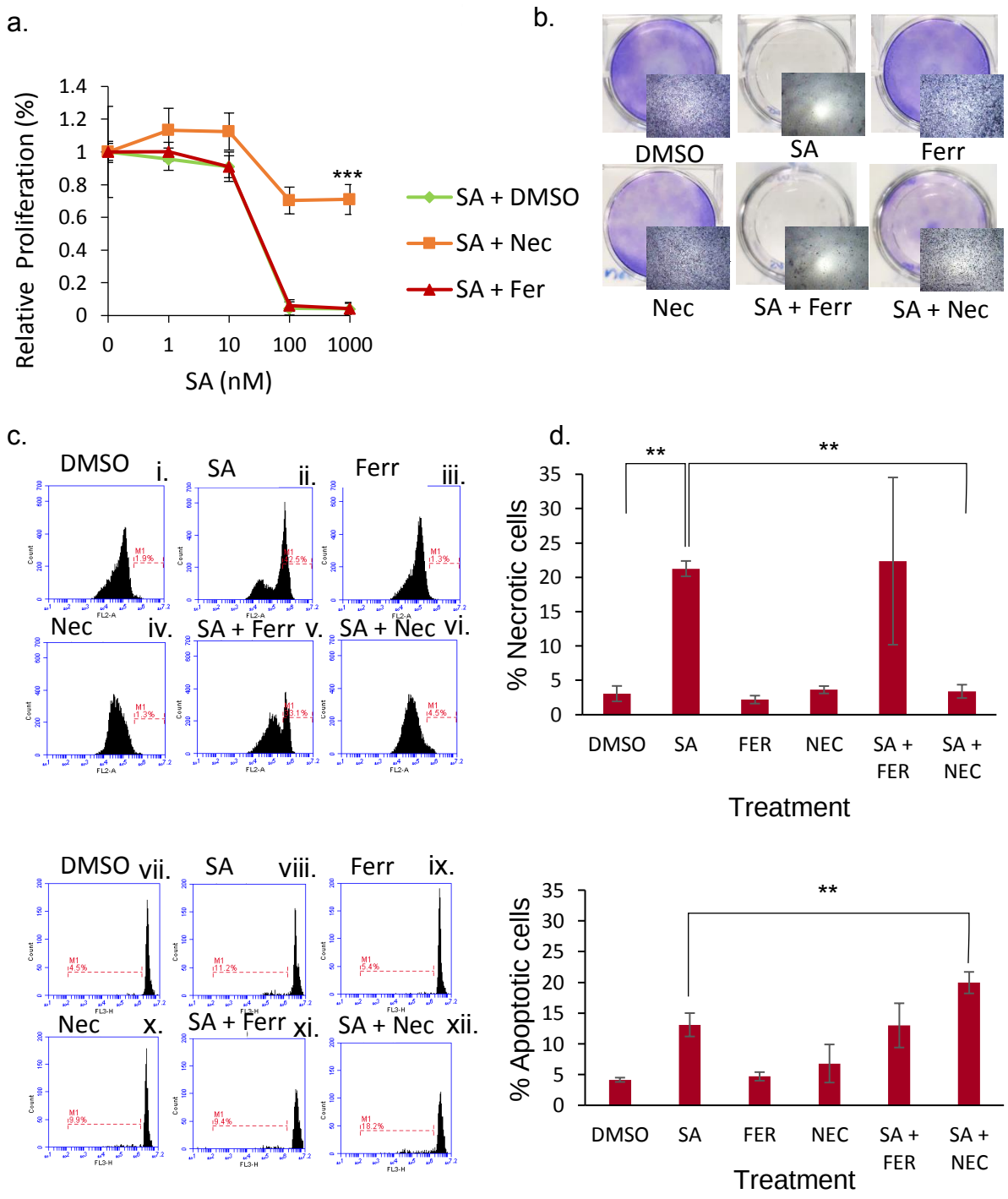

Figure 4.2: PC3 cells treated with succinylacetone can be rescued in the presence of necrostatin-1. PC3 were plated at a seeding density of 2 x 10^3 per well of a 96 well plate. Cells were treated with drugs succinylacetone (0 - 1000 µm), ferrostatin-1 (10 µM) and necrostatin-1 (40 µM) for 24 hours and left for six days before they were harvested and stained with propidium iodide. Averages of the mean ± SE from two separate experiments were calculated (unless otherwise stated) and paired two-tailed T-tests were performed to measure statistical significance (* = P < 0.05, ** = P < 0.01 and *** = P < 0.001) between DMSO, succinylacetone only and succinylacetone drug treatments. Cells were plated in a 24-well plate and kept in an incubator in hormone-depleted DMEM at 37 ˚C and 5 % carbon dioxide in air Crystal violet (CV) assays were measured at 590 nm. a. Relative proliferation of cells after

treatment with ferrostatin-1 ± succinylacetone and necrostatin-1 ± succinylacetone. DMSO was used as a control. b. CV growth assay. PC3 cells were plated in a 12-well plate at a seeding density of 5 x 10^4 per well of a 12 well plate c. Flow cytometry analyses of cellular demise detected using propidium iodide. (i-vi): Flow cytometry analyses of numbers of necrotic PC3 cells using propidium iodide staining. (vii-xii): Flow cytometry displaying numbers of the cells dying via apoptosis using a DNA hypoploidy assay propidium iodide assay. d. (top and bottom) quantitative data of i-vi and iv-xii displayed as percentage of cells undergoing necrosis and apoptosis respectively.

4.3 Inhibition of the Haem Synthesis Pathway Sensitises PC3 to ROS

Cancer cells often have high levels of ROS produced due to cell stress caused by hypoxia (Pelicano *et al.*, 2004). The haemoproteins (e.g. cytoglobin) downstream of porphyrin synthesis are known to protect against ROS damage (McRonald *et al.*, 2012). It was therefore hypothesised that inhibition of haem synthesis would sensitise cells to ROS damage. To investigate this, PC3 were treated with SA and H_2O_2 (to induce ROS). PC3 cells were plated in a 24-well plate at a seeding density of 4 x 10^4 and after 24 hours were treated with a sub-lethal concentration of succinylacetone (50 µM). After 5 days, cells were treated with 300 µM H_2O_2 and left for a further 24 hours. Cells were prepared for flow cytometry as described previously. Treatment with SA and H_2O_2 separately did not induce cell death. However, when cells were treated with SA and H_2O_2, necroptosis was significantly increased (Figure 4.3a and Figure 4.3b). Apoptosis was not induced by this co-treatment (Figure 4.3c and Figure 4.3d)

To see if this sensitisation to ROS damage was specific to cancer cells, the experiment was repeated in BPH1 cells. BPH-1 cells were plated in a 12-well plate at a seeding density 4 x 10^4 per well and left for 24 hours before being treated with 50 µM succinylacetone. After 5 days, cells were treated with H_2O_2 from 0 – 500 µM and left for a further 24 hours later prior to harvesting and PI staining. PI and DNA hypoploidy assays demonstrated low levels of necroptosis and apoptosis respectively (Figure 4.4). In contrast to PC3, SA did not sensitise BPH1 to H_2O_2, with necroptosis and apoptosis remaining at a low level irrespective of the treatment. This therefore suggests that SA can selectively tumour cells to ROS damage, although further cell lines would need to be investigated to confirm this.

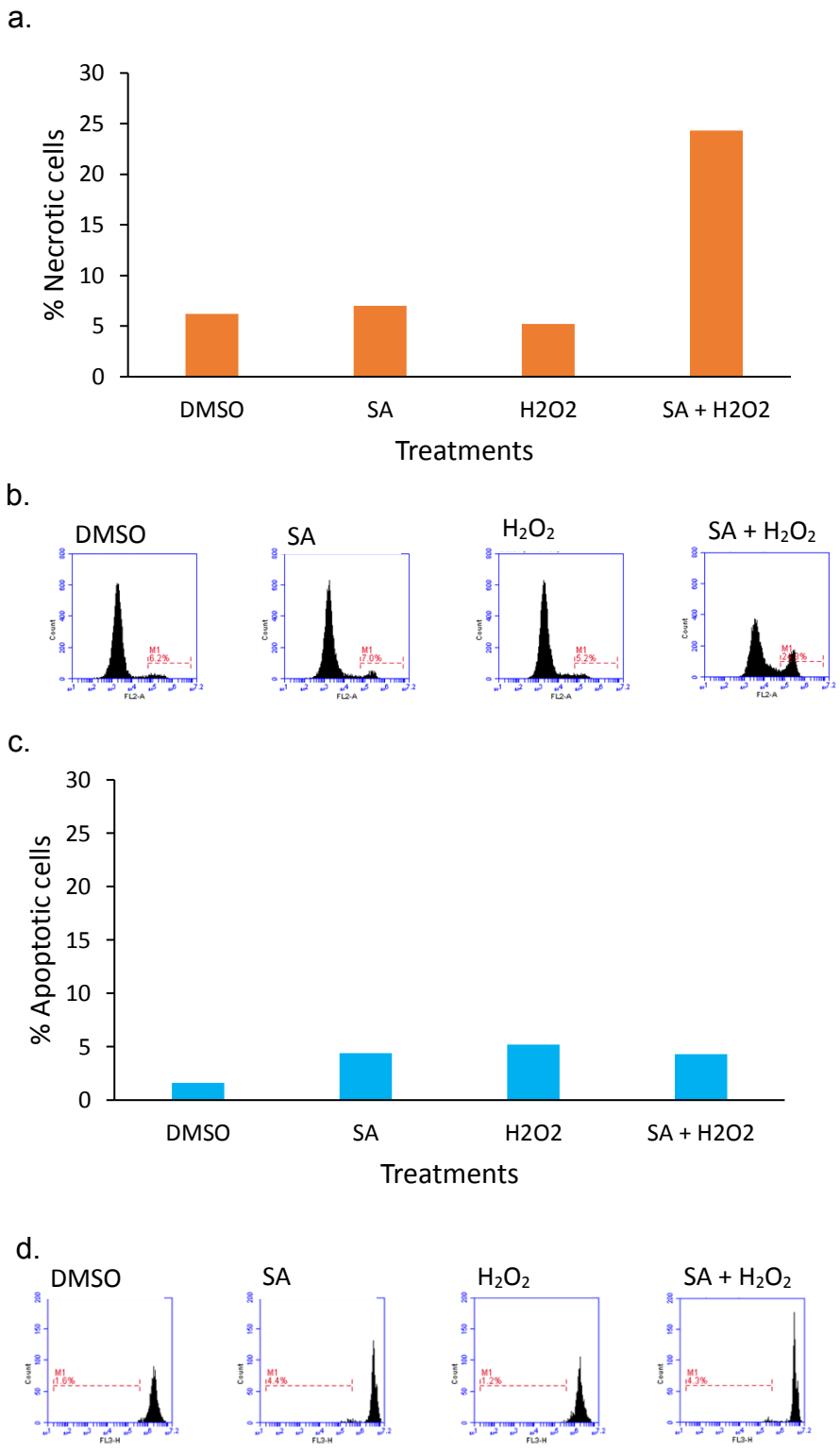

Figure 4.3: PC3 cells treated with succinylacetone in hypoxic conditions. PC3 cells were plated at a seeding density of 2 x 10^4 per well of a 12 well plate. Cells were treated with drugs succinylacetone (SA) (100 nm), left for 5 days before hydrogen peroxide was added. Cells were left for 24 hours before they were harvested for flow cytometry experiments. Cells were kept in RPMI media supplemented with 10 % FBS and 5 % PSG. a. Propidium iodide inclusion assay with H_2O_2 treatment (0-500 nM) used to detect necrotic cells. b. Flow cytometry graphs

of necrotic cells using flow cytometry propidium iodide inclusion assay. c. DNA hypoploidy assay using flow cytometry, with H_2O_2 treatment (0-500 nM) to detect apoptotic cells. d. Flow cytometry graphs of apoptotic cells using a DNA hypoploidy assay. These data demonstrate results from a single repeat.

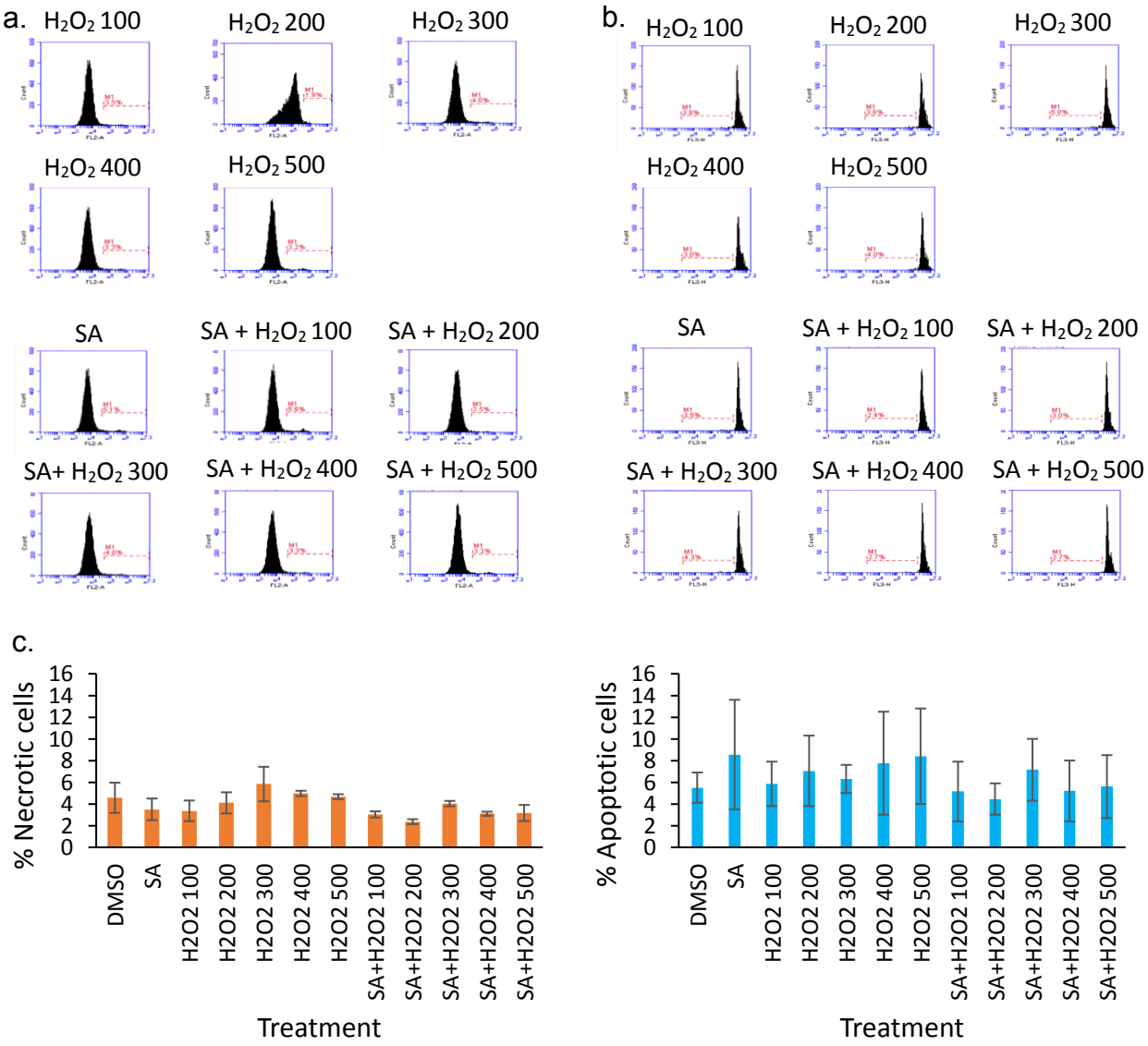

Figure 4.4: BPH-1 cells treated with succinylacetone in hypoxic conditions. BPH-1 cells were plated at a seeding density of 5 x 10^4 per well of a 12 well plate. Cells were treated with drugs succinylacetone (SA) (100 nm), left for 5 days before hydrogen peroxide was added. Cells were left for 24 hours before they were harvested for flow cytometry experiments. Averages of the mean ± SE from three separate experiments were calculated and paired two-tailed T-tests were performed to measure statistical significance (* = $P < 0.05$, ** = $P < 0.005$ and *** = $P < 0.0005$). Cells were kept in RPMI media supplemented with 10 % FBS and 5 % PSG. a. Propidium iodide inclusion assay with H_2O_2 treatment (0-500 nM) used to detect necrotic cells. b. DNA hypoploidy assay using flow cytometry, with H_2O_2 treatment (0-500 nM) to detect apoptotic cells. c. Quantitative analyses of data from sections a. and b.

4.4 Inhibition of haem synthesis reduces the proliferation of other cancer cell lines

Targeting the haem synthesis pathway using succinylacetone effectively inhibited PC3 proliferation. Allafi et al. (Unpub.) has also demonstrated that succinylacetone can effectively inhibit the proliferation of other PCa cell lines (e.g. DU145 and LNCaP). To see if targeting haem synthesis is also effective in other cancer types, proliferation assays were performed in cells lines from pancreatic cancer (PANC1), breast cancer (MCF-7), colorectal cancer (COLO-205), lung cancer (A549) and a mouse fibrobast cell line (L929). Cells were plated in 96-well plates at seeding densities ranging from 2-4 x 10^3. 24 hours after plating, cells were treated with a range of succinylacetone concentrations from 0 nM – 1 mM. Cells were left for 6 days before being fixed and stained with 0.02% crystal violet. 10 % acetic acid was then added and wells were read in an Omega plate reader. These assays demonstrated that increasing concentrations of succinylacetone decreased cell proliferation in all cell lines, with PANC1 and L929 being least effected (Figure 4.5). KMS-5 was the most affected by SA treatment at concentrations of 100-1000 µM. SA efficacy is therefore cell line dependent.

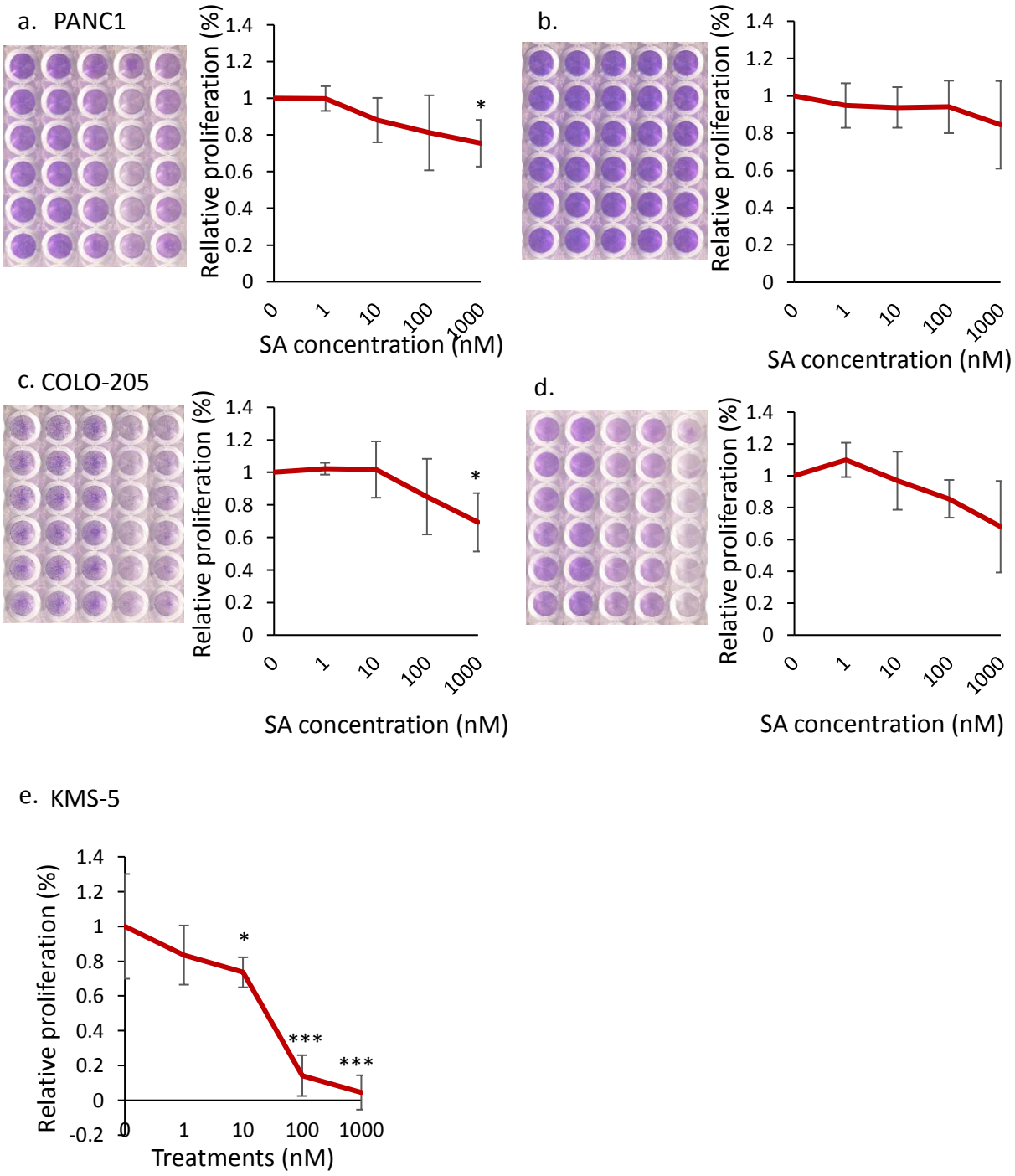

Figure 4.5: Effect of proliferation when the haem synthesis pathway is inhibited in other cancer cell lines. A succinylacetone dose range from 0 – 1000 nM. Cells were treated 24 hours after plating at a range of cell densities from 2-4 x 10^3. Cells were incubated for 6 days before preparation for crystal violet proliferation assays. Cells were read in an Omega plate reader at 590 nm wavelength. (Left of figures) Crystal violet growth assay. (Right of figures) quantitative data from the crystal violet data. a. PANC1 cells were plated at a seeding density of 4 x 10^3. b. L929 cells were plated at a seeding density of 2 x 10^3. c. COLO-205 cells were plated at a seeding density of 2 x 10^3. d. A549 cells were plated at a seeding density of 2 x 10^3.e. KMS-5 cells were plated at a seeding density of 2 x 10^3.

4.5 ALAS1 levels are elevated in some PCa cell lines

From the previous experiments, it appears that that targeting haem synthesis is a promising therapeutic target for PCa, however, there is the risk of off-target effects as haem synthesis is essential for e.g. haemoglobin. To reduce the likelihood of off-target effects, I propose to target the first and rate limiting step of porphyrin synthesis, performed by ALAS1 or ALAS2. ALAS2 is specifically expressed in erythroid cells (Kubota *et al.*, 2016) and hence targeting ALAS1 should reduce these potential off-target effects. To investigate ALAS1 expression in PCa immunoblotting was performed on a range of cell lines representing different stages o the disease, from normal/benign (PNT1A and BPH1) to androgen sensitive (e.g. LNCaP) to castrate resistant (e.g. DU145). ALAS1 was found to be elevated in the majority of PCa cell lines compared to the normal/benign lines (Figure 4.6).

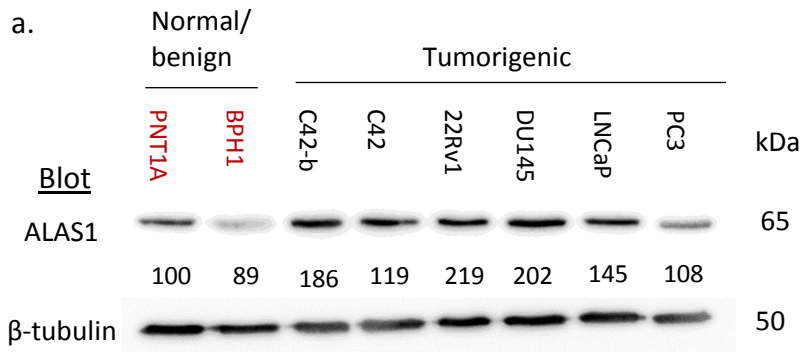

Figure 4.6: Detection of ALAS-1 in a range of prostate cancer cell lines. a. The presence of ALAS-1 in a range of prostate cancer cell lines. β–tubulin was used as a control. Highlighted in red are the non-cancerous cell lines. Number indicate densitometry values normalised to β–tubulin

4.6 siRNA Knockdown of Aminolevulinate Synthase 1 and The Effect on PC3 Cell Proliferation

After finding that ALAS1 levels appear to be upregulated in PCa, the effect of siRNA depletion of ALAS1 upon cell proliferation was assessed in PC3 cells. To confirm knock-down, cells were plated in 6-well plates at a seeding density of 2 x 10^5 per well and transfected with either mock (transfection reagent only), non-targeting control siRNA or ALAS1 targeting siRNA 24 hours after plating. Cells were incubated for 48 and 72 hrs prior to harvesting for qPCR and immunoblot analysis respectively. Successful knockdown was first confirmed at both the RNA (Figure 4.7a) and protein (Figure 4.7b) levels. These analyses demonstrated that ALAS1 is depleted by approximately 80% at both the RNA and protein level.

To investigate the effect of ALAS1 depletion upon proliferation, cells were plated in 24 well plates and transfected ± siRNA as described above. After three days cells were fixed and stained with crystal violet and imaged using brightfield microscopy (Figure 4.7c). There was little difference in cell number between mock and NTC transfected cells. In contrast, there was a significant reduction in cell number when cells were transfected with siRNA targeting ALAS1. To quantify this, crystal violet was solubilised with 10% acetic acid and absorbance measured (Figure 4.7d). In agreement with the microscopy images, PC3 proliferation was reduced by approximately 60% when ALAS1 was depleted. Targeting ALAS1 therefore appears to be a viable option to inhibit PCa.

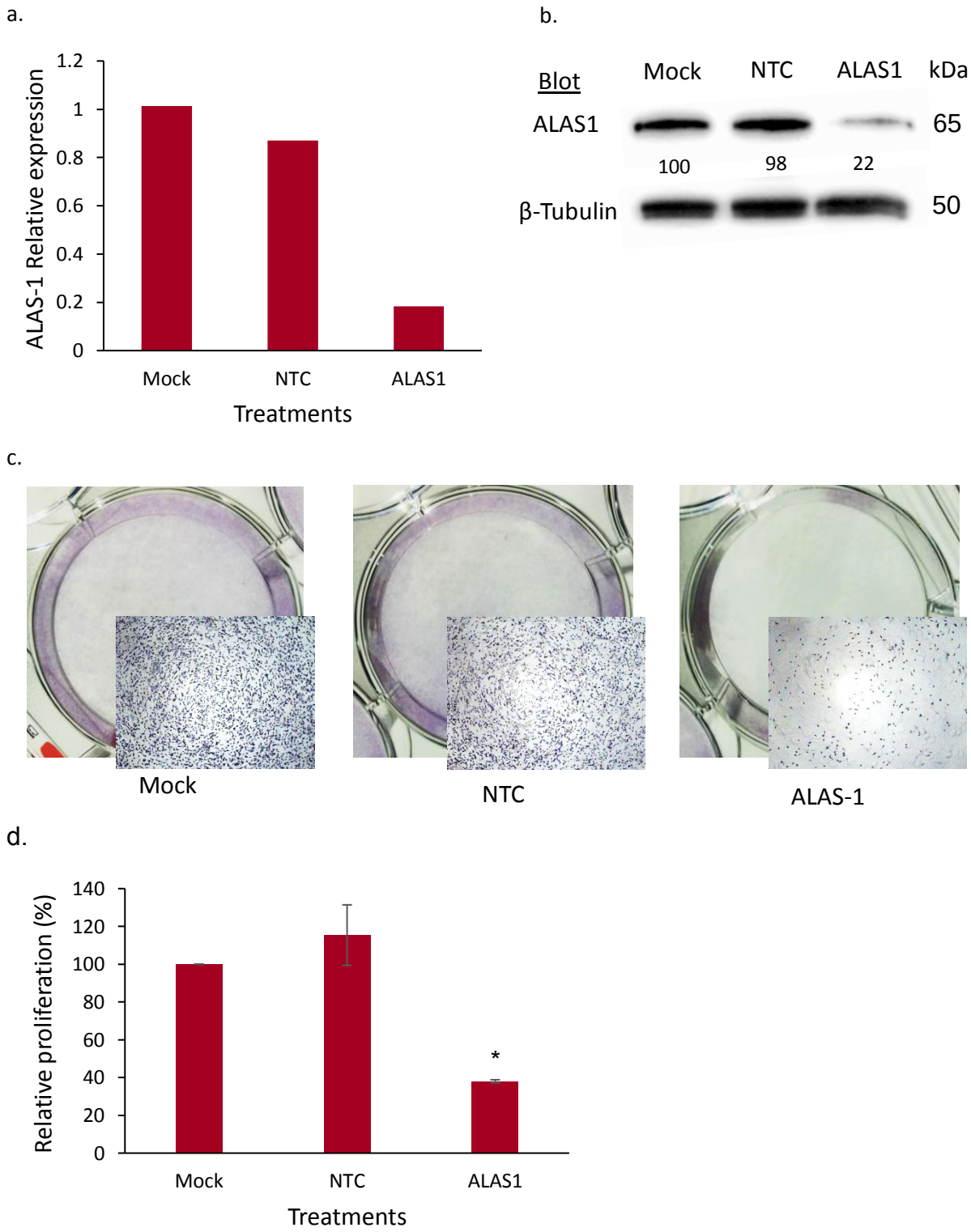

Figure 4.7: ALAS-1 knockdown in PC3 cells decreases their proliferation. PC3 were plated at a seeding density of 2 x 10^5 per well. Cells were treated after 24 hours with siRNA and left for three days before they were harvested. Mock was used as a control with transfection reagent only. Averages of the mean ± SE from three separate experiments were calculated and paired two-tailed T-tests were performed to measure statistical significance (* = P < 0.05, ** = P < 0.005 and *** = P < 0.0005) between NTC and ALAS-1 KD. There was statistical significance between these conditions. Cells were plated in a 24-well plate and kept

in an incubator in hormone-depleted DMEM. a. & b. Western blot and qPCR analyses (respectively) to confirm successful knockdown of 5'-aminolevulinate synthase-1 (ALAS-1). L19 was used as a control gene (not shown) c. Crystal violet (CV) proliferation assays demonstrated that ALAS-1 knockdown affected cell proliferation. d. Quantitative analyses of CV assay showing relative proliferation (%). Crystal violet (CV) assays were measured at 590 nm.

4.7. Protein Expression of Human Aminolevulinate Synthase 1 and 2 in BL21(DE3) *Escherichia coli* cells

Inhibiting the haem synthesis pathway reduced PCa proliferation therefore ALAS1 was deemed a potential target for future therapeutics. Currently no crystal structures exist for hALAS1 and 2. To aid in the development of small molecules specific to hALAS1, the 2 enzymes were cloned and expressed in *Escherichia coli* cells in preparation for crystallographic studies. Two constructs were generated for each enzyme, full-length and a truncated version that lacked the mitochondrial targeting peptide (Figure 4.8a).

Human ALAS1 FL was synthesised into a shuttle vector (pCMV3_ALAS1) by Sino Biological Inc. The primers designed to generate the full-length and truncated versions of ALAS1 were synthesised with NheI and HindIII restriction enzyme sites 5' to 3' respectively. All constructs were cloned into the pET28a^{+} bacterial expression vector (Figure 4.8b). Following a PCR amplification of ALAS1, the gene (full-length and truncated) was digested with NheI and HindIII to generate sticky ends, PCR products separated using gel electrophoresis, the product gel extracted and ligated into pET28^{+}, which was also digested with the same restriction enzymes. Successful insertion was confirmed using a diagnostic digest (Figure 4.8c). The digest gave rise to bands of 5.300 bp and 2,000 bp which represents the vector backbone and ALAS1 full-length respectively (Figure 4.8c). Also, bands of 5,000 bp and 1,800 bp were observed for truncated ALAS1 (vector backbone and insert respectively, Figure 4.8c).

To clone ALAS2, RNA was extracted from K562 cells and reverse transcribed into cDNA. A PCR reaction was then performed with primers designed to amplify full-length and truncated ALAS2, with the addition of NheI and HindIII restriction sites. The PCR products were separated using gel electrophoresis, gel extracted and ligated into pET28^{+}. Successful insertion of the constructs was confirmed using diagnostic digests. The digest gave rise to bands of 5,303 bp and 1,784 bp which represented the vector backbone and ALAS2 full-length insert respectively (Figure 4.8c). Bands of 5,314 bp and 1,623 bp were observed for truncated

ALAS2 vector backbone and insert respectively (Figure 4.8c). These four constructs were then transformed into BL21(DE3) cells in preparation for protein expression.

Initially, protein expression was investigated for the truncated ALAS1 and ALAS2. The BL21(DE3) cells were inoculated with Luria Broth supplemented with kanamycin and grown to an optical density 600 (OD_{600}) of 0.4 - 0.5. Once this density was reached, a 1 ml sample of cells was removed and pelleted. The remaining culture was induced with 0.5 mM IPTG and left to incubate at either 37 °C for 4 hours or 18˚C overnight. After the incubation time, 1 ml of cells was removed and pelleted. These 1 ml samples were used for SDS-PAGE analyses and Coomassie blue staining (Figure 4.9). The remaining cultures were also pelleted and the cells were lysed by sonication for analyses of soluble and insoluble fractions (Figure 4.9b and Figure 4.9c respectively), which were also prepared for SDS-PAGE analysis. The whole cell lysate for ALAS1 T (~67.65 kDa with His-tag) and ALAS2 T (~ 61.71 kDa with His-tag) demonstrated that these proteins was successfully expressed in all conditions (Figure 4.9a). The presence of our protein was not observed in the soluble fraction in all conditions (Figure 4.9b). However, in the insoluble fraction, proteins were seen in all conditions (Figure 4.9c). Therefore, it appears that the truncated proteins are insoluble. To investigate if the full-length proteins were soluble, proteins were expressed as described previously. Gels demonstrated low levels of expression for ALAS2 at 37 °C for 4 hours whereas none was observed for cells exposed to 18˚C, overnight (Figure 4.9d). It also appears that ALAS1 full-length expression was not induced. Further optimisation is therefore necessary before large-scale protein expression and purification can be performed.

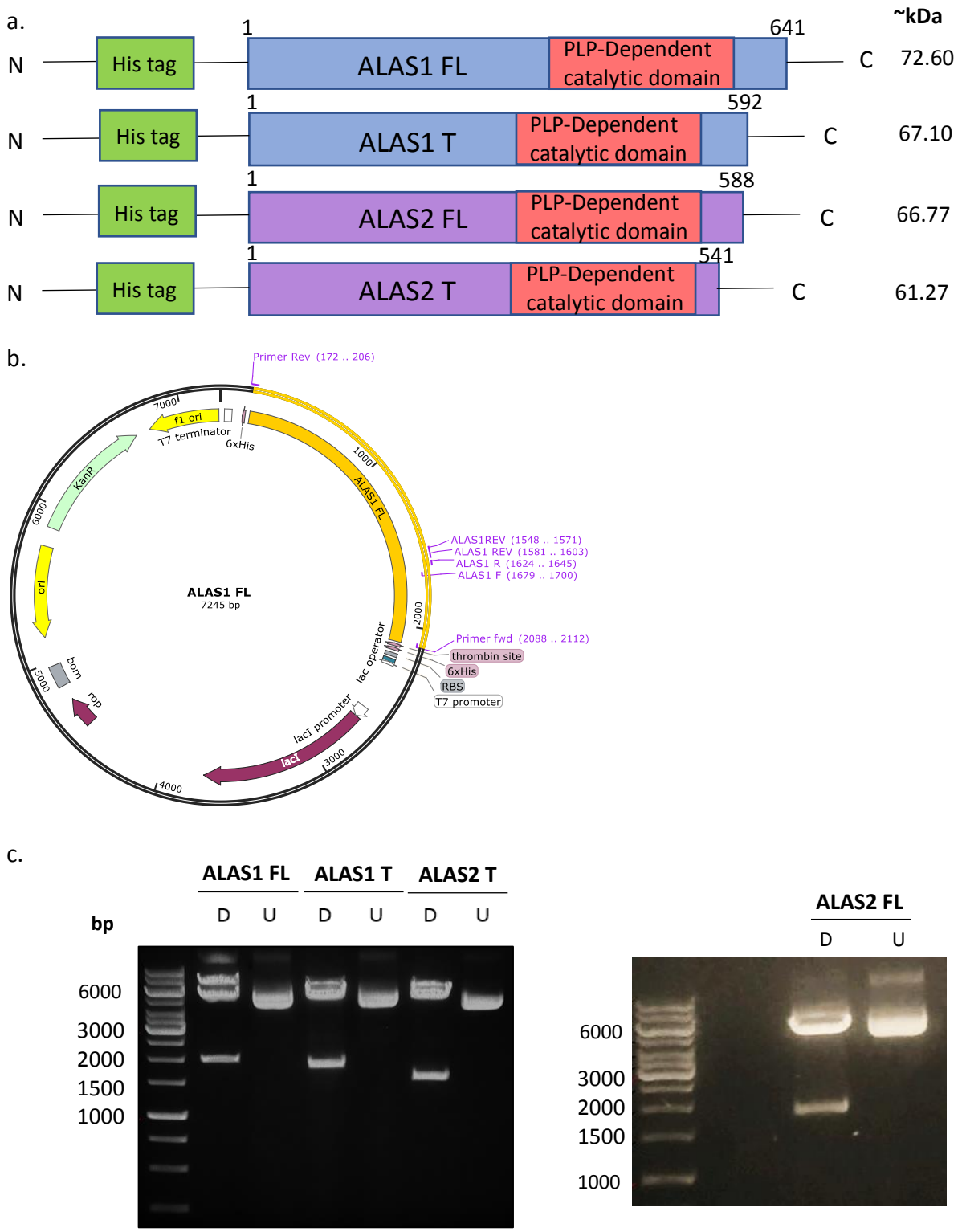

Figure 4.8: Cloning of aminolevulinate synthase 1 (ALAS1) and aminolevulinate synthase 2 (ALAS2) full length (FL) and truncated (T) into expression vector pET28a^{+}. a. Schematic of designed ALAS1 and ALAS2 FL and T constructs with a Histidine tag. Numbers represent amino acid number. b. Plasmid construct of ALAS1 in pET28^{+}. This image was made using SnapGene Viewer Version 4.1. c. Digestion diagnosis of ALAS1 and ALAS2 full length and truncated plasmid constructs. Plasmids were digested with restriction enzymes NheI and HindIII.

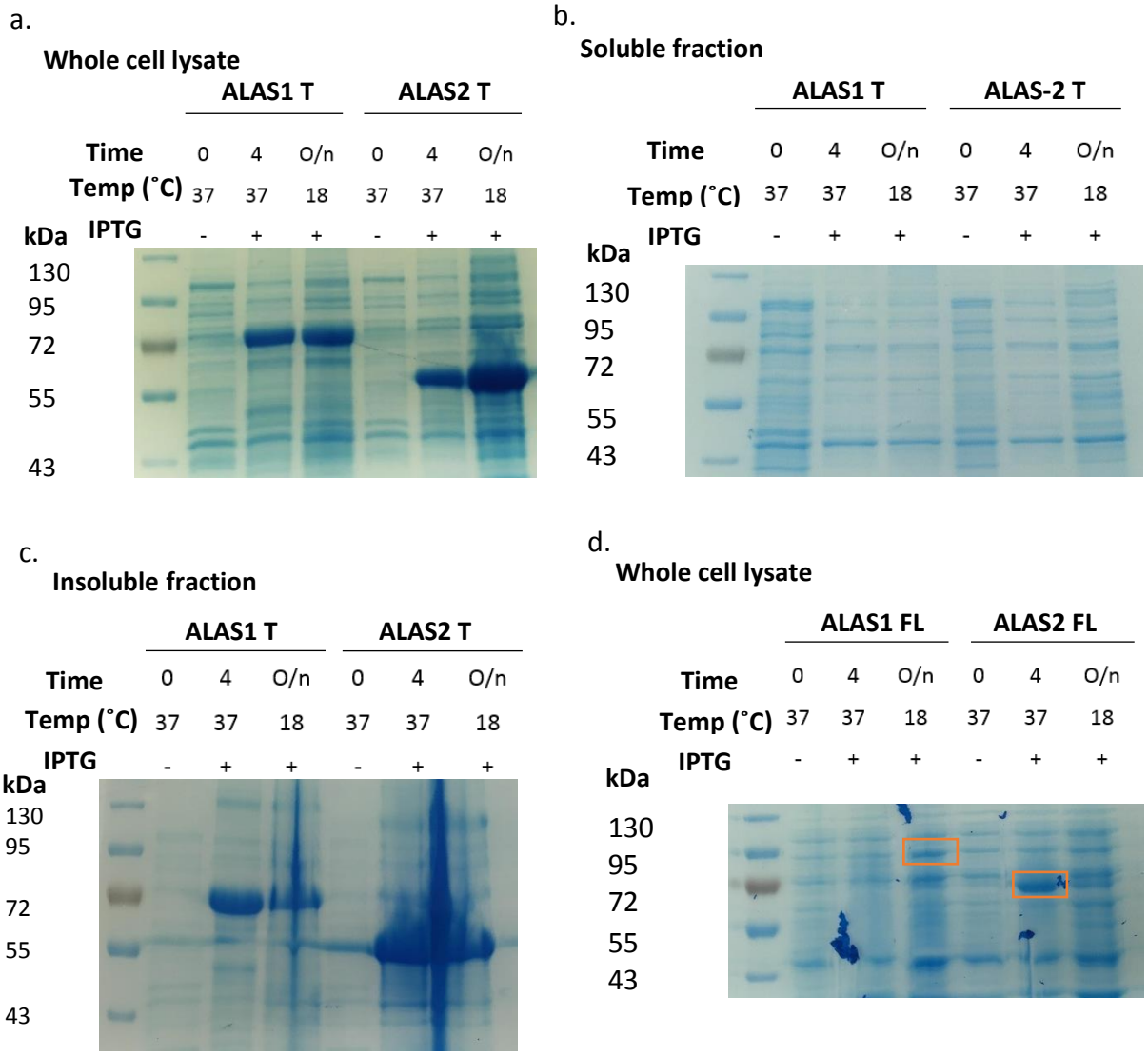

Figure 4.9 Expression of full length and truncated human aminolevulinate synthase 1 and 2 in *Escherichia* coli BL21(DE3) cells. a. Constructs of aminolevulinate synthase (ALAS)1 and ALAS2 truncated (T) and full length (FL) designed for protein expression experiments. b. Plasmid map example of ALAS1 FL in the pET28a^{+} plasmid. c. Digestion diagnostic to ensure successful cloning of ALAS1 and ALAS2 FL and T into pET28a^{+}. BL21(DE3) cells were transformed with ALAS1 and ALAS2 constructs. Expression was induced with 0.5 mM IPTG once an optical density (OD_{600}) was reached. Cells were exposed to two different conditions: 37 °C for four hours or 18 ˚C overnight. Samples were then prepared for SDS-PAGE analyses and stained with Coomassie blue. d. Whole cell lysate of ALAS1 and ALAS2 T. Cells were then sonicated to produce the soluble (e.) and insoluble fractions (f.). Whole cell lysate as described before was also produced for ALAS1 and ALAS2 FL. Orange boxes determine successful protein expression.

Chapter 5 – Discussion

5.1 The role of FUS and the lncRNA HOTAIR in Androgen Receptor signalling

The AR is the main driver of PCa proliferation at all stages of the disease (Jernberg *et al.*, 2017). Underlying this, the AR has dynamic interactions with a range of co-factors as well as lncRNAs to further finetune its signalling process (Brooke and Bevan, 2009; Zhang *et al.*, 2016). However, the complexity of these co-factors and lncRNAs which regulate the AR is not well understood. FUS and HOTAIR were selected for further investigation and it was hypothesised that these components will affect AR activity.

To optimise conditions for the reporter assay experiments, a mibolerone dose range was performed. As expected, AR activity was enhanced as mibolerone concentrations increased. This appears to be due to increased stability of the receptor in the presence of its ligand (Zhou *et al.*, 1995), as evidenced by immunoblotting analysis of receptor levels (Figure 3.1a). Indeed, the NTD together with the LBD form a steady complex dependent upon ligand binding (Centenera *et al.*, 2008). This allows slow dissociation of the hormone, which stabilises the AR and decreases its degradation rate (Centenera *et al.*, 2008). It is known that the AR can be degraded rapidly (Kemppainen *et al.*, 1992), which corresponds with our results showing low activity and the low level of AR in western blots in control experiments as well as low mibolerone concentrations (Figure 3.1b). It is postulated that AR degradation is mediated via the ubiquitin proteasome system, regulated predominantly by E3 ligases (Lee and Chang, 2003; Li *et al.*, 2014). A phosphorylated peptide degradation motif (PEST), a sequence rich in amino acids corresponding to its name, has been noted within the hinge region of the AR which appears to facilitate this process (Clinckemalie *et al.*, 2012).

The RNA-binding protein FUS has transactivation properties and is known to interact with nuclear receptors. FUS can act as a co-factor of the AR, however, it is unclear if it acts as a co-repressor or a co-activator due to conflicting evidence. Haile *et al*., (2011) suggested that FUS acts as a co-activator whereas Brooke *et al*., (Unpub.) demonstrated the opposite. The

data presented here also demonstrated that FUS acts as a co-repressor of the AR. The difference in results may be as a result in different methods used by Haile *et al.*, (2011) as they used a different luciferase reporter (ARR3-tk-LUC). This reporter contains six ARE sites and is therefore likely to be highly sensitive to androgen signalling. Further, FUS regulation of AR activity could be promoter-specific as described by Haile *et al.*, (2011) who suggested that certain target genes may be enhanced in the presence of FUS. This differential regulation of target genes could be a result of different types of response elements, including palindromic and direct sequences, which may alter the behaviour of the AR at these different target sites (Zhou *et al.*, 1997). A more global approach, e.g. RNA-seq and ChIP-seq, could be performed to confirm the role of FUS in androgen signalling and it is hypothesised that FUS can act as a co-activator and co-repressor dependent upon promoter context.

FUS is known to be a nuclear protein (Schwartz *et al.*, 2014) and it has been demonstrated that FUS levels are inversely correlated with Gleason grade (Brooke *et al.*, 2011). Interestingly, Brooke *et al.,* (Unpub.) demonstrated that FUS levels are elevated in CRPC and that the protein has both nuclear and cytoplasmic localisation. To see if altered FUS localisation affects its ability to repress AR activity, which could subsequently lead to enhanced AR signalling and therefore promote disease progression, a mutation was inserted into the FUS NLS (K510E). This was selected from previous studies in Amyloid Lateral Sclerosis which demonstrated that FUS with NLS mutations partially mislocalised to the cytoplasm (Vance *et al.*, 2013). Using immunofluorescent imaging, it was observed that FUS K510E localised to both the cytoplasm and the nucleus whereas WT FUS was nuclear, as expected (Vance *et al.*, 2013). The reduced nuclear localisation of K510E could be due to reduced affinity for transportin-1, leading to inefficient nuclear trafficking (Twyffels *et al.*, 2014). FUS aggregates were also observed in the cytoplasm, agreeing with previous studies which showed that FUS can form direct protein-protein interactions with itself and accumulate (Vance *et al.*, 2013).

High expression of HOTAIR has been observed in different cancers and correlates with metastasis (Gupta *et al.*, 2010). HOTAIR expression has not been well characterised in PCa

but it has been stated there it is at increased levels as the disease progresses to CRPC (Zhang *et al.*, 2015). Reporter assays demonstrated that HOTAIR represses AR activity. This is not in agreement with a previous study which showed an increase in AR activity in the presence of HOTAIR (Zhang *et al.*, 2015). Zhang *et al*., (2015) mainly focussed on DNA binding events in in response to elevated levels of HOTAIR. After finding increased binding events in the presence of overexpressed HOTAIR, the effect upon target gene expression was analysed. They demonstrated that androgen-regulated genes were significantly enriched and that androgen-activated genes and androgen-repressed genes were significantly up- or downregulated respectively (Zhang *et al.*, 2015). As discussed above, the effect of HOTAIR upon AR activity may differ dependent upon promoter context (Wilson *et al.*, 2016; Zhou *et al.*, 1997).

Various studies have investigated AR co-factors (Bevan *et al.*, 1999; Haile *et al.*, 2011; Heemers and Tindall, 2007). To further characterise these co-factors the Proximity-Dependent Biotin Identification technique will be used. The advantage of this technique over other strategies is that interacting proteins throughout the signalling pathway can be identified. The AR was successfully cloned downstream of biotinylase and the tagged protein was demonstrated to function similarly to the un-tagged receptor. The characterisation of novel interacting proteins could aid in the identification of novel therapeutic strategies to inhibit AR signalling.

5.2 Targeting The Haem Synthesis Pathway As A Novel Therapeutic Approach For Prostate Cancer

The AR regulates many genes required for cell division, including factors involved in metabolism (McNair *et al.*, 2017). Metabolic processes are more rapid in cancerous cells as a result of their abnormal proliferation rate (Kalyanaraman, 2017). Using an siRNA screen, Allafi *et al.,* (Unpub.) demonstrated that UROS, a member of the haem synthesis pathway, is a key regulator of PCa proliferation and motility. Haem is an essential compound in the cell as it is required for fundamental enzymes such as cytochrome c (Zámocký *et al.*, 2015).

Succinylacetone is an inhibitor of the second step of the haem synthesis pathway, performed by ALAD. Treatment of the PC3 line with succinylacetone successfully inhibited proliferation and flow cytometry demonstrated that cell death was predominantly via necroptosis/necrosis/ferroptosis. Co-treatment with inhibitors of necroptosis and ferroptosis confirmed that cell death is as a result of necroptosis. This lack of proliferation and cell demise is understandable due to the downstream effects that the lack of haem would have on the cell. Haem is required for many proteins such as cytochrome c, essential in the electron transport chain for oxidative phosphorylation (Hooda *et al.*, 2015), micro RNA transcriptional processing (Weitz *et al.*, 2014) and as a co-factor in haem peroxidases (Zámocký *et al.*, 2015). Therefore, inhibiting haem synthesis would have a significant impact on cellular processes. The observation that targeting haem synthesis promotes necroptosis differs from a previous study in neuronal cells whereby apoptosis was triggered (Sengupta *et al.*, 2005). The pathways triggered may differ due to the different tissues studied.

The findings that succinylacetone promotes necroptosis is a significant finding. Recently it has been shown that caspase-independent cell death enhances tumour clearance via synergistic interactions with the host's immune system (Giampazolias *et al.*, 2017). Indeed, necroptosis attracts phagocytes to the area which generates ROS in the process of phagocytosis (Dupre-Crochet *et al.*, 2013). This can then further amplify cellular death as cancer cells will be sensitive to ROS species when their haem synthesis pathway is inhibited.

Cancer cells are often exposed to hypoxic conditions, resulting in increased levels of ROS (Liou and Storz, 2010). To see if inhibition of haem synthesis sensitises cells to ROS damage, cells were co-treated with succinylacetone and H_2O_2. Interestingly, succinylacetone did sensitise PC3 cells to ROS damage. In contrast, cell death was not induced in the control cell line BPH-1 when cells were treated with succinylacetone and H_2O_2. This therefore suggests that this therapeutic strategy is selective for cancer cells. Metabolism in the prostate differs to other tissues (Cutruzzolà *et al.*, 2017). Further, the Kreb's cycle is restored in PCa which aids proliferation as it becomes energy-efficient (Cutruzzolà *et al.*, 2017). Inhibition of haem biosynthesis may therefore destabilise respiration and other important processes within the cell. Diminishing these crucial processes would prevent cancer progression.

Haem synthesis is ubiquitous within the body and therefore targeting this pathway could have significant off-target effects. To mitigate this, I propose to target the first and rate-limiting step in haem synthesis, performed by ALAS1 or ALAS2. ALAS1 is found in the mitochondria and performs the first step of the haem synthesis pathway except for in erythrocytes whereby it is performed by ALAS2 (Kubota *et al.*, 2016). To avoid targeting erythroid cells, ALAS1 will therefore be targeted. Importantly, ALAS1 was found to be up-regulated in the majority of prostate cancer cell lines and siRNA depletion of ALAS1 significantly reduced proliferation. This increase in ALAS1 in cancer compared to non-tumorigenic controls was also noted in a previous study in non-small cell lung cancer (Hooda *et al.*, 2013).

Overall, the results showed that targeting the haem synthesis pathway significantly reduces PCa proliferation without affecting normal cells, providing a promising approach for a novel therapeutic. Small molecules targeting ALAS1 do not exist and the identification of such molecules is hampered by the lack of structural information for the enzyme. In preparation for crystallography analysis full-length and truncated forms of ALAS1 and ALAS2 were expressed in BL21(DE3) *Escherchia coli* cells. The results demonstrated successful expression of these proteins, however, they appeared to be insoluble. Multiple factors are important to consider

when expressing proteins in bacteria to achieve successful purification. Adjustment of expression levels such as the use of low copy number plasmids could help to form soluble proteins (Rosano and Ceccarelli, 2014). Producing an insoluble protein is considered undesirable due to the more expensive and timely protein refolding procedure, although at times, this is the chosen method (Sørensen and Mortensen, 2005). It is important to determine whether these proteins will form monomeric or multimeric complexes when expressed as aggregations often affect the solubility (Ventura, 2005). Switching the Histidine tag to the C-terminal domain or swapping tags may also help with purification procedures (Sørensen and Mortensen, 2005). Lastly, protein expression may be improved using a different bacterial strain. For example, the Lemo21(DE3) strain contains tuneable expression which can be useful for proteins which are insoluble-prone.

In summary, targeting haem synthesis significantly reduced proliferation with cells dying mainly via necroptosis. Also, targeting haem synthesis in the presence of hypoxic conditions enhanced cell death.

5.3 Future Work

CRPC is an advanced aggressive stage of the disease with poor prognosis for patients. Treatment options for this stage of the disease are limited and therefore further characterisation of disease progression and the identification of novel therapeutic strategies are much needed. Elucidating novel co-regulators which interact with the AR during different phases of its signalling cascade could help identify novel therapeutic targets. We have found that BioID-AR behaves the same as WT AR when exposed to mibolerone and antiandrogens. Additional experiments are required to further confirm that the addition of the biotinylase enzyme does not affect AR activity. For example, to ensure that the localisation of AR and nuclear translocation is not affected, fluorescent imaging could be performed. Also, to confirm that the receptor can bind to DNA, chromatin immunoprecipitation should be performed. Protein interactions with a range of previously validated co-factors could also be performed to ensure BioID-AR is interacting correctly. Lastly, correct expression within the cell would need to be investigated using western blot analyses. If successful, Proximity-Dependent Biotin Identification and mass spectrometry can be utilised to find novel interacting proteins throughout the entire AR signalling cascade.

To characterise the potential crosstalk between FUS, HOTAIR and the AR, reporter assays should be performed with cell co-transfected with these factors. If cross-talk between HOTAIR and FUS is identified, mammalian two-hybrid assays could be performed to identify which regions of the AR that FUS and HOTAIR are interacting with.

Both full length and truncated ALAS1 and ALAS2 were successfully expressed in *Escherichia coli* BL21(DE3) cells. However, all proteins appeared to be insoluble, therefore it is necessary to optimise the conditions to ensure that the proteins are expressed in the soluble fraction. Conditions such as temperature, IPTG concentration, optical density upon induction and bacterial growth time will need to be modified. Alternatively, the vector and/or bacterial strain could be substituted.

The novel approach of targeting haem synthesis in PCa is promising, particularly when non-cancerous cells were not affected by the treatments. However, it is necessary to continue this treatment in more PCa cell lines as well as other non-tumorigenic control lines. Moreover, once ALAS1 and ALAS2 structures are identified and further testing has been performed, this work should eventually move into relevant pre-clinical animal models and patient derived xenografts to validate and ensure safety of targeting this pathway. The data generated would support subsequently support clinical trials.

Supplementary data

```
FUS         186 METSSGGGSGGGYGNQDQSGGGGSGGYGQQDRGGRGRGGSGGGGGGGGGGYNRSSGGYEP
FUS           1 METSSGGASGGGYGNQDQSGGGGSGGYGQQDRGGRGRGGXCGGGGGGGGGGYNRSSGGYEP
                ******* ******************************  ******************

FUS         246 RGRGGGRGGRGGMETGGSDRGGFNKFGGPRDQGSRHDSEQDNSDNNTIFVQGLGENVTIE
FUS          61 RGRGGGRGGRGGMETGGSDRGGFNKFGGPRDQGSRHDSEQDNSDNNTIFVQGLGENVTIE
                ************************************************************

FUS         306 SVADYFKQIGIIKTNKKTGQPMETINLYTDRETGKLKGEATVSFDDPPSAKAAIDWFDGK
FUS         121 SVADYFKQIGIIKTNKKTGQPMETINLYTDRETGKLKGEATVSFDDPPSAKAAIDWFDGK
                ************************************************************

FUS         366 EFSGNPIKVSFATRRADFNRGGGNGRGGRGRGGPMETGRGGYGGGGSGGGGRGGFPSGGG
FUS         181 EFSGNPIKVSFATRRADFNRGGGNGRGGRGRGGPMETGRGGYGGGGSGGGGRGGFPSGGG
                ************************************************************

FUS         426 GGGGQQRAGDWKCPNPTCENMETNFSWRNECNQCKAPKPDGPGGGPGGSHMETGGNYGDD
FUS         241 GGGGQQRAGDWKCPNPTCENMETNFSWRNECNQCKAPKPDGPGGGPGGSHMETGGNYGDD
                ************************************************************

FUS         486 RRGGRGGYDRGGYRGRGGDRGGFRGGRGGGDRGGFGPGKMETDSRGEHRQDRRERPYSTO
FUS         301 RRGGRGGYDRGGYRGRGGDRGGFRGGRGGGDRGGFGPGEMETDSRGEHRQDRRERPYSTO
                ************************************ ********************

FUS         546 P
FUS         361 P
                *
```

Figure S1.1: Fused in Sarcoma (FUS) mutant (K510E) in the N-terminal domain of the protein. A mutation was introduced into the N-terminal domain of FUS.

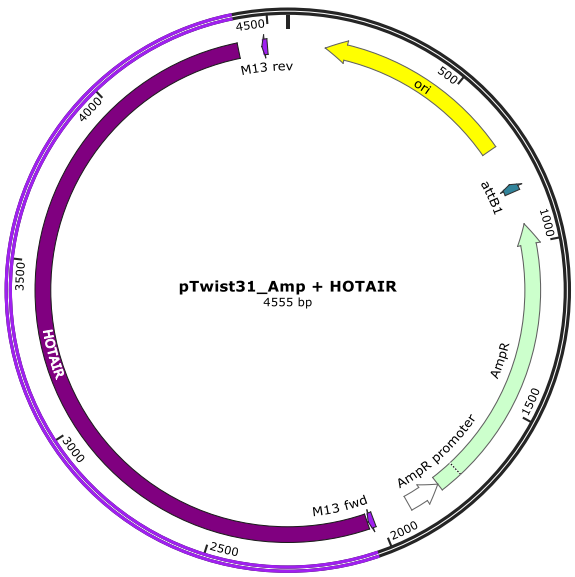

Figure S1.2: Hox Transcript Antisense Intergenic RNA (HOTAIR) cloned into shuttle vector pTWIST_Amp-HOTAIR. This plasmid was industrially synthesised with HOTAIR by TWIST Bioscience. This image was made using SnapGene® Viewer version 4.1**.**

Barfeld, S. J., Itkonen, H. M., Urbanucci, A. and Mills, I. G. (2014) Androgen-regulated metabolism and biosynthesis in prostate cancer. *Endocr Relat Cancer,* **21**, T57-66.
Bourque, S. L., Benjamin, C. D., Adams, M. A. and Nakatsu, K. (2010) Lack of hemodynamic effects after extended heme synthesis inhibition by succinylacetone in rats. *J Pharmacol Exp Ther,* **333**, 290-6.
Brooke, G. N., Culley, R. L., Dart, D. A., Mann, D. J., Gaughan, L., McCracken, S. R., Robson, C. N., Spencer-Dene, B., Gamble, S. C., Powell, S. M., Wait, R., Waxman, J., Walker, M. M. and Bevan, C. L. (2011) FUS/TLS is a novel mediator of androgen-dependent cell-cycle progression and prostate cancer growth. *Cancer Res,* **71**, 914-24.
Brooke, G. N., Gamble, S. C., Hough, M. A., Begum, S., Dart, D. A., Odontiadis, M., Powell, S. M., Fioretti, F. M., Bryan, R. A., Waxman, J., Wait, R. and Bevan, C. L. (2015) Antiandrogens Act as Selective Androgen Receptor Modulators at the Proteome Level in Prostate Cancer Cells. *Molecular & Cellular Proteomics,* **14**, 1201.
Davey, R. A. and Grossmann, M. (2016) Androgen Receptor Structure, Function and Biology: From Bench to Bedside. *The Clinical biochemist. Reviews,* **37**, 3-15.
Haile, S., Lal, A., Myung, J.-K. and Sadar, M. D. (2011) FUS/TLS Is a Co-Activator of Androgen Receptor in Prostate Cancer Cells. *PLoS ONE,* **6**, e24197.
Hooda, J., Cadinu, D., Alam, M. M., Shah, A., Cao, T. M., Sullivan, L. A., Brekken, R. and Zhang, L. (2013) Enhanced heme function and mitochondrial respiration promote the progression of lung cancer cells. *PLoS One,* **8**, e63402.
Kalyanaraman, B. (2017) Teaching the basics of cancer metabolism: Developing antitumor strategies by exploiting the differences between normal and cancer cell metabolism. *Redox biology,* **12**, 833-842.
Kubota, Y., Nomura, K., Katoh, Y., Yamashita, R., Kaneko, K. and Furuyama, K. (2016) Novel Mechanisms for Heme-dependent Degradation of ALAS1 Protein as a Component of Negative Feedback Regulation of Heme Biosynthesis. *J Biol Chem,* **291**, 20516-29.
Le Sage, V., Cinti, A. and Mouland, A. J. (2016) Proximity-Dependent Biotinylation for Identification of Interacting Proteins. *Curr Protoc Cell Biol,* **73**, 17.19.1-17.19.12.
McRonald, F. E., Risk, J. M. and Hodges, N. J. (2012) Protection from intracellular oxidative stress by cytoglobin in normal and cancerous oesophageal cells. *PLoS One,* **7**, e30587.
Misawa, A., Takayama, K. i. and Inoue, S. (2017) Long non-coding RNAs and prostate cancer. *Cancer Science,* **108**, 2107-2114.
Osguthorpe, D. J. and Hagler, A. T. (2011) Mechanism of androgen receptor antagonism by bicalutamide in the treatment of prostate cancer. *Biochemistry,* **50**, 4105-13.
Pelicano, H., Carney, D. and Huang, P. (2004) ROS stress in cancer cells and therapeutic implications. *Drug Resistance Updates,* **7**, 97-110.
Vance, C., Scotter, E. L., Nishimura, A. L., Troakes, C., Mitchell, J. C., Kathe, C., Urwin, H., Manser, C., Miller, C. C., Hortobágyi, T., Dragunow, M., Rogelj, B. and Shaw, C. E. (2013) ALS mutant FUS disrupts nuclear localization and sequesters wild-type FUS within cytoplasmic stress granules. *Human Molecular Genetics,* **22**, 2676-2688.
Xie, Y., Hou, W., Song, X., Yu, Y., Huang, J., Sun, X., Kang, R. and Tang, D. (2016) Ferroptosis: process and function. *Cell death and differentiation,* **23**, 369-379.
Zámocký, M., Hofbauer, S., Schaffner, I., Gasselhuber, B., Nicolussi, A., Soudi, M., Pirker, K. F., Furtmüller, P. G. and Obinger, C. (2015) Independent evolution of four heme peroxidase superfamilies. *Archives of Biochemistry and Biophysics,* **574**, 108-119.

Aaron, L., Franco, O. and Hayward, S. W. (2016) Review of Prostate Anatomy and Embryology and the Etiology of BPH. *The Urologic clinics of North America,* **43**, 279-288.

Abate-Shen, C. and Shen, M. M. (2000) Molecular genetics of prostate cancer. *Genes Dev,* **14**, 2410-34.

Agbor, T. A., Demma, Z., Mrsny, R. J., Castillo, A., Boll, E. J. and McCormick, B. A. (2014) The oxido-reductase enzyme glutathione peroxidase 4 (GPX4) governs Salmonella Typhimurium-induced neutrophil transepithelial migration. *Cellular Microbiology,* **16**, 1339-1353.

Ahn, J., Kibel, A. S., Park, J. Y., Rebbeck, T. R., Rennert, H., Stanford, J. L., Ostrander, E. A., Chanock, S., Wang, M. H., Mittal, R. D., Isaacs, W. B., Platz, E. A. and Hayes, R. B. (2011) Prostate cancer predisposition loci and risk of metastatic disease and prostate cancer recurrence. *Clin Cancer Res,* **17**, 1075-81.

Ajioka, R. S., Phillips, J. D. and Kushner, J. P. (2006) Biosynthesis of heme in mammals. *Biochimica et Biophysica Acta (BBA) - Molecular Cell Research,* **1763**, 723-736.

Aneck-Hahn, N. H., Schulenburg, G. W., Bornman, M. S., Farias, P. and de Jager, C. (2007) Impaired semen quality associated with environmental DDT exposure in young men living in a malaria area in the Limpopo Province, South Africa. *Journal of andrology,* **28**, 423-434.

Antonioli, E., Della-Colleta, H. H. and Carvalho, H. F. (2004) Smooth muscle cell behavior in the ventral prostate of castrated rats. *J Androl,* **25**, 50-6.

Astner, I., Schulze, J. O., van den Heuvel, J., Jahn, D., Schubert, W.-D. and Heinz, D. W. (2005) Crystal structure of 5-aminolevulinate synthase, the first enzyme of heme biosynthesis, and its link to XLSA in humans. *The EMBO Journal,* **24**, 3166-3177.

Ayala, A. G., Ro, J. Y., Babaian, R., Troncoso, P. and Grignon, D. J. (1989) The prostatic capsule: does it exist? Its importance in the staging and treatment of prostatic carcinoma. *The American journal of surgical pathology,* **13**, 21-27.

Baechtold, H., Kuroda, M., Sok, J., Ron, D., Lopez, B. S. and Akhmedov, A. T. (1999) Human 75-kDa DNA-pairing protein is identical to the pro-oncoprotein TLS/FUS and is able to promote D-loop formation. *J Biol Chem,* **274**, 34337-42.

Banach-Petrosky, W., Jessen, W. J., Ouyang, X., Gao, H., Rao, J., Quinn, J., Aronow, B. J. and Abate-Shen, C. (2007) Prolonged Exposure to Reduced Levels of Androgen Accelerates Prostate Cancer Progression in Nkx3.1; Pten Mutant Mice. *Cancer Research,* **67**, 9089.

Banjac, A., Perisic, T., Sato, H., Seiler, A., Bannai, S., Weiss, N., Kölle, P., Tschoep, K., Issels, R. D., Daniel, P. T., Conrad, M. and Bornkamm, G. W. (2007) The cystine/cysteine cycle: a redox cycle regulating susceptibility versus resistance to cell death. *Oncogene,* **27**, 1618.

Bao, B. Y., Pao, J. B., Huang, C. N., Pu, Y. S., Chang, T. Y., Lan, Y. H., Lu, T. L., Lee, H. Z., Chen, L. M., Ting, W. C., Hsieh, C. J. and Huang, S. P. (2012) Significant associations of prostate cancer susceptibility variants with survival in patients treated with androgen-deprivation therapy. *Int J Cancer,* **130**, 876-84.

Barfeld, S. J., Itkonen, H. M., Urbanucci, A. and Mills, I. G. (2014) Androgen-regulated metabolism and biosynthesis in prostate cancer. *Endocr Relat Cancer,* **21**, T57-66.

Beer, T. M., Armstrong, A. J., Rathkopf, D. E., Loriot, Y., Sternberg, C. N., Higano, C. S., Iversen, P., Bhattacharya, S., Carles, J., Chowdhury, S., Davis, I. D., de Bono, J. S., Evans, C. P., Fizazi, K., Joshua, A. M., Kim, C.-S., Kimura, G., Mainwaring, P., Mansbach, H., Miller, K., Noonberg, S. B., Perabo, F., Phung, D., Saad, F., Scher, H. I., Taplin, M.-E., Venner, P. M. and Tombal, B. (2014) Enzalutamide in Metastatic Prostate Cancer before Chemotherapy. *New England Journal of Medicine,* **371**, 424-433.

Berney, D. M., Beltran, L., Fisher, G., North, B. V., Greenberg, D., Møller, H., Soosay, G., Scardino, P. and Cuzick, J. (2016) Validation of a contemporary prostate cancer grading system using prostate cancer death as outcome. *British Journal Of Cancer,* **114**, 1078.

Bevan, C. L., Hoare, S., Claessens, F., Heery, D. M. and Parker, M. G. (1999) The AF1 and AF2 Domains of the Androgen Receptor Interact with Distinct Regions of SRC1. *Molecular and Cellular Biology,* **19**, 8383-8392.

Bhat, S. A., Ahmad, S. M., Mumtaz, P. T., Malik, A. A., Dar, M. A., Urwat, U., Shah, R. A. and Ganai, N. A. (2016) Long non-coding RNAs: Mechanism of action and functional utility. *Non-coding RNA Research,* **1**, 43-50.

Bhavsar, A. and Verma, S. (2014) Anatomic imaging of the prostate. *Biomed Res Int,* **2014**, 728539.

Bird, I. M. (2012) In the zone: understanding zona reticularis function and its transformation by adrenarche. *J Endocrinol,* **214**, 109-11.

Bishop, D. F., Henderson, A. S. and Astrin, K. H. (1990) Human delta-aminolevulinate synthase: assignment of the housekeeping gene to 3p21 and the erythroid-specific gene to the X chromosome. *Genomics,* **7**, 207-14.

Blana, A., Walter, B., Rogenhofer, S. and Wieland, W. F. (2004) High-intensity focused ultrasound for the treatment of localized prostate cancer: 5-year experience. *Urology,* **63**, 297-300.

Boon, R. A., Jaé, N., Holdt, L. and Dimmeler, S. (2016) Long Noncoding RNAs. *From Clinical Genetics to Therapeutic Targets?,* **67**, 1214-1226.

Bourque, S. L., Benjamin, C. D., Adams, M. A. and Nakatsu, K. (2010) Lack of hemodynamic effects after extended heme synthesis inhibition by succinylacetone in rats. *J Pharmacol Exp Ther,* **333**, 290-6.

Brawer, M. K. (2005) Prostatic Intraepithelial Neoplasia: An Overview. *Reviews in Urology,* **7**, S11-S18.

Brooke, G. N. and Bevan, C. L. (2009) The Role of Androgen Receptor Mutations in Prostate Cancer Progression. *Current Genomics,* **10**, 18-25.

Brooke, G. N., Culley, R. L., Dart, D. A., Mann, D. J., Gaughan, L., McCracken, S. R., Robson, C. N., Spencer-Dene, B., Gamble, S. C., Powell, S. M., Wait, R., Waxman, J., Walker, M. M. and Bevan, C. L. (2011) FUS/TLS is a novel mediator of androgen-dependent cell-cycle progression and prostate cancer growth. *Cancer Res,* **71**, 914-24.

Brooke, G. N., Gamble, S. C., Hough, M. A., Begum, S., Dart, D. A., Odontiadis, M., Powell, S. M., Fioretti, F. M., Bryan, R. A., Waxman, J., Wait, R. and Bevan, C. L. (2015) Antiandrogens Act as Selective Androgen Receptor Modulators at the Proteome Level in Prostate Cancer Cells. *Molecular & Cellular Proteomics,* **14**, 1201.

Burd, C. J., Morey, L. M. and Knudsen, K. E. (2006) Androgen receptor corepressors and prostate cancer. *Endocrine-Related Cancer,* **13**, 979-994.

Burris, T. P., Busby, S. A. and Griffin, P. R. (2012) Targeting Orphan Nuclear Receptors for Treatment of Metabolic Diseases and Autoimmunity. *Chemistry & biology,* **19**, 51-59.

Cairns, R. A., Harris, I. S. and Mak, T. W. (2011) Regulation of cancer cell metabolism. *Nat Rev Cancer,* **11**, 85-95.

Centenera, M. M., Harris, J. M., Tilley, W. D. and Butler, L. M. (2008) The contribution of different androgen receptor domains to receptor dimerization and signaling. *Mol Endocrinol,* **22**, 2373-82.

Chang, C. Y. and McDonnell, D. P. (2005) Androgen receptor-cofactor interactions as targets for new drug discovery. *Trends Pharmacol Sci,* **26**, 225-8.

Chang, J., Xu, W., Du, X. and Hou, J. (2018) MALAT1 silencing suppresses prostate cancer progression by upregulating miR-1 and downregulating KRAS. *OncoTargets and therapy,* **11**, 3461-3473.

Chang, K.-H., Li, R., Papari-Zareei, M., Watumull, L., Zhao, Y. D., Auchus, R. J. and Sharifi, N. (2011) Dihydrotestosterone synthesis bypasses testosterone to drive castration-resistant prostate cancer. *Proceedings of the National Academy of Sciences of the United States of America,* **108**, 13728-13733.

Chau, B. L., Ng, K. P., Li, K. K. and Lee, K. A. (2016) RGG boxes within the TET/FET family of RNA-binding proteins are functionally distinct. *Transcription,* **7**, 141-51.

Chen, H., Jin, S., Guo, J., Kombairaju, P., Biswal, S. and Zirkin, B. R. (2015) Knockout of the transcription factor Nrf2: Effects on testosterone production by aging mouse Leydig cells. *Molecular and Cellular Endocrinology,* **409**, 113-120.

Chen, N. and Zhou, Q. (2016) The evolving Gleason grading system. *Chinese Journal of Cancer Research,* **28**, 58-64.

Cheng, Z., Jie, W., Yuxiao, Z., Yuan, H., Gong, C. and Lixin, H. (2017) Efficacy and toxicity between luteinising hormone

releasing hormone analogue therapy and maximal

androgen blockade therapy in patients with

advanced prostate cancer in China. International Journal of Clinical and Experimental Medicine.

Choudhuri, S. (2010) Small noncoding RNAs: biogenesis, function, and emerging significance in toxicology. *J Biochem Mol Toxicol,* **24**, 195-216.

Chu, C., Quinn, J. and Chang, H. Y. (2012) Chromatin isolation by RNA purification (ChIRP). *J Vis Exp*.

Claessens, F., Denayer, S., Van Tilborgh, N., Kerkhofs, S., Helsen, C. and Haelens, A. (2008) Diverse roles of androgen receptor (AR) domains in AR-mediated signaling. *Nuclear Receptor Signaling,* **6**, e008.

Clinckemalie, L., Vanderschueren, D., Boonen, S. and Claessens, F. (2012) The hinge region in androgen receptor control. *Molecular and Cellular Endocrinology,* **358**, 1-8.

Cohen, R. J., Shannon, B. A., Phillips, M., Moorin, R. E., Wheeler, T. M. and Garrett, K. L. (2008) Central zone carcinoma of the prostate gland: a distinct tumor type with poor prognostic features. *J Urol,* **179**, 1762-7; discussion 1767.

Cooney, K. A. (2017) Inherited Predisposition to Prostate Cancer: From Gene Discovery to Clinical Impact. *Transactions of the American Clinical and Climatological Association,* **128**, 14-23.

Costello, L. C. and Franklin, R. B. (2006) The clinical relevance of the metabolism of prostate cancer; zinc and tumor suppression: connecting the dots. *Molecular Cancer,* **5**, 17-17.

Cutruzzolà, F., Giardina, G., Marani, M., Macone, A., Paiardini, A., Rinaldo, S. and Paone, A. (2017) Glucose Metabolism in the Progression of Prostate Cancer. *Frontiers in Physiology,* **8**, 97.

Dammer, E. B., Fallini, C., Gozal, Y. M., Duong, D. M., Rossoll, W., Xu, P., Lah, J. J., Levey, A. I., Peng, J., Bassell, G. J. and Seyfried, N. T. (2012) Coaggregation of RNA-binding proteins in a model of TDP-43 proteinopathy with selective RGG motif methylation and a role for RRM1 ubiquitination. *PLoS One,* **7**, e38658.

Davey, R. A. and Grossmann, M. (2016) Androgen Receptor Structure, Function and Biology: From Bench to Bedside. *The Clinical biochemist. Reviews,* **37**, 3-15.

De Leon, J. T., Iwai, A., Feau, C., Garcia, Y., Balsiger, H. A., Storer, C. L., Suro, R. M., Garza, K. M., Lee, S., Sang Kim, Y., Chen, Y., Ning, Y.-M., Riggs, D. L., Fletterick, R. J., Guy, R. K., Trepel, J. B., Neckers, L. M. and Cox, M. B. (2011) Targeting the regulation of androgen receptor signaling by the heat shock protein 90 cochaperone FKBP52 in prostate cancer cells. *Proceedings of the National Academy of Sciences,* **108**, 11878-11883.

De Marzo, A. M., Meeker, A. K., Zha, S., Luo, J., Nakayama, M., Platz, E. A., Isaacs, W. B. and Nelson, W. G. (2003) Human prostate cancer precursors and pathobiology. *Urology,* **62**, 55-62.

de Ronde, W., van der Schouw, Y. T., Muller, M., Grobbee, D. E., Gooren, L. J. G., Pols, H. A. P. and de Jong, F. H. (2005) Associations of Sex-Hormone-Binding Globulin (SHBG) with Non-SHBG-Bound Levels of Testosterone and Estradiol in Independently Living Men. *The Journal of Clinical Endocrinology & Metabolism,* **90**, 157-162.

de Rooij, M., Hamoen, E. H. J., Witjes, J. A., Barentsz, J. O. and Rovers, M. M. (2016) Accuracy of Magnetic Resonance Imaging for Local Staging of Prostate Cancer: A Diagnostic Meta-analysis. *European Urology,* **70**, 233-245.

Dhar, S. K., Zhang, J., Gal, J., Xu, Y., Miao, L., Lynn, B. C., Zhu, H., Kasarskis, E. J. and St Clair, D. K. (2014) FUsed in sarcoma is a novel regulator of manganese superoxide dismutase gene transcription. *Antioxid Redox Signal,* **20**, 1550-66.

Di Lorenzo, G., Buonerba, C., Autorino, R., De Placido, S. and Sternberg, C. N. (2010) Castration-resistant prostate cancer: current and emerging treatment strategies. *Drugs,* **70**, 983-1000.

Diamanti-Kandarakis, E., Bourguignon, J.-P., Giudice, L. C., Hauser, R., Prins, G. S., Soto, A. M., Zoeller, R. T. and Gore, A. C. (2009) Endocrine-Disrupting Chemicals: An Endocrine Society Scientific Statement. *Endocrine Reviews,* **30**, 293-342.

Ding, W., Ren, J., Ren, H. and Wang, D. (2017) Long Noncoding RNA HOTAIR Modulates MiR-206-mediated Bcl-w Signaling to Facilitate Cell Proliferation in Breast Cancer. *Scientific Reports,* **7**, 17261.

Dixon, S. J. and Stockwell, B. R. (2013) The role of iron and reactive oxygen species in cell death. *Nature Chemical Biology,* **10**, 9.

Dormann, D., Rodde, R., Edbauer, D., Bentmann, E., Fischer, I., Hruscha, A., Than, M. E., Mackenzie, I. R. A., Capell, A., Schmid, B., Neumann, M. and Haass, C. (2010) ALS-associated fused in sarcoma (FUS) mutations disrupt Transportin-mediated nuclear import. *The EMBO Journal,* **29**, 2841-2857.

Dubbink, H. J., Hersmus, R., Verma, C. S., van der Korput, H. A. G. M., Berrevoets, C. A., van Tol, J., Ziel-van der Made, A. C. J., Brinkmann, A. O., Pike, A. C. W. and Trapman, J. (2004) Distinct Recognition Modes of FXXLF and LXXLL Motifs by the Androgen Receptor. *Molecular Endocrinology,* **18**, 2132-2150.

Dueregger, A., Heidegger, I., Ofer, P., Perktold, B., Ramoner, R., Klocker, H. and Eder, I. E. (2014) The Use of Dietary Supplements to Alleviate Androgen Deprivation Therapy Side Effects during Prostate Cancer Treatment. *Nutrients,* **6**, 4491-4519.

Dupre-Crochet, S., Erard, M. and Nubetae, O. (2013) ROS production in phagocytes: why, when, and where? *J Leukoc Biol,* **94**, 657-70.

Dutt, S. S. and Gao, A. C. (2009) Molecular mechanisms of castration-resistant prostate cancer progression. *Future oncology (London, England),* **5**, 1403-1413.

Dwyer, Daniel J., Camacho, Diogo M., Kohanski, Michael A., Callura, Jarred M. and Collins, James J. (2012) Antibiotic-Induced Bacterial Cell Death Exhibits Physiological and Biochemical Hallmarks of Apoptosis. *Molecular Cell,* **46**, 561-572.

Ederle, H. and Dormann, D. (2017) TDP-43 and FUS en route from the nucleus to the cytoplasm. *FEBS Letters,* **591**, 1489-1507.

Edwards, J. and Bartlett, J. M. S. (2005) The androgen receptor and signal-transduction pathways in hormone-refractory prostate cancer. Part 2: androgen-receptor cofactors and bypass pathways. *BJU International,* **95**, 1327-1335.

Evans, A. J. (2018) Treatment effects in prostate cancer. *Modern Pathology,* **31**, S110.

Fang, Y. and Fullwood, M. J. (2016) Roles, Functions, and Mechanisms of Long Non-coding RNAs in Cancer. *Genomics, Proteomics & Bioinformatics,* **14**, 42-54.

Fanzani, A. and Poli, M. (2017) Iron, Oxidative Damage and Ferroptosis in Rhabdomyosarcoma. *International Journal of Molecular Sciences,* **18**, 1718.

Fernie, A. R., Carrari, F. and Sweetlove, L. J. (2004) Respiratory metabolism: glycolysis, the TCA cycle and mitochondrial electron transport. *Curr Opin Plant Biol,* **7**, 254-61.

Ferreira, G. C., Neame, P. J. and Dailey, H. A. (1993) Heme biosynthesis in mammalian systems: evidence of a Schiff base linkage between the pyridoxal 5'-phosphate cofactor and a lysine residue in 5-aminolevulinate synthase. *Protein Sci,* **2**, 1959-65.

Festjens, N., Vanden Berghe, T. and Vandenabeele, P. (2006) Necrosis, a well-orchestrated form of cell demise: Signalling cascades, important mediators and concomitant immune response. *Biochimica et Biophysica Acta (BBA) - Bioenergetics,* **1757**, 1371-1387.

Fitzwalter, B. E. and Thorburn, A. (2017) A caspase-independent way to kill cancer cells. *Nat Cell Biol,* **19**, 1014-1015.

Foster, A. D., Sivarapatna, A. and Gress, R. E. (2011) The aging immune system and its relationship with cancer. *Aging health,* **7**, 707-718.

Fraietta, R., Zylberstejn, D. S. and Esteves, S. C. (2013) Hypogonadotropic Hypogonadism Revisited. *Clinics,* **68**, 81-88.

Franken, A. C. W., Lokman, B. C., Ram, A. F. J., Punt, P. J., van den Hondel, C. A. M. J. J. and de Weert, S. (2011) Heme biosynthesis and its regulation: towards understanding and improvement of heme biosynthesis in filamentous fungi. *Applied Microbiology and Biotechnology,* **91**, 447-460.

Franz, M. C., Anderle, P., Bürzle, M., Suzuki, Y., Freeman, M. R., Hediger, M. A. and Kovacs, G. (2013) Zinc transporters in prostate cancer. *Molecular aspects of medicine,* **34**, 735-741.

Galluzzi, L. and Kroemer, G. (2008) Necroptosis: A Specialized Pathway of Programmed Necrosis. *Cell,* **135**, 1161-1163.

Gaschler, M. M. and Stockwell, B. R. (2017) Lipid peroxidation in cell death. *Biochemical and biophysical research communications,* **482**, 419-425.

Geisler, S., Lojek, L., Khalil, A. M., Baker, K. E. and Coller, J. (2012) Decapping of long non-coding RNAs regulates inducible genes. *Molecular Cell,* **45**, 279-291.

Giampazolias, E., Zunino, B., Dhayade, S., Bock, F., Cloix, C., Cao, K., Roca, A., Lopez, J., Ichim, G., Proics, E., Rubio-Patino, C., Fort, L., Yatim, N., Woodham, E., Orozco, S., Taraborrelli, L., Peltzer, N., Lecis, D., Machesky, L., Walczak, H., Albert, M. L., Milling, S., Oberst, A., Ricci, J. E., Ryan, K. M., Blyth, K. and Tait, S. W. G. (2017) Mitochondrial permeabilization engages NF-kappaB-dependent anti-tumour activity under caspase deficiency. *Nat Cell Biol,* **19**, 1116-1129.

Giampietri, C., Starace, D., Petrungaro, S., Filippini, A. and Ziparo, E. (2014) Necroptosis: molecular signalling and translational implications. *Int J Cell Biol,* **2014**, 490275.

Gibb, E. A., Brown, C. J. and Lam, W. L. (2011) The functional role of long non-coding RNA in human carcinomas. *Molecular Cancer,* **10**, 38-38.

Gisk, B., Yasui, Y., Kohchi, T. and Frankenberg-Dinkel, N. (2010) Characterization of the haem oxygenase protein family in Arabidopsis thaliana reveals a diversity of functions. *Biochem J,* **425**, 425-34.

Gordetsky, J. and Epstein, J. (2016) Grading of prostatic adenocarcinoma: current state and prognostic implications. *Diagnostic Pathology,* **11**, 25.

Grossmann, M. E., Huang, H. and Tindall, D. J. (2001) Androgen Receptor Signaling in Androgen-Refractory Prostate Cancer. *JNCI: Journal of the National Cancer Institute,* **93**, 1687-1697.

Gupta, R. A., Shah, N., Wang, K. C., Kim, J., Horlings, H. M., Wong, D. J., Tsai, M.-C., Hung, T., Argani, P., Rinn, J. L., Wang, Y., Brzoska, P., Kong, B., Li, R., West, R. B., van de Vijver, M. J., Sukumar, S. and Chang, H. Y. (2010) Long noncoding RNA HOTAIR reprograms chromatin state to promote cancer metastasis. *Nature,* **464**, 1071-1076.

Gutschner, T. and Diederichs, S. (2012) The hallmarks of cancer. *RNA Biology,* **9**, 703-719.

Guttman, M., Amit, I., Garber, M., French, C., Lin, M. F., Feldser, D., Huarte, M., Zuk, O., Carey, B. W., Cassady, J. P., Cabili, M. N., Jaenisch, R., Mikkelsen, T. S., Jacks, T., Hacohen, N., Bernstein, B. E., Kellis, M., Regev, A., Rinn, J. L. and Lander, E. S. (2009) Chromatin signature reveals over a thousand highly conserved large non-coding RNAs in mammals. *Nature,* **458**, 223.

Haile, S., Lal, A., Myung, J.-K. and Sadar, M. D. (2011) FUS/TLS Is a Co-Activator of Androgen Receptor in Prostate Cancer Cells. *PLoS ONE,* **6**, e24197.

Haiman, C. A., Patterson, N., Freedman, M. L., Myers, S. R., Pike, M. C., Waliszewska, A., Neubauer, J., Tandon, A., Schirmer, C., McDonald, G. J., Greenway, S. C., Stram, D. O., Le Marchand, L., Kolonel, L. N., Frasco, M., Wong, D., Pooler, L. C., Ardlie, K., Oakley-Girvan, I., Whittemore, A. S., Cooney, K. A., John, E. M., Ingles, S. A., Altshuler, D., Henderson, B. E. and Reich, D. (2007) Multiple regions within 8q24 independently affect risk for prostate cancer. *Nat Genet,* **39**, 638-44.

Harnden, P., Shelley, M. D., Coles, B., Staffurth, J. and Mason, M. D. (2007) Should the Gleason grading system for prostate cancer be modified to account for high-grade tertiary components? A systematic review and meta-analysis. *Lancet Oncol,* **8**, 411-9.

Hay, N. (2016) Reprogramming glucose metabolism in cancer: can it be exploited for cancer therapy? *Nature reviews. Cancer,* **16**, 635-649.

Heemers, H. V. and Tindall, D. J. (2007) Androgen Receptor (AR) Coregulators: A Diversity of Functions Converging on and Regulating the AR Transcriptional Complex. *Endocrine Reviews,* **28**, 778-808.

Hess-Wilson, J. K. and Knudsen, K. E. (2006) Endocrine disrupting compounds and prostate cancer. *Cancer Letters,* **241**, 1-12.

Hooda, J., Alam, M. and Zhang, L. (2015) Measurement of Heme Synthesis Levels in Mammalian Cells. *Journal of Visualized Experiments : JoVE*, 51579.

Hooda, J., Cadinu, D., Alam, M. M., Shah, A., Cao, T. M., Sullivan, L. A., Brekken, R. and Zhang, L. (2013) Enhanced heme function and mitochondrial respiration promote the progression of lung cancer cells. *PLoS One,* **8**, e63402.

Hotte, S. J. and Saad, F. (2010) Current management of castrate-resistant prostate cancer. *Current Oncology,* **17**, S72-S79.

Hua, J. T., Ahmed, M., Guo, H., Zhang, Y., Chen, S., Soares, F., Lu, J., Zhou, S., Wang, M., Li, H., Larson, N. B., McDonnell, S. K., Patel, P. S., Liang, Y., Yao, C. Q., van der Kwast, T., Lupien, M., Feng, F. Y., Zoubeidi, A., Tsao, M.-S., Thibodeau, S. N., Boutros, P. C. and He, H. H. (2018) Risk SNP-Mediated Promoter-Enhancer Switching Drives Prostate Cancer through lncRNA PCAT19. *Cell,* **174**, 564-575.e18.

Huarte, M. (2015) The emerging role of lncRNAs in cancer. *Nat Med,* **21**, 1253-61.

Hunter, G. A. and Ferreira, G. C. (1999) Lysine-313 of 5-Aminolevulinate Synthase Acts as a General Base during Formation of the Quinonoid Reaction Intermediates. *Biochemistry,* **38**, 12526.

Iko, Y., Kodama, T. S., Kasai, N., Oyama, T., Morita, E. H., Muto, T., Okumura, M., Fujii, R., Takumi, T., Tate, S.-i. and Morikawa, K. (2004) Domain Architectures and Characterization of an RNA-binding Protein, TLS. *Journal of Biological Chemistry,* **279**, 44834-44840.

Jernberg, E., Bergh, A. and Wikström, P. (2017) Clinical relevance of androgen receptor alterations in prostate cancer. *Endocrine connections,* **6**, R146-R161.

Jiang, Y., Palma, J. F., Agus, D. B., Wang, Y. and Gross, M. E. (2010) Detection of Androgen Receptor Mutations in Circulating Tumor Cells in Castration-Resistant Prostate Cancer. *Clinical Chemistry,* **56**, 1492.

Joniau, S., Goeman, L., Pennings, J. and Van Poppel, H. (2005) Prostatic Intraepithelial Neoplasia (PIN): Importance and Clinical Management. *European Urology,* **48**, 379-385.

Kafina, M. D. and Paw, B. H. (2017) Intracellular iron and heme trafficking and metabolism in developing erythroblasts. *Metallomics,* **9**, 1193-1203.

Kalyanaraman, B. (2017) Teaching the basics of cancer metabolism: Developing antitumor strategies by exploiting the differences between normal and cancer cell metabolism. *Redox biology,* **12**, 833-842.

Kantari, C. and Walczak, H. (2011) Caspase-8 and Bid: Caught in the act between death receptors and mitochondria. *Biochimica et Biophysica Acta (BBA) - Molecular Cell Research,* **1813**, 558-563.

Kaufmann, S. H., Desnoyers, S., Ottaviano, Y., Davidson, N. E. and Poirier, G. G. (1993) Specific proteolytic cleavage of poly(ADP-ribose) polymerase: an early marker of chemotherapy-induced apoptosis. *Cancer Res,* **53**, 3976-85.

Kemppainen, J. A., Lane, M. V., Sar, M. and Wilson, E. M. (1992) Androgen receptor phosphorylation, turnover, nuclear transport, and transcriptional activation. Specificity for steroids and antihormones. *J Biol Chem,* **267**, 968-74.

Kim, J. W. and Dang, C. V. (2006) Cancer's molecular sweet tooth and the Warburg effect. *Cancer Res,* **66**, 8927-30.

Kirby, M., Hirst, C. and Crawford, E. D. (2011) Characterising the castration-resistant prostate cancer population: a systematic review. *Int J Clin Pract,* **65**, 1180-92.

Kluth, L. A., Shariat, S. F., Kratzik, C., Tagawa, S., Sonpavde, G., Rieken, M., Scherr, D. S. and Pummer, K. (2014) The hypothalamic-pituitary-gonadal axis and prostate cancer: implications for androgen deprivation therapy. *World J Urol,* **32**, 669-76.

Koochekpour, S. (2010) Androgen receptor signaling and mutations in prostate cancer. *Asian Journal of Andrology,* **12**, 639-657.
Koryakina, Y., Ta, H. Q. and Gioeli, D. (2014) Phosphorylation of the Androgen Receptor. *Endocrine-related cancer,* **21**, T131-T145.
Kroemer, G. and Pouyssegur, J. (2008) Tumor Cell Metabolism: Cancer's Achilles' Heel. *Cancer Cell,* **13**, 472-482.
Kubota, Y., Nomura, K., Katoh, Y., Yamashita, R., Kaneko, K. and Furuyama, K. (2016) Novel Mechanisms for Heme-dependent Degradation of ALAS1 Protein as a Component of Negative Feedback Regulation of Heme Biosynthesis. *J Biol Chem,* **291**, 20516-29.
Kumar, R. and McEwan, I. J. (2012) Allosteric Modulators of Steroid Hormone Receptors: Structural Dynamics and Gene Regulation. *Endocrine Reviews,* **33**, 271-299.
Kumar, V. L. and Majumder, P. K. (1995) Prostate gland: Structure, functions and regulation. *International Urology and Nephrology,* **27**, 231-243.
Lagier-Tourenne, C. and Cleveland, D. W. (2009) Rethinking ALS: the FUS about TDP-43. *Cell,* **136**, 1001-4.
Lane, J. A., Oliver, S. E., Appleby, P. N., Lentjes, M. A. H., Emmett, P., Kuh, D., Stephen, A., Brunner, E. J., Shipley, M. J., Hamdy, F. C., Neal, D. E., Donovan, J. L., Khaw, K. T. and Key, T. J. (2017) Prostate cancer risk related to foods, food groups, macronutrients and micronutrients derived from the UK Dietary Cohort Consortium food diaries. *European Journal of Clinical Nutrition,* **71**, 274-283.
Lashley, T., Rohrer, J. D., Bandopadhyay, R., Fry, C., Ahmed, Z., Isaacs, A. M., Brelstaff, J. H., Borroni, B., Warren, J. D., Troakes, C., King, A., Al-Saraj, S., Newcombe, J., Quinn, N., Ostergaard, K., Schrøder, H. D., Bojsen-Møller, M., Braendgaard, H., Fox, N. C., Rossor, M. N., Lees, A. J., Holton, J. L. and Revesz, T. (2011) A comparative clinical, pathological, biochemical and genetic study of fused in sarcoma proteinopathies. *Brain,* **134**, 2548-2564.
Lawson, D. A., Zong, Y., Memarzadeh, S., Xin, L., Huang, J. and Witte, O. N. (2010) Basal epithelial stem cells are efficient targets for prostate cancer initiation. *Proceedings of the National Academy of Sciences,* **107**, 2610-2615.
Layer, G., Reichelt, J., Jahn, D. and Heinz, D. W. (2010) Structure and function of enzymes in heme biosynthesis. *Protein Science : A Publication of the Protein Society,* **19**, 1137-1161.
Le Sage, V., Cinti, A. and Mouland, A. J. (2016) Proximity-Dependent Biotinylation for Identification of Interacting Proteins. *Curr Protoc Cell Biol,* **73**, 17.19.1-17.19.12.
Lee, D. K. and Chang, C. (2003) Expression and Degradation of Androgen Receptor: Mechanism and Clinical Implication. *The Journal of Clinical Endocrinology & Metabolism,* **88**, 4043-4054.
Lewerenz, J., Hewett, S. J., Huang, Y., Lambros, M., Gout, P. W., Kalivas, P. W., Massie, A., Smolders, I., Methner, A., Pergande, M., Smith, S. B., Ganapathy, V. and Maher, P. (2013) The Cystine/Glutamate Antiporter System x(c)(−) in Health and Disease: From Molecular Mechanisms to Novel Therapeutic Opportunities. *Antioxidants & Redox Signaling,* **18**, 522-555.
Li, B., Lu, W. and Chen, Z. (2014) Regulation of Androgen Receptor by E3 Ubiquitin Ligases: for More or Less. *Receptors & clinical investigation,* **1**, 10.14800/rci.122.
Li, S., Li, J., Chen, C., Zhang, R. and Wang, K. (2017) Pan-cancer analysis of long non-coding RNA NEAT1 in various cancers. *Genes & diseases,* **5**, 27-35.
Li, Y., Chan, S. C., Brand, L. J., Hwang, T. H., Silverstein, K. A. T. and Dehm, S. M. (2013) Androgen receptor splice variants mediate enzalutamide resistance in castration-resistant prostate cancer cell lines. *Cancer research,* **73**, 483-489.
Li, Y., Luo, H., Xiao, N., Duan, J., Wang, Z. and Wang, S. (2018) Long Noncoding RNA SChLAP1 Accelerates the Proliferation and Metastasis of Prostate Cancer via Targeting miR-198 and Promoting the MAPK1 Pathway. *Oncol Res,* **26**, 131-143.
Linkermann, A. and Green, D. R. (2014) Necroptosis. *The New England journal of medicine,* **370**, 455-465.

Liou, G.-Y. and Storz, P. (2010) Reactive oxygen species in cancer. *Free radical research,* **44**, 479-496.
Lipsky, B. A., Byren, I. and Hoey, C. T. (2010) Treatment of Bacterial Prostatitis. *Clinical Infectious Diseases,* **50**, 1641-1652.
Liu, C., Kelnar, K., Liu, B., Chen, X., Calhoun-Davis, T., Li, H., Patrawala, L., Yan, H., Jeter, C., Honorio, S., Wiggins, J. F., Bader, A. G., Fagin, R., Brown, D. and Tang, D. G. (2011) Identification of miR-34a as a potent inhibitor of prostate cancer progenitor cells and metastasis by directly repressing CD44. *Nature medicine,* **17**, 211-215.
Liu, X., Niu, C., Ren, J., Zhang, J., Xie, X., Zhu, H., Feng, W. and Gong, W. (2013) The RRM domain of human fused in sarcoma protein reveals a non-canonical nucleic acid binding site. *Biochimica et Biophysica Acta (BBA) - Molecular Basis of Disease,* **1832**, 375-385.
Lu, C. and Luo, J. (2013) Decoding the androgen receptor splice variants. *Translational Andrology and Urology,* **2**, 178-186.
Marker, P. C., Donjacour, A. A., Dahiya, R. and Cunha, G. R. (2003) Hormonal, cellular, and molecular control of prostatic development. *Developmental Biology,* **253**, 165-174.
Massard, C. and Fizazi, K. (2011) Targeting Continued Androgen Receptor Signaling in Prostate Cancer. *Clinical Cancer Research,* **17**, 3876.
McNair, C., Urbanucci, A., Comstock, C. E. S., Augello, M. A., Goodwin, J. F., Launchbury, R., Zhao, S. G., Schiewer, M. J., Ertel, A., Karnes, J., Davicioni, E., Wang, L., Wang, Q., Mills, I. G., Feng, F. Y., Li, W., Carroll, J. S. and Knudsen, K. E. (2017) Cell cycle-coupled expansion of AR activity promotes cancer progression. *Oncogene,* **36**, 1655-1668.
McRonald, F. E., Risk, J. M. and Hodges, N. J. (2012) Protection from intracellular oxidative stress by cytoglobin in normal and cancerous oesophageal cells. *PLoS One,* **7**, e30587.
Meijer, O. C., Steenbergen, P. J. and de Kloet, E. R. (2000) Differential Expression and Regional Distribution of Steroid Receptor Coactivators SRC-1 and SRC-2 in Brain and Pituitary*. *Endocrinology,* **141**, 2192-2199.
Michalik, K. M., You, X., Manavski, Y., Doddaballapur, A., Zornig, M., Braun, T., John, D., Ponomareva, Y., Chen, W., Uchida, S., Boon, R. A. and Dimmeler, S. (2014) Long noncoding RNA MALAT1 regulates endothelial cell function and vessel growth. *Circ Res,* **114**, 1389-97.
Micheau, O., Thome, M., Schneider, P., Holler, N., Tschopp, J., Nicholson, D. W., Briand, C. and Grutter, M. G. (2002) The long form of FLIP is an activator of caspase-8 at the Fas death-inducing signaling complex. *J Biol Chem,* **277**, 45162-71.
Miller, W. L. and Auchus, R. J. (2011) The Molecular Biology, Biochemistry, and Physiology of Human Steroidogenesis and Its Disorders. *Endocrine Reviews,* **32**, 81-151.
Misawa, A., Takayama, K. i. and Inoue, S. (2017) Long non‐coding RNAs and prostate cancer. *Cancer Science,* **108**, 2107-2114.
Moeller, A., Cookson, M. and Patel, S. G. (2018) Metastatic Castrate-Resistant Prostate Cancer Practical Review. *Physician Assistant Clinics,* **3**, 11-21.
Monahan, Z., Ryan, V. H., Janke, A. M., Burke, K. A., Rhoads, S. N., Zerze, G. H., O'Meally, R., Dignon, G. L., Conicella, A. E., Zheng, W., Best, R. B., Cole, R. N., Mittal, J., Shewmaker, F. and Fawzi, N. L. (2017) Phosphorylation of the FUS low‐complexity domain disrupts phase separation, aggregation, and toxicity. *The EMBO Journal,* **36**, 2951-2967.
Mostaghel, E. A. (2013) Steroid hormone synthetic pathways in prostate cancer. *Translational Andrology and Urology,* **2**, 212-227.
Munakata, H., Sun, J. Y., Yoshida, K., Nakatani, T., Honda, E., Hayakawa, S., Furuyama, K. and Hayashi, N. (2004) Role of the heme regulatory motif in the heme-mediated inhibition of mitochondrial import of 5-aminolevulinate synthase. *J Biochem,* **136**, 233-8.
Mundy, G. R. (2002) Metastasis to bone: causes, consequences and therapeutic opportunities. *Nature Reviews Cancer,* **2**, 584.
Murashima, A., Kishigami, S., Thomson, A. and Yamada, G. (2015) Androgens and mammalian male reproductive tract development. *Biochim Biophys Acta,* **1849**, 163-70.

Myung, J.-K., Banuelos, C. A., Fernandez, J. G., Mawji, N. R., Wang, J., Tien, A. H., Yang, Y. C., Tavakoli, I., Haile, S., Watt, K., McEwan, I. J., Plymate, S., Andersen, R. J. and Sadar, M. D. (2013) An androgen receptor N-terminal domain antagonist for treating prostate cancer. *The Journal of Clinical Investigation,* **123**, 2948-2960.

Nadal, M., Prekovic, S., Gallastegui, N., Helsen, C., Abella, M., Zielinska, K., Gay, M., Vilaseca, M., Taulès, M., Houtsmuller, A. B., van Royen, M. E., Claessens, F., Fuentes-Prior, P. and Estébanez-Perpiñá, E. (2017) Structure of the homodimeric androgen receptor ligand-binding domain. *Nature Communications,* **8**, 14388.

Nelson, K. A. and Witte, J. S. (2002) Androgen receptor CAG repeats and prostate cancer. *Am J Epidemiol,* **155**, 883-90.

Nickel, J. C., Gilling, P., Tammela, T. L., Morrill, B., Wilson, T. H. and Rittmaster, R. S. (2011) Comparison of dutasteride and finasteride for treating benign prostatic hyperplasia: the Enlarged Prostate International Comparator Study (EPICS). *BJU International,* **108**, 388-394.

Niu, C., Zhang, J., Gao, F., Yang, L., Jia, M., Zhu, H. and Gong, W. (2012) FUS-NLS/Transportin 1 complex structure provides insights into the nuclear targeting mechanism of FUS and the implications in ALS. *PLoS One,* **7**, e47056.

Osguthorpe, D. J. and Hagler, A. T. (2011) Mechanism of androgen receptor antagonism by bicalutamide in the treatment of prostate cancer. *Biochemistry,* **50**, 4105-13.

Ozdilek, B. A., Thompson, V. F., Ahmed, N. S., White, C. I., Batey, R. T. and Schwartz, J. C. (2017) Intrinsically disordered RGG/RG domains mediate degenerate specificity in RNA binding. *Nucleic Acids Research,* **45**, 7984-7996.

Parimi, V., Goyal, R., Poropatich, K. and Yang, X. J. (2014) Neuroendocrine differentiation of prostate cancer: a review. *American Journal of Clinical and Experimental Urology,* **2**, 273-285.

Pelicano, H., Carney, D. and Huang, P. (2004) ROS stress in cancer cells and therapeutic implications. *Drug Resistance Updates,* **7**, 97-110.

Penning, T. M. (2014) Androgen biosynthesis in castration-resistant prostate cancer. *Endocrine-related cancer,* **21**, T67-T78.

Perlmutter, M. A. and Lepor, H. (2007) Androgen Deprivation Therapy in the Treatment of Advanced Prostate Cancer. *Reviews in Urology,* **9**, S3-S8.

Petrunak, E. M., DeVore, N. M., Porubsky, P. R. and Scott, E. E. (2014) Structures of human steroidogenic cytochrome P450 17A1 with substrates. *J Biol Chem,* **289**, 32952-64.

Pietri, E., Conteduca, V., Andreis, D., Massa, I., Melegari, E., Sarti, S., Cecconetto, L., Schirone, A., Bravaccini, S., Serra, P., Fedeli, A., Maltoni, R., Amadori, D., De Giorgi, U. and Rocca, A. (2016) Androgen receptor signaling pathways as a target for breast cancer treatment. *Endocrine-Related Cancer,* **23**, R485-R498.

Poulos, T. L. (2014) Heme Enzyme Structure and Function. *Chemical reviews,* **114**, 3919-3962.

Pritchard, C. C., Mateo, J., Walsh, M. F., De Sarkar, N., Abida, W., Beltran, H., Garofalo, A., Gulati, R., Carreira, S., Eeles, R., Elemento, O., Rubin, M. A., Robinson, D., Lonigro, R., Hussain, M., Chinnaiyan, A., Vinson, J., Filipenko, J., Garraway, L., Taplin, M. E., AlDubayan, S., Han, G. C., Beightol, M., Morrissey, C., Nghiem, B., Cheng, H. H., Montgomery, B., Walsh, T., Casadei, S., Berger, M., Zhang, L., Zehir, A., Vijai, J., Scher, H. I., Sawyers, C., Schultz, N., Kantoff, P. W., Solit, D., Robson, M., Van Allen, E. M., Offit, K., de Bono, J. and Nelson, P. S. (2016) Inherited DNA-Repair Gene Mutations in Men with Metastatic Prostate Cancer. *N Engl J Med,* **375**, 443-53.

Prostate Cancer UK. (2019) Treatments, https://prostatecanceruk.org/prostate-information/treatments Accessed on: 16 January 2019

Rabbitts, T. H., Forster, A., Larson, R. and Nathan, P. (1993) Fusion of the dominant negative transcription regulator CHOP with a novel gene FUS by translocation t(12;16) in malignant liposarcoma. *Nature Genetics,* **4**, 175.

Ricke, W. A., Wang, Y., Kurita, T., Hayward, S. W. and Cunha, G. R. (2005) Hormonal and stromal regulation of normal and neoplastic prostatic growth. *Prog Mol Subcell Biol,* **40**, 183-216.

Rishi, I., Baidouri, H., Abbasi, J. A., Bullard-Dillard, R., Kajdacsy-Balla, A., Pestaner, J. P., Skacel, M., Tubbs, R. and Bagasra, O. (2003) Prostate cancer in African American men is associated with downregulation of zinc transporters. *Appl Immunohistochem Mol Morphol,* **11**, 253-60.

Robinson-Rechavi, M., Escriva Garcia, H. and Laudet, V. (2003) The nuclear receptor superfamily. *J Cell Sci,* **116**, 585-6.

Rock, K. L. and Kono, H. (2008) The inflammatory response to cell death. *Annual review of pathology,* **3**, 99-126.

Rodriguez-Martinez, H., Kvist, U., Ernerudh, J., Sanz, L. and Calvete, J. J. (2011) Seminal plasma proteins: what role do they play? *Am J Reprod Immunol,* **66 Suppl 1**, 11-22.

Roney, J. R., Simmons, Z. L. and Lukaszewski, A. W. (2010) Androgen receptor gene sequence and basal cortisol concentrations predict men's hormonal responses to potential mates. *Proceedings of the Royal Society B: Biological Sciences,* **277**, 57.

Rosano, G. L. and Ceccarelli, E. A. (2014) Recombinant protein expression in Escherichia coli: advances and challenges. *Frontiers in Microbiology,* **5**, 172.

Sah, V. K., Wang, L., Min, X., Feng, Z., Rizal, R., Li, L., Deng, M., Liu, J. and Li, H. (2015) Multiparametric MR imaging in diagnosis of chronic prostatitis and its differentiation from prostate cancer. *Radiology of Infectious Diseases,* **1**, 70-77.

Salameh, A., Lee, A. K., Cardo-Vila, M., Nunes, D. N., Efstathiou, E., Staquicini, F. I., Dobroff, A. S., Marchio, S., Navone, N. M., Hosoya, H., Lauer, R. C., Wen, S., Salmeron, C. C., Hoang, A., Newsham, I., Lima, L. A., Carraro, D. M., Oliviero, S., Kolonin, M. G., Sidman, R. L., Do, K. A., Troncoso, P., Logothetis, C. J., Brentani, R. R., Calin, G. A., Cavenee, W. K., Dias-Neto, E., Pasqualini, R. and Arap, W. (2015) PRUNE2 is a human prostate cancer suppressor regulated by the intronic long noncoding RNA PCA3. *Proc Natl Acad Sci U S A,* **112**, 8403-8.

Sanderson, J. T. (2006) The Steroid Hormone Biosynthesis Pathway as a Target for Endocrine-Disrupting Chemicals. *Toxicological Sciences,* **94**, 3-21.

Schiffer, L., Arlt, W. and Storbeck, K.-H. (2018) Intracrine androgen biosynthesis, metabolism and action revisited. *Molecular and Cellular Endocrinology,* **465**, 4-26.

Schreiber, E., Leong, H., Berosik, S., Schneider, S., Marks, J., George, W., Lim, Y. P., Chan, E. and Gerstner, A. New software for detecting somatic mutations at low level in Sanger sequencing traces. *European Journal of Cancer,* **61**, S16.

Schwartz, J. C., Podell, E. R., Han, S. S., Berry, J. D., Eggan, K. C. and Cech, T. R. (2014) FUS is sequestered in nuclear aggregates in ALS patient fibroblasts. *Mol Biol Cell,* **25**, 2571-8.

Sciarra, A., Mariotti, G., Salciccia, S., Autran Gomez, A., Monti, S., Toscano, V. and Di Silverio, F. (2008) Prostate growth and inflammation. *J Steroid Biochem Mol Biol,* **108**, 254-60.

Sengupta, A., Hon, T. and Zhang, L. (2005) Heme deficiency suppresses the expression of key neuronal genes and causes neuronal cell death. *Molecular Brain Research,* **137**, 23-30.

Shaffer, P. L., Jivan, A., Dollins, D. E., Claessens, F. and Gewirth, D. T. (2004) Structural basis of androgen receptor binding to selective androgen response elements. *Proc Natl Acad Sci U S A,* **101**, 4758-63.

Soff, G. A., Sanderowitz, J., Gately, S., Verrusio, E., Weiss, I., Brem, S. and Kwaan, H. C. (1995) Expression of plasminogen activator inhibitor type 1 by human prostate carcinoma cells inhibits primary tumor growth, tumor-associated angiogenesis, and metastasis to lung and liver in an athymic mouse model. *J Clin Invest,* **96**, 2593-600.

Stephan, C. (2011) Prostate-Specific Antigen. *In:* Schwab, M. (ed.) *Encyclopedia of Cancer.* Berlin, Heidelberg: Springer Berlin Heidelberg.

Sukocheva, O. A., Li, B., Due, S. L., Hussey, D. J. and Watson, D. I. (2015) Androgens and esophageal cancer: What do we know? *World Journal of Gastroenterology : WJG,* **21**, 6146-6156.

Sørensen, H. P. and Mortensen, K. K. (2005) Soluble expression of recombinant proteins in the cytoplasm of Escherichia coli. *Microbial cell factories,* **4**, 1-1.

Tan, A. Y., Riley, T. R., Coady, T., Bussemaker, H. J. and Manley, J. L. (2012) TLS/FUS (translocated in liposarcoma/fused in sarcoma) regulates target gene transcription via single-stranded DNA response elements. *Proceedings of the National Academy of Sciences,* **109**, 6030-6035.

Tan, M. H. E., Li, J., Xu, H. E., Melcher, K. and Yong, E.-l. (2014) Androgen receptor: structure, role in prostate cancer and drug discovery. *Acta Pharmacologica Sinica,* **36**, 3.

Toivanen, R. and Shen, M. M. (2017) Prostate organogenesis: tissue induction, hormonal regulation and cell type specification. *Development (Cambridge, England),* **144**, 1382-1398.

Twyffels, L., Gueydan, C. and Kruys, V. (2014) Transportin-1 and Transportin-2: protein nuclear import and beyond. *FEBS Lett,* **588**, 1857-68.

Untergasser, G., Madersbacher, S. and Berger, P. (2005) Benign prostatic hyperplasia: age-related tissue-remodeling. *Exp Gerontol,* **40**, 121-8.

van der Steen, T., Tindall, D. J. and Huang, H. (2013) Posttranslational Modification of the Androgen Receptor in Prostate Cancer. *International Journal of Molecular Sciences,* **14**, 14833-14859.

Vance, C., Scotter, E. L., Nishimura, A. L., Troakes, C., Mitchell, J. C., Kathe, C., Urwin, H., Manser, C., Miller, C. C., Hortobágyi, T., Dragunow, M., Rogelj, B. and Shaw, C. E. (2013) ALS mutant FUS disrupts nuclear localization and sequesters wild-type FUS within cytoplasmic stress granules. *Human Molecular Genetics,* **22**, 2676-2688.

Vargas, H. A., Akin, O., Franiel, T., Goldman, D. A., Udo, K., Touijer, K. A., Reuter, V. E. and Hricak, H. (2012) Normal central zone of the prostate and central zone involvement by prostate cancer: clinical and MR imaging implications. *Radiology,* **262**, 894-902.

Vaupel, P. (2010) Metabolic microenvironment of tumor cells: a key factor in malignant progression. *Experimental oncology,* **32**, 125-127.

Ventura, S. (2005) Sequence determinants of protein aggregation: tools to increase protein solubility. *Microbial cell factories,* **4**, 11-11.

Verze, P., Cai, T. and Lorenzetti, S. (2016) The role of the prostate in male fertility, health and disease. *Nat Rev Urol,* **13**, 379-86.

Wang, X., Julio, M. K.-d., Economides, K. D., Walker, D., Yu, H., Halili, M. V., Hu, Y.-P., Price, S. M., Abate-Shen, C. and Shen, M. M. (2009) A luminal epithelial stem cell that is a cell of origin for prostate cancer. *Nature,* **461**, 495.

Weitz, S. H., Gong, M., Barr, I., Weiss, S. and Guo, F. (2014) Processing of microRNA primary transcripts requires heme in mammalian cells. *Proceedings of the National Academy of Sciences,* **111**, 1861.

Wetherill, Y. B., Fisher, N. L., Staubach, A., Danielsen, M., de Vere White, R. W. and Knudsen, K. E. (2005) Xenoestrogen Action in Prostate Cancer: Pleiotropic Effects Dependent on Androgen Receptor Status. *Cancer Research,* **65**, 54.

Wilson, S., Qi, J. and Filipp, F. V. (2016) Refinement of the androgen response element based on ChIP-Seq in androgen-insensitive and androgen-responsive prostate cancer cell lines. *Scientific Reports,* **6**, 32611.

Winterbourn, C. C. (1995) Toxicity of iron and hydrogen peroxide: the Fenton reaction. *Toxicol Lett,* **82-83**, 969-74.

Woenckhaus, J. and Fenic, I. (2008) Proliferative inflammatory atrophy: a background lesion of prostate cancer? *Andrologia,* **40**, 134-7.

Xie, Y., Hou, W., Song, X., Yu, Y., Huang, J., Sun, X., Kang, R. and Tang, D. (2016) Ferroptosis: process and function. *Cell death and differentiation,* **23**, 369-379.

Xu, J., Meyers, D., Freije, D., Isaacs, S., Wiley, K., Nusskern, D., Ewing, C., Wilkens, E., Bujnovszky, P., Bova, G. S., Walsh, P., Isaacs, W., Schleutker, J., Matikainen, M., Tammela, T., Visakorpi, T., Kallioniemi, O. P., Berry, R., Schaid, D., French, A., McDonnell, S., Schroeder, J., Blute, M., Thibodeau, S., Gronberg, H., Emanuelsson, M., Damber, J. E., Bergh, A., Jonsson, B. A., Smith, J., Bailey-Wilson, J., Carpten, J., Stephan, D., Gillanders, E., Amundson, I., Kainu, T., Freas-Lutz, D., Baffoe-Bonnie, A., Van Aucken, A., Sood, R., Collins, F., Brownstein, M. and Trent, J.

(1998) Evidence for a prostate cancer susceptibility locus on the X chromosome. *Nat Genet,* **20**, 175-9.

Yamashita, S., Mori, A., Sakaguchi, H., Suga, T., Ishihara, D., Ueda, A., Yamashita, T., Maeda, Y., Uchino, M. and Hirano, T. (2012) Sporadic juvenile amyotrophic lateral sclerosis caused by mutant FUS/TLS: possible association of mental retardation with this mutation. *J Neurol,* **259**, 1039-44.

Yang, L., Gal, J., Chen, J. and Zhu, H. (2014) Self-assembled FUS binds active chromatin and regulates gene transcription. *Proceedings of the National Academy of Sciences,* **111**, 17809-17814.

Zhan, F., Shen, J., Wang, R., Wang, L., Dai, Y., Zhang, Y. and Huang, X. (2018) Role of exosomal small RNA in prostate cancer metastasis. *Cancer management and research,* **10**, 4029-4038.

Zhang, A., Zhao, Jonathan C., Kim, J., Fong, K.-w., Yang, Yeqing A., Chakravarti, D., Mo, Y.-Y. and Yu, J. (2015) LncRNA HOTAIR Enhances the Androgen-Receptor-Mediated Transcriptional Program and Drives Castration-Resistant Prostate Cancer. *Cell Reports,* **13**, 209-221.

Zhang, Z., Zhou, N., Huang, J., Ho, T.-T., Zhu, Z., Qiu, Z., Zhou, X., Bai, C., Wu, F., Xu, M. and Mo, Y.-Y. (2016) Regulation of androgen receptor splice variant AR3 by PCGEM1. *Oncotarget,* **7**, 15481-15491.

Zheng, J. (2012) Energy metabolism of cancer: Glycolysis versus oxidative phosphorylation (Review). *Oncol Lett,* **4**, 1151-1157.

Zheng, X., Ji, P., Mao, H. and Hu, J. (2012) A comparison of virtual touch tissue quantification and digital rectal examination for discrimination between prostate cancer and benign prostatic hyperplasia. *Radiol Oncol,* **46**, 69-74.

Zhou, Y., Bolton, E. C. and Jones, J. O. (2015) Androgens and androgen receptor signaling in prostate tumorigenesis. *J Mol Endocrinol,* **54**, R15-29.

Zhou, Z., Corden, J. L. and Brown, T. R. (1997) Identification and characterization of a novel androgen response element composed of a direct repeat. *J Biol Chem,* **272**, 8227-35.

Zhou, Z. X., Lane, M. V., Kemppainen, J. A., French, F. S. and Wilson, E. M. (1995) Specificity of ligand-dependent androgen receptor stabilization: receptor domain interactions influence ligand dissociation and receptor stability. *Mol Endocrinol,* **9**, 208-18.

Zinszner, H., Sok, J., Immanuel, D., Yin, Y. and Ron, D. (1997) TLS (FUS) binds RNA in vivo and engages in nucleo-cytoplasmic shuttling. *J Cell Sci,* **110 (Pt 15)**, 1741-50.

Zong, W. X. and Thompson, C. B. (2006) Necrotic death as a cell fate. *Genes Dev,* **20**, 1-15.

Zámocký, M., Hofbauer, S., Schaffner, I., Gasselhuber, B., Nicolussi, A., Soudi, M., Pirker, K. F., Furtmüller, P. G. and Obinger, C. (2015) Independent evolution of four heme peroxidase superfamilies. *Archives of Biochemistry and Biophysics,* **574**, 108-119.